

THE ROLES OF THE *DROSOPHILA* PROTEIN TRIBBLES IN OOGENESIS AND
INSULIN SIGNALING PATHWAY

A DISSERTATION IN
Molecular Biology and Biochemistry
and
Cell Biology and Biophysics

Presented to the faculty of the University
of Missouri-Kansas City in partial fulfillment
of the requirements for the degree

DOCTOR OF PHILOSOPHY

By Rahul Das

B.Sc., University of Calcutta, 2006
M.Sc., University of Calcutta, 2008
M.S., University of Missouri-Kansas City, 2011

Kansas City, Missouri

2015

© 2015

Rahul Das

All Rights Reserved

THE ROLES OF THE *DROSOPHILA* PROTEIN TRIBBLES IN OOGENESIS AND INSULIN SIGNALING PATHWAY

Rahul Das, Candidate for the Doctor of Philosophy Degree
University of Missouri-Kansas City, 2015

ABSTRACT

In this dissertation, I examined the molecular mechanism of function of the *Drosophila melanogaster* protein Tribbles (Trbl) during oogenesis and larval development. Trbl is the founding member of an evolutionarily conserved family of kinase proteins that play diverse roles in cell signaling and energy homeostasis. In addition to the central Serine/Threonine kinase domain, members of the Tribbles gene family (Trib) shares C terminal mitogen activated protein kinase kinase MEK1 and E3 ubiquitin ligase COP1 binding motifs, the latter required for the degradation of target proteins via proteasome. During oogenesis, Trbl controls border cell (BC) cluster migration by mediating degradation of C/EBP transcription factor Slbo. I first investigated Trbl's role during oogenesis using a Trbl specific antisera. Trbl localizes to the nucleus of main body follicle cells (MBFC) up to stage 10 of oogenesis. In the case of BC, Trbl expresses in a complementary pattern to Slbo expression. The Trbl level decreases gradually as the BC cluster delaminates from the epithelium and starts migrating when Slbo protein level increases. Moreover, Slbo was found to be essential but not sufficient to decrease the Trbl level required for BC migration.

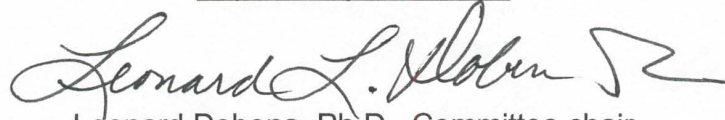
In a wing misexpression screen for Trbl interacting proteins, I identified the Serine/Threonine protein kinase Akt, a major mediator of insulin signaling. In recent years, mammalian Trib3 and Trib2 proteins have been implicated in the regulation of

Insulin signaling by inhibiting the activating phosphorylation of Akt, Given the central role of Akt in insulin signaling, I tested whether the function of Trib family in insulin signaling is evolutionarily conserved. Using *Drosophila* larval development as a model system, I found that Trbl has a conserved role in binding and inhibiting Akt phosphorylation-activation, implicating Trib proteins as novel sites of signaling pathway integration that link nutrient availability with cell growth and proliferation. Finally, I have identified a previously unknown motif (R141) in Trib proteins essential for their function to regulate insulin signaling mediated growth and metabolism.


APPROVAL PAGE

The faculty listed below, appointed by the Dean of School of Graduate Studies have examined a dissertation titled "The Roles of the *Drosophila* Protein Tribbles in Oogenesis and Insulin Signaling Pathway" presented by Rahul Das, candidate for the Doctor of Philosophy degree, and certify that in their opinion it is worthy of acceptance.

Supervisory committee

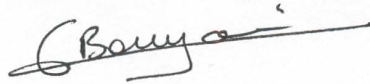


Leonard L. Dobens, Ph.D., Committee chair
Associate Professor, Division of Molecular Biology and Biochemistry



Jeffrey L. Price, Ph.D.
Associate Professor, Division of Molecular Biology and Biochemistry

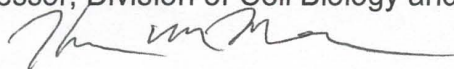
Samuel Bouyain, DPhil.
Associate Professor, Division of Molecular Biology and Biochemistry



Erika Geisbrecht, Ph.D.
Associate Professor, Division of Cell Biology and Biophysics



Thomas Menees, Ph.D.
Associate Professor, Division of Cell Biology and Biophysics



CONTENTS

ABSTRACT iii

LIST OF ILLUSTRATIONS..... vii

LIST OF TABLES ix

ABBREVIATIONS x

ACKNOWLEDGEMENT xii

CHAPTER

1. BACKGROUND AND SIGNIFICANCE 1

2. THE KINASE DOMAIN OF *DROSOPHILA* TRIBBLES IS REQUIRED FOR
TURNOVER OF FLY C/EBP DURING CELL MIGRATION 12

3. *DROSOPHILA* TRIBBLES ANTAGONIZES INSULIN SIGNALING-
MEDIATED GROWTH AND METABOLISM VIA INTERACTIONS
WITH AKT KINASE-----43

4. EVOLUTIONARILY CONSERVED ARGININE 141 OF *DROSOPHILA*
TRIBBLES PLAYS CRUCIAL ROLES IN THE REGULATION OF THE
INSULIN-SIGNALING PATHWAY -----76

5. APPENDIX----- 104

6. FUTURE DIRECTIONS ----- 106

REFERENCES ----- 111

VITA ----- 128

ILLUSTRATIONS

Figure	Page
1.1 Schematic of Trib protein structure-----	2
2.1 Trbl accumulates in the nuclei of non-migratory FC groups -----	20
2.2 <i>slbo</i> and <i>trbl</i> have opposing effects in migratory FC groups-----	23
2.3 Slbo is not sufficient to repress Trbl expression -----	24
2.4 Construction of a <i>trbl</i> null allele-----	27
2.5 Characterization of Trbl antisera -----	28
2.6 Trbl kinase domain is required to block BC migration -----	32
2.7 Trbl kinase domain is required for Slbo binding in vitro (Y2H) -----	36
2.8 Trbl kinase domain is required for Slbo turnover in vivo -----	40
3.1 Akt is a Trbl interacting gene in a wing misexpression screen -----	55
3.2 Larval fat body specific overexpression of Trbl suppresses growth and Delays development -----	58
3.3 Trbl affects circulatory sugar and total lipid level -----	61
3.4 Trbl binds Akt and suppresses Akt mediated growth phenotypes-----	64
3.5 The Trbl kinase domain is required to block Akt activation-----	66
3.6 Trbl blocks insulin signaling -----	68
3.7 Trbl reduces FoxO phosphorylation; a model for Trbl action -----	71
4.1 Human Trib3 Q84 position is highly conserved and contains R in most Trib proteins-----	91
4.2 R141 plays crucial role in the inhibition of dAkt activation -----	93
4.3 Trbl 141Q is a less potent inhibitor of larval growth and metabolism-----	95

ILLUSTRATIONS

Figure

Page

4.4 R141 plays a crucial role only in Trbl's physical interaction with Akt and the regulation of insulin signaling-----	100
5.1 mouse Trib2 can inhibit endogenous dAkt activation in fat body-----	105

TABLES

Table	Page
1. Genetic interactions between <i>trbl</i> and <i>slbo</i> during BC migration	30
2. Misexpression assay of UAS- <i>Trbl</i> , UAS- <i>Trbl</i> mutant transgenes and UAS- <i>Trbl</i> RNAi	33
3. Yeast Two hybrid interaction between <i>Trbl</i> and <i>Trbl</i> mutations with <i>Slbo</i>	35

ABBREVIATIONS

ACC	Acetyl coA carboxylase
Arm	Armadillo
BC	Border Cell
BMP	Bone Morphogenetic Protein
Bun	Bunched
C/EBP	CAAT Enhancer Binding Protein
CMFC	Centripetally Migrating Follicle Cell
COP1	Constitutive photomorphogenic protein 1
Cyc	Cyclin
Dig	Discs Large
DN	Dominant Negative
DPP	Decapentaplegic
En	Engrailed
Fas2	Fasciclin II
FC	Follicle Cell
FLP	Flipase
FoxO	Forkhead transcription factor subgroup X
FRT	Flipase Recognition target
GFP	Green Fluorescent Protein
GSK	Glycogen synthase kinase
GOF	Gain of Function
HS	heat shock

PH	Pleckstrin homology
Ppl	Pumpless
PI3K	Phosphatidylinositol-3-kinase
PIP2	Phosphatidylinositol 3, 4,-Bisphosphate
PIP3	Phosphatidylinositol 3, 4, 5-Trisphosphate
PKB	Protein kinase B (Akt)
PPAR	Peroxisome Proliferator-Activated receptor
Pten	Phosphatase and tensin homolog ten
Slbo	Slow Border Cell
SNP	Single nucleotide polymorphism
UAS	Upstream Activating
Ubi-GFP	Ubiquitous Green Fluorescence protein
WT	Wild Type

ACKNOWLEDGEMENTS

I would like to thank my committee members Dr. Leonard Dobens, Dr. Jeffrey Price, Dr. Samuel Bouyain, Dr. Thomas Menees and Dr. Erika Geisbrecht for their guidance and advice through the work represented in this thesis. I would especially like to express my gratitude to my committee chair, Dr. Leonard Dobens, for being a perfect mentor and teaching me numerous valuable lessons during the course of this dissertation. I would also like to thank fellow members of the lab for their cooperation and assistance; Elizabeth Dobens, Venessa Masoner, Laramie Pence, Zach Sebo, Zach Fischer and Anna Shipman.

Support for this research came from the National Science Foundation (Award Number: 0920613), University of Missouri Research Board and School of Graduate studies of UMKC.

DEDICATION

This dissertation is dedicated to my beloved grandfather late Bidur Bhattacharya, Grandmother Nanibala Das and Maya Bhattacharya for their support and inspiration throughout. I would like to express gratitude to my father Basudeb Das, mother Ruma Das, wife Madhurima Das and sister Susmita Das for their help and encouragement.

CHAPTER 1

BACKGROUND AND SIGNIFICANCE

A brief history of Tribbles protein family

The *trbl* gene was first identified over a decade ago in genetic screens for mutations that control cell migration during oogenesis (Rorth et al., 2000) and cell division during embryogenesis (Seher and Leptin 2000). Trbl binds and degrades String/Twine phosphatase to block cell division both early during the mid-blastula transition and later in the invaginating mesoderm during gastrulation (Farrell and O'Farrell 2013; Grosshans and Wieschaus 2000; Mata et al., 2000). During oogenesis, Trbl regulates BC migration by mediating the turnover of the C/EBP transcription factor homolog Slow Border Cells (Slbo)(Rorth et al., 2000). Afterwards, three Trbl orthologs namely Trib1, Trib2 and Trib3 (Wilkin et al., 1996) (Mayumi-Matsuda et al., 1999; Wilkin et al., 1997) were discovered in higher animals.

Structural features Of Trib proteins

The N-terminal and the C-terminal region of Trib proteins are not evolutionarily well conserved across species except for two motifs present in the C-terminus region: an E3 ubiquitin ligase COP1 binding motif and a Mitogen activated protein kinase kinase (MAPKK) MEK1 binding motif. In contrast, the central domain resembling catalytic domain of protein Serine/Threonine kinase is highly conserved in all Tribs. However, the central domain lacks three key motifs thought to be needed for kinase's catalytic activity; (1) a VAIK motif which binds ATP (2) a central HRD

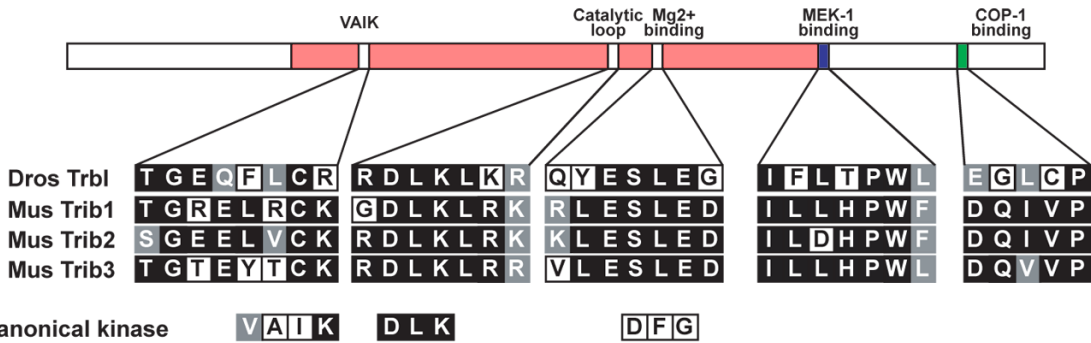
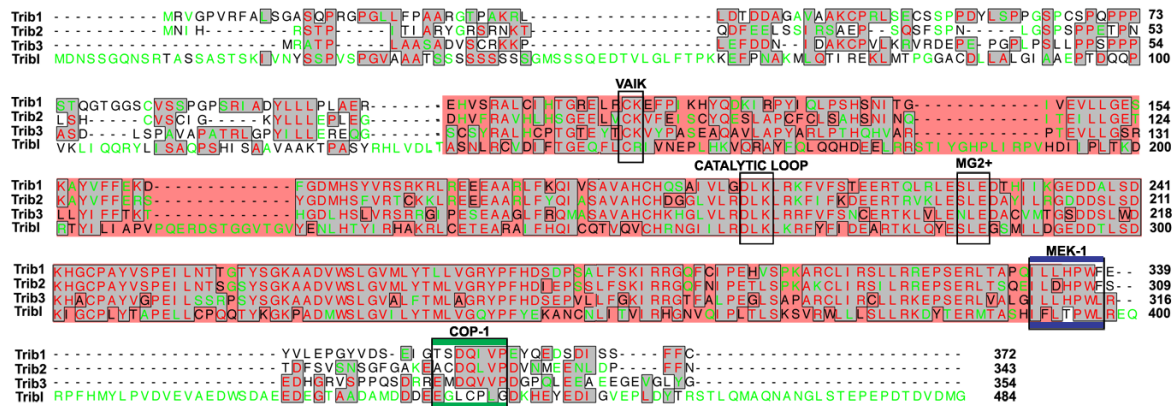


Figure 1.1 Schematic of Trib protein structure.

(A.) Clustal alignment of *Drosophila* Trbl with mammalian Tribbles reveals a conserved central kinase domain (red) with key features boxed, and conserved MEK1 (blue) and COP1 (green) binding domains. Common identical residues shown in black, conserved residues shaded. (B.) Tribbles protein schematic with key residues found in the Trbl family contrasted with those found in canonical kinases. Figure adapted from (Dobens and Bouyain 2012)

domain in which the catalytic aspartic acid residue functions as a base acceptor during proton transfer and (3) a DFG motif required for Mg^{2+} co-ordination [reviewed in (Dobens and Bouyain 2012)]. These deviations from the consensus sequence of the protein kinase superfamily led to the postulation that Tribl proteins do not possess catalytic activity and they act as pseudo-kinase or decoy kinase. However, the sequences that replace the VAIK, DFG and HRD motifs are extremely conserved in all Tribs, indicating that Trib proteins may represent a divergent group of kinases with catalytic activity. Indeed, a very recent discovery shows that Trib2 is an active kinase and it can undergo auto-phosphorylation (Bailey et al., 2015), a key feature of many kinases.

Function of Trib proteins in development and disease

In a genetic screen conducted in the ovarian follicle cell epithelium, Tribl misexpression was found to specifically blocks border cell (BC) cluster migration. Border cells delaminate from the anterior tip of follicular epithelium at stage 9 of oogenesis and migrate as a cluster (of up to 10 cells) between the nurse cells to reach the nurse cell-oocyte boundary by stage 10, later forming the micropyle, a tube like structure that allows sperm access to the egg. It was discovered that Tribl binds to and promotes proteasomal degradation of the fly C/EBP (CAAT enhancer binding protein, a group of transcription factors) homolog encoded by the gene 'Slow border cells' (*slbo*), a key mediator of border cell migration. Further studies on mammalian Tribs showed that Trib-C/EBP interaction is highly conserved in Trib1 and Trib 2. For example, in acute myelogenous leukemia (AML) tumors, Trib1 promotes degradation of C/EBP α and upregulation of C/EBP β occurs in Trib1

knockout mice (Keeshan et al., 2008; Yamamoto et al., 2007). Similarly, overexpression of Trib2 induces proteasomal degradation of C/EBP α , which is thought to be required for myeloid differentiation during acute myelogenous leukemia (Keeshan et al., 2006). However, unlike Trib1 and Trib2, Trib3 doesn't appear to target C/EBP proteins for degradation. It was shown that Trib3 could not induce proteasomal degradation of C/EBP α required for onset of AML (Dedhia et al., 2010). Finally, Trib2 (but not Trib3) increases degradation of C/EBP β , resulting in suppression of differentiation of 3T3-L1 preadipocytes (Naiki et al., 2007).

Two independent screens designed to identify mutations that inhibit mesodermal invagination also identified *Trbl* as a candidate. Loss of function of *trbl* gene results in migration inhibition and over-proliferation of mesodermal cells (Grosshans and Wieschaus 2000; Seher and Leptin 2000). During normal gastrulation, the ventral mesodermal cells stop dividing and undergo ingression and dorsal migration. It was found that *Trbl* induces degradation of String phosphatase, which removes an inhibitory phosphate from the Cyclin/cdc2 complex. This inhibition of cell division perhaps accommodates epithelial to mesenchymal cell shape changes incompatible with cell rounding that typically occur during division. Indeed, double mutants for *trbl* and *string* invaginate normally. Snail transcription factor triggers the shape changes of ventral cells to form 'ventral furrow' that brings the mesoderm anlage into the interior of the embryo during gastrulation. Injection of *trbl* mRNA in wild-type embryo is sufficient to block cell divisions, but injection into *snail* mutant embryos does not prevent cell division, suggesting that Snail activates expression of a *Trbl* co-activator, whose identity and mechanism of activity remains

undetermined (Grosshans and Wieschaus 2000). Knockdown of *trib3* in tumor cells leads to down-regulation of Twist and Snail resulting in the inhibition of the tumor metastasis (Hua et al., 2011). Thus the interactions among Twist, Snail and Trbl to control cell migration during development seems to be evolutionarily conserved (Ciruna and Rossant 2001; Ip and Gridley 2002). An inhibitory role of Trbl in somatic cell division seems to be global as *trbl* mutations suppress eye overgrowth phenotypes resulting from overexpression of Unpaired, a ligand of Jak/Stat pathway (Mukherjee et al., 2006) and Trbl misexpression enhances while *trbl* mutants suppress expression of Wee1 kinase that phosphorylates and inhibits Cdc2/Cdk activity.

In contrast to Trbl's ability to inhibit cell division in the somatic cells described above, Trbl actually induces proliferation of germ line cells. Trbl misexpression in the germ line triggers an extra round of cell division during oocyte differentiation (Mata et al., 2000). Complementarily, mutation in *trbl* gene reduces the number of the germ cells in ovary and the oocyte does not differentiate properly (Huynh and St Johnston 2004). Trbl misexpression induces amplification of the male gamete precursors (Schulz et al., 2004). Prospero, a transcription factor that negatively regulates spermatogonial stem cell proliferation, was found to downregulate *trbl* mRNA expression (Choksi et al., 2006). Taken together, these observations suggest that Trbl induces germ cell division, opposite to its role in inhibiting cell division (Price et al., 2002).

Mammalian Trib proteins, especially Trib3 and Trib2 also play a major role in metabolism and energy homeostasis by regulating insulin-signaling pathway. Akt

kinase is a major downstream mediator of insulin signaling. In response to insulin, mTORC2 protein complex phosphorylates Ser473 (Ser505 in *Drosophila*) of Akt in the activation loop, resulting in the activation of the kinase activity of Akt. Mammalian Trib3 and Trib2 have been demonstrated to bind Akt and block activation without targeting Akt for proteasomal degradation, resulting in impaired insulin signaling in hepatocytes, adipocytes, skeletal muscle, liver, fat, and pancreas (Du et al., 2003; Koh et al., 2006; Liu et al., 2010; Qi et al., 2006). Consistent with a role in reducing insulin outputs, increased Trib3 expression occurs (1) following either starvation or exercise in mice, (2) in db/db diabetic mice (Matsushima et al., 2006) and (3) following experimental treatments such as high-fructose feeding or chronic ethanol consumption that lead to impaired insulin responses (Bi et al., 2008; He et al., 2006). Aberrantly high Trib3 levels are detected in insulin-resistant humans (Liu et al., 2010; Oberkofler et al., 2010; Prudente et al., 2009) and a population variant Trib3Q/R84 associated with predisposition to metabolic disease and diabetes dominantly blocks Akt activation in vitro and in vivo (Andreozzi et al., 2008; Prudente et al., 2005; Prudente et al., 2013).

The notion that Trib3 binds Akt to 'dial-down' the insulin response in peripheral tissues is contradicted by genetic analysis showing that rat Trib3 knockdown has no effect on Akt activity (; Weismann et al., 2011) and mouse Trib3 knockout has no effect on metabolism at all (Okamoto et al., 2007); phenotypes that may be caused by overlapping functions with Trib1 and Trib2.

Overview of my dissertation research

My dissertation research can be divided into 2 broad sections: (i) regulation and function of Trbl during *Drosophila* oogenesis (ii) regulation of insulin signaling pathway by Trbl.

Since the initial series of publications, several genetic screens identified Trbl as either an antagonist or promoter of cell division, depending on the context (described in earlier sections). However, the regulation of Trbl itself or the functions of individual Trib domains have not been studied. I first focused on the regulation of Trbl in BC migration. Using a newly generated Trbl specific antibody, I observed that Trbl is expressed in the follicle cells up to stage 10B of oogenesis with low level of expression in migrating BC and centripetal cells (CMFC). In the border cells, Trbl level drops gradually during the course of migration, indicating involvement of Slbo in the regulation of Trbl. Indeed, using a *slbo* mutant allele, I was able to show that Slbo downregulates Trbl as migration starts. However, misexpression of Slbo was not sufficient to reduce Trbl level, indicating that other factor(s) that work in combination with Slbo play a crucial role in Trbl downregulation. Research by other members of the lab showed that Trbl physically interacts with Slbo through Trbl's kinase domain and this interaction is essential for the proper turnover of Slbo during the BC migration.

My second project was focused on the genetic regulation of the *Drosophila* insulin signaling pathway and the function of Trbl in Insulin signaling. As described in previous section, several findings strongly suggest that Trib proteins, especially Trib3 and Trib2 have important regulatory functions in insulin signaling pathway.

Surprisingly, deletion of the *trb3* gene has no effect on insulin signaling (including Akt inhibition) and glucose homeostasis in rodent liver. Similarly, overexpression of Trib3 in rat primary hepatocyte does not change the phosphorylation level of Akt or Akt mediated phosphorylation of Glycogen synthase kinase 3 (GSK3) (Okamoto et al., 2007). Knockout of *trb2* gene also has no effect on the development of mouse (Takasato et al., 2008). Both Trib2 and Trib3 are expressed in a variety of organs including muscle, bone and kidney in overlapping and non-overlapping patterns (Ashton-Chess et al., 2008; Okamoto et al., 2007). Together the shared expression patterns, the absence of phenotypic effects when individual genes are deleted, and the high degree of sequence homologies in the kinase domain among Trib proteins raise the possibility that all Trib family members exert overlapping functions, perhaps through their central kinase domain. On the other hand, non-conserved N and C terminal domains might be required for tissue or developmental stage specific functions.

To test if the insulin signaling inhibitory function of Trib proteins is evolutionarily conserved, I examined the ability of Trbl to inhibit the *Drosophila* insulin signaling pathway in different tissues and different stages of development. I performed immunostaining of larval tissues and observed Trbl expression in fat body (equivalent to mammalian adipose tissue and liver), salivary gland and skeletal muscle. Fat body specific overexpression of Trbl delayed pupation and eclosion. Using western blot, I found that Trbl prevents the activating phosphorylation of dAkt kinase (at Ser505, equivalent to Ser473 in mammalian Akt) whereas a mutant version of Trbl bearing point mutation in Kinase domain (D/NLK) failed to prevent

dAkt phosphorylation. Complimentarily, *trbl* knockdown by several RNAi lines increased active Akt level. Lipid analysis of the larval tissue showed that fat body specific Trbl overexpression decreases and *trbl* knock down increases total lipid level. I also found that Trbl overexpression increases larval circulatory glucose and trehalose (main circulatory sugar in insects) concentrations. In case of skeletal muscle, *trbl* misexpression or knockdown does not have any visible effect on larval phenotype. However, co-misexpression of Trbl can rescue embryonic lethality (or muscle hypertrophy at permissive temperature) caused by muscle specific misexpression of dAkt. A wing misexpression assay revealed the position of Trbl in the Insulin signaling pathway; Trbl acts upstream and at the level of dAkt but not downstream of dAkt. Finally, using yeast two-hybrid assay, I showed that Trbl physically interacts with dAkt via its kinase domain. Taken together, these data show that Trbl acts as a negative regulator of insulin signaling pathway and co-ordinates nutrient availability with developmental timing.

A single nucleotide polymorphism (dsSNP ID: rs2295490) of human Trib3 associated with insulin resistance has recently been described. This non-synonymous polymorphism changes amino acid Glutamine (Q) at position 84 to arginine (R). Carriers of the R84 allele are predisposed to develop insulin resistance and early onset Type 2 Diabetes Mellitus (T2DM) in different human populations (Gong et al., 2009; Prudente et al., 2010; Prudente et al., 2005). Cell culture studies indicate that 84R is a stronger inhibitor of Akt activation than the more prevalent Q84 allele (Andreozzi et al., 2008; Prudente et al., 2005). All Trib proteins share an extensive sequence homology at their central kinase domain (Hegedus et al., 2006)

that is associated with binding and preventing Akt activation (Das et al., 2014; Du et al., 2003). This encouraged me to check if Q84 is conserved in other Trib proteins as well. I performed an extensive sequence alignment between *Drosophila* Trbl and all mammalian Trib proteins. Very surprisingly, I observed that R and not Q actually occupies the position corresponding to Trib3 84 in almost all Trib proteins; it is conserved in *Drosophila* Trbl (position R141) and all mammalian Trib1 and Trib2s (Figure 4.1A). Additionally, R but not Q was found in most other mammalian Trib3s (including chimpanzee Trib3); only human and neanderthal Trib3 contain Q at this position. I sought to determine if this extremely conserved R residue plays an important role in the insulin signaling pathway and the function of Trbl in general. Therefore, I generated a mutant Trbl carrying Q at that site (changing R with Q; R141Q, referred as 141Q hereafter) and compared its activity with WT Trbl in relevant fly tissues.

I was able to show that 141Q is indeed a less potent inhibitor of Akt activation in adipose tissue: misexpression of 141Q did not prevent activating phosphorylation of dAkt to the same extent as WT Trbl did and consequently 141Q acted as a weaker inhibitor of insulin action, as demonstrated by effects of misexpression on developmental timing and various metabolite contents. I also observed that R141 is specifically involved with the regulation of insulin signaling, as misexpression of 141Q does not change WT Trbl's regulatory action on other cellular processes such as cell migration and division. Using in vivo and in vitro methods I showed that 141Q increases Trbl's physical interaction strength with Akt but not with C/EBP transcription factor, a known binding partner of Trbl (Masoner et al., 2013),

confirming that the 141Q mutation has effects specific for metabolism. I further verified the conserved role of R141 by showing that mouse Trib3 (containing R at the conserved position) was not only able to prevent Akt activation when introduced in the *Drosophila* adipose tissue, but also it did so with a potency similar to WT Trib3 and significantly higher than that of 141Q. Taken together, my observations indicate that Trib3 Q84 appeared late during the course of evolution and suggest that human and neanderthal Trib3 variant conferred more avid interaction strength with Akt kinase, but reduced the potency of Akt inhibition, compared to related Trib3s.

Specific contribution of other members of the lab

Several past and present members of our lab contributed significantly to the work presented in this thesis. Following list shows each member's contribution in the experiments depicted in the corresponding figures of this thesis.

- Leonard Dobens Figure 2.4 (A, C, D), 3.1, 3.5 (A-I)
- Venessa Masoner Figure 2.6 and 2.8
- Laramie Pence Figure 2.7 and 4.4D
- Zachary Sebo Figure 3.5(K-R)
- Anna Shipman Figure 4.4E

CHAPTER 2

THE KINASE DOMAIN OF *DROSOPHILA* TRIBBLES IS REQUIRED FOR TURNOVER OF FLY C/EBP DURING CELL MIGRATION

Introduction

Cell migration is a tightly regulated process, in which loss of polarity and delamination of epithelial cells is followed by changes in cell adhesion and the formation and extension of cellular processes during a migratory phase. During normal development as well as abnormal tumor progression, the levels of key regulatory proteins that trigger, direct and terminate cell migration are strictly controlled. The *Drosophila* ovary presents two excellent model tissues to study collective cell migration: (1) the border cells (BC), which delaminate as a small cluster and migrate through the nurse cells to reach the posterior oocyte from stages 9-10B and (2) the centripetal follicle cells (centripetal migrating FC or CMFC) which migrate as a cell sheet between the nurse cells and oocyte from stages 10B-13 (Figure. 2.1A). A key regulator of migration in both these tissues is the C/EBP protein Slow border cells (Slbo). Levels of Slbo are critical for proper migration, and negative feedback regulates Slbo expression both transcriptionally (Levine et al., 2010) and post-transcriptionally. A search for genes that regulate Slbo protein levels during BC migration identified the gene *tribbles*.

During mammalian and fly development, Tribbles regulate cell proliferation during tissue differentiation (Ables and Drummond-Barbosa 2010; Dobens and Bouyain 2012). In flies, Trbl blocks (1) embryonic cell division during mesodermal migration (Grosshans and Wieschaus 2000; Seher and Leptin 2000) (2) the step-

wise cell division connected to patterning of the bristle primordia in the peripheral neurons (Abdelilah-Seyfried et al., 2000; Fichelson and Gho 2004; Norga et al., 2003) and (3) stem cell proliferation during germ line differentiation (Mata et al., 2000; Schulz et al., 2004). Mammalian Trib isoforms regulate differentiation linked to cell division during hematopoiesis (Eder et al., 2008b; Lin et al., 2007; Sathyanarayana et al., 2008), myogenesis (Kato and Du 2007; Sung et al., 2007), lymphogenesis (Selim et al., 2007) and adipogenesis (Naiki et al., 2007). The connections observed between Tribs and diverse cell signaling pathways regulating cell growth, proliferation and differentiation likely underlie the involvement of Tribs in cancer and disease (Angyal and Kiss-Toth 2012; Kiss-Toth 2011; Prudente et al., 2012; Yokoyama and Nakamura 2011).

One common mechanistic feature shared by all Tribs is the ability to bind key regulatory proteins and either block their activity or direct their turnover by the proteasome. In the mesoderm and germ line of the fly, Trbl degrades String/cdc25 phosphatase to regulate the entry into S phase (Grosshans and Wieschaus 2000; Seher and Leptin 2000). In mouse osteoblasts, Trib3 binds and degrades SMURF1, an E3 ubiquitin ligase specific for the BMP mediator Smad, effectively stabilizing Smads (Chan et al., 2007). During adipogenesis, Trib3 binds and degrades acetyl coenzyme A carboxylase1 (ACC1), the rate-limiting enzyme in fatty acid synthesis (Qi et al., 2006). As well, Trib3 (and Trib2 less effectively) binds to Akt to inhibit phosphorylation of Foxo1 to permit adipocyte development to proceed (Naiki et al., 2007). During BC migration, Trbl binds to Slbo to direct its degradation by the proteasome, and this interaction is conserved in mammals, where Trib1 and Trib2

accelerate degradation of C/EBP α and C/EBP β , respectively, during normal tissue differentiation and in tumors (Keeshan et al., 2008; Naiki et al., 2007; Yamamoto et al., 2007).

Here I show, using a cell migration model in the fly ovary that Slbo and Trbl have a complex negative feedback whereby Slbo represses Trbl expression and Trbl – via its conserved DLK motif – directs Slbo turnover. These results shed light on the conserved mechanism of Trbl function, and assign a role for Trbl interactions in a negative feedback loop regulating C/EBP-regulated cell migration.

Materials and methods

Drosophila strains

Stocks used were (1) $P\{w+(mC)=AyGal4\}25 P\{w+(mC)=UAS-GFP.S65T\}T2/CyO$ (Pignoni and Zipursky, 1997), (2) $slbo^{01310}/CyO$ (Montell et al., 1992), (3) $P\{XP\}trbl^{d07751}$, (4) $P\{XP\}trbl^{d03251}$ [3 and 4 are from the Harvard Stock Center; (Thibault et al., 2004)], (5) $hsFLP1$ (Xu and Rubin 1993) (6) $UAS-Trbl$, (7) $trbl^{EP1119}$, (8) $trbl^{EP3519}$ [7-8 are gifts from Pernille Rorth; (Rorth et al., 2000)], (9) $hsSlbo$, (10) $w^{1118}; \{Ubi-GFP(S65T)nls\}3L P\{neoFRT\}80B/TM3$ (Xu and Rubin 1993), (11) $trbl^{P\{GawB\}NP3530}$, (12) $CG33969^{EP20583}$, (13) $fb1^1$, (14) $Df(3L)rdgC-co2$, (15) $y^1w^1; P\{w+(mW.hs)=en2.4-Gal4\}e22c/SM5$ (10-15 are from the Bloomington Stock Center), (16) $UAS-Trbl IR^{22114}$ and (17) $UAS-Trbl IR^{22113}$ (16 and 17 are from the Vienna Stock Center).

Generation of clones and immunochemistry

Flp-out clones misexpressing UAS-transgenes were created as described previously (Levine et al., 2010). The productions of mitotic clones and

Immunohistochemistry procedures have been described (Levine et al., 2010). Following primary antisera were used: (1) polyclonal antisera were raised against the peptide CZDKHEYEDIGVEPLDYTR in chickens and affinity purified with the peptide (Aves Lab, Tigard, OR) and was used at 1:1000 (in PBS+ 1% BSA+ 0.5% Triton-X100 solution after pre-adsorption to ovarian tissue); (2) rabbit anti- β -galactosidase (1:50,000 following preadsorption to ovarian tissue; Cappell, West Chester, PA); (3) rabbit anti-Slbo at 1:2000 (Szafranski and Goode 2004) (4) monoclonal mouse and rabbit GFP (Invitrogen) were used at 1:200 and 1:1000, respectively; Secondary antibodies used were goat anti-rabbit, mouse and chicken AlexaFluor®488, 594 and 647 (1:200; Invitrogen). Confocal images were collected on an Olympus Fluoview 300 confocal microscope or Nikon 90i microscope with Optigrid paddle and Metamorph Image acquisition software. DIC images were collected on a Nikon TE-2000 with attached Colorview camera and 'Analysis' image acquisition software. Figures were prepared using Photoshop CS.

Fluorescence intensity (measured in arbitrary units) was obtained by collecting confocal sections through the BC cluster taken under identical settings and the section with maximum *slbo* expression was selected using 'plot Z axis profile' function of the ImageJ software (<http://rsbweb.nih.gov/ij/>). The corresponding Trbl fluorescence intensity in that section was measured by the 'measure' function of ImageJ and the background intensity (calculated by averaging maximum intensities of three separate empty spots within a specific egg chamber) subtracted. Finally, the Trbl intensities obtained from multiple egg chambers of a given genotype were

averaged and used for plotting. The graphs and statistical analysis were done using GraphPad Prism software.

Design and construction of Trbl mutants

Construction of FLAGTrbl^{WT}

The complete ORF of *trbl* was amplified from cDNA using the oligonucleotides

ATGGATTACAAGGATGACGACGATAAGATGGATAACAGTAGCGGTC and TCAGCCCATGTCCACATCCGTATCGGGTTC to generate a N-terminal FLAG fusion (FLAG sequence in bold), cloned into pSTBlue-1 (AccepTor Vector kit, Novagen) and confirmed by DNA sequencing. An *EcoRI* fragment containing the full-length FLAGTrbl was then cloned into pUASTattB and again confirmed by DNA sequencing.

Construction of UAS-FLAGTrbl^{D/NLK}, UAS-FLAGTrbl^{FLCR/A}, and UAS-FLAGTrbl^{SLE/G}

Mutated versions of Trbl were generated from pSTBlue-1+FLAGTrbl using the QuikChange II XL Site-Directed Mutagenesis Kit (Stratagene) and oligonucleotides were designed as described therein (FLAGTrbl^{D/NLK}:

CGGGATTATCCTCAGGA**AA**CCTCAAGCTCAAGCG and

CGCTTGAGCTTGAGGTT**CC**TGAGGATAATCCCG; UAS-FLAGTrbl^{FLCR/A}:

GGGAGCAGTTCCTCTGC**GC**TATTGTAAACGAACCGTTG and

CAAGCGTTCGTTTACAATAG**CG**CAGAGGAACTGCTCCC; UAS-FLAGTrbl^{SLE/G}:

GCAGTATGAATCACTGG**G**AGGCTCAATGATCCTCG and

CGAGGATCATTGAGCCT**CCC**AGTGATTCATACTGC). Site-directed mutations

(shown in bold) were confirmed by DNA sequencing. FLAGTrbl^{SLE/G} was constructed slightly differently by adding flanking *attB1* and *attB2* sites (using the oligonucleotides

GGGGACAAGTTTGTACAAAAAAGCAGGCTTCATGGATTACAAGGATGACGAC
GATAAG and

GGGGACCACTTTGTACAAGAAAGCTGGGTCTCAGCCCATGTCCACATCCGTAT
C; *attB1* and *attB2* sequences in bold), using recombination to insert the fragment into the GATEWAY donor vector pDONR-21 and then into the destination vector pUASgattB (Bischof and Basler 2008). Embryo injections were performed as a fee-for-service (Genetic Services, Inc., Cambridge, MA) and transgenic lines established were confirmed for the presence of the WT or mutant transgene by sequencing of PCR product.

Yeast two-hybrid interaction screen

The ProQuest Two-Hybrid System (Invitrogen) was used to perform yeast two-hybrid interaction tests. Plasmid DNA transformations of *Saccharomyces cerevisiae* strain MaV203 were performed as outlined in the kit manual and grown on SC media lacking both tryptophan and leucine to confirm the presence of both the bait and prey plasmids. The cells were then transferred to a series of plates to test for interactions: SC-Leu-Trp-His, SC-Leu-Trp-His+3AT (at various concentrations). A quantitative β -galactosidase assay was performed on transformants grown in SC-Leu-Trp broth using CPRG as a substrate.

To construct bait and prey plasmids FLAGTrbl, FLAGTrbl^{D/NLK}, and Slbo cDNAs were amplified using PCR to add flanking *attB1* and *attB2* sites. Forward

and reverse primers for FLAGTrbl and FLAGTrbl^{D/NLK} were, respectively: 5'-

GGGGACAAGTTTGTACAAAAAGCAGGCTTCATGGATTACAAGGATGACGAC

GATAAG -3', 5'-

GGGGACCACTTTGTACAAGAAAGCTGGGTCTCAGCCCATGTCCACATCCGTAT

C -3'; and for SLBO, respectively, 5'-

GGGGACAAGTTTGTACAAAAAGCAGGCTTCATGCTGAACATGGAGTCGCCG

CAG-3', 5'-

GGGGACCACTTTGTACAAGAAAGCTGGGTCTACAGCGAGTGTTTCGTTGGTG

TTG-3' (*attB1* and *attB2* sequences in bold). The PCR product was cloned into the

donor vector pDONR-21 and then into either pDEST32 (bait vector) or pDEST22

(prey vector). All constructs were confirmed by DNA sequencing.

Construction of pDEST32 UAS-FLAGTrblCOP-1

pDEST32 UAS-FLAGTrblCOP-1 mutant was generated from previously constructed pDEST32 UAS-FLAGTrbl using the QuikChange Kit and the following oligonucleotides: FLAGTrblCOP-1: 5'-

GATGGATGATGACGAG**GC**AGGACTCTGTCCCTTGG-3' and 5'-

CCAAGGGACAGAGTCCT**GC**CCTCGTCATCATCCATC-3' (mutated nucleotides in

bold). Site-directed mutations were confirmed by DNA sequencing.

Results

Trbl is a nuclear protein expressed in non-migratory follicle cells whose expression is

repressed by Slbo (C/EBP)

To examine the endogenous expression of Trbl in the egg chamber, I took two approaches. First, I evaluated available *trbl* enhancer trap reporter genes and

found one (*trbl*^{P{GawB}NP3530}) that expressed in the FC with high levels in the main body FC and at low levels in the centripetal FC (CMFC) and border cells (BC), two cell types that express high levels of Slbo protein (Figure. 2.1B). To examine directly Trbl protein levels in this tissue, I used antisera to Trbl protein and detected a protein that migrates at ~65kDa (Figure. 2.2) with widespread nuclear expression in the somatic follicle cells and germ line nurse cells from stages 2-10 of oogenesis (Figure 2.1C-F). Counterstaining for a *slbo-lacZ* reporter gene (*slbo*⁰¹³¹⁰) revealed that, like expression of *trbl*^{P{GawB}NP3530}, Trbl protein levels are low in both the border cells and in the leading edge CMFC (Figure. 2.1C,D). At later stages the subcellular accumulation of Trbl in the main body FC is dynamic: I noticed strong nuclear accumulation at stage 10 (Figure. 2.1E) that decreases to low levels in the cytoplasm by stage 12 (Figure. 2.1F).

Closer examination revealed that Trbl expression is high at the beginning of BC delamination (stage 7, Figure 2.2A and stage 8, Figure 2.2B) but decreases markedly when the border cells arrive at the nurse cell/oocyte boundary (stage 10B, Figure 2.2C,E). Based on the complementary expression of Trbl and Slbo during BC and CMFC migration, I tested the interaction between these genes in these two tissues in several ways. First I examined the effect of *slbo* mutations and Slbo misexpression on Trbl levels, measured with Trbl antisera. In the *slbo* mutant background (*slbo*⁰¹³¹⁰/*slbo*⁰¹³¹⁰), Trbl expression increased in the border cells and centripetal FC (Figure 2.2D) both at stages 9 and 10B (Figure 2.2F), indicating that *slbo* is required for Trbl repression throughout BC migration. In contrast, Flp-out

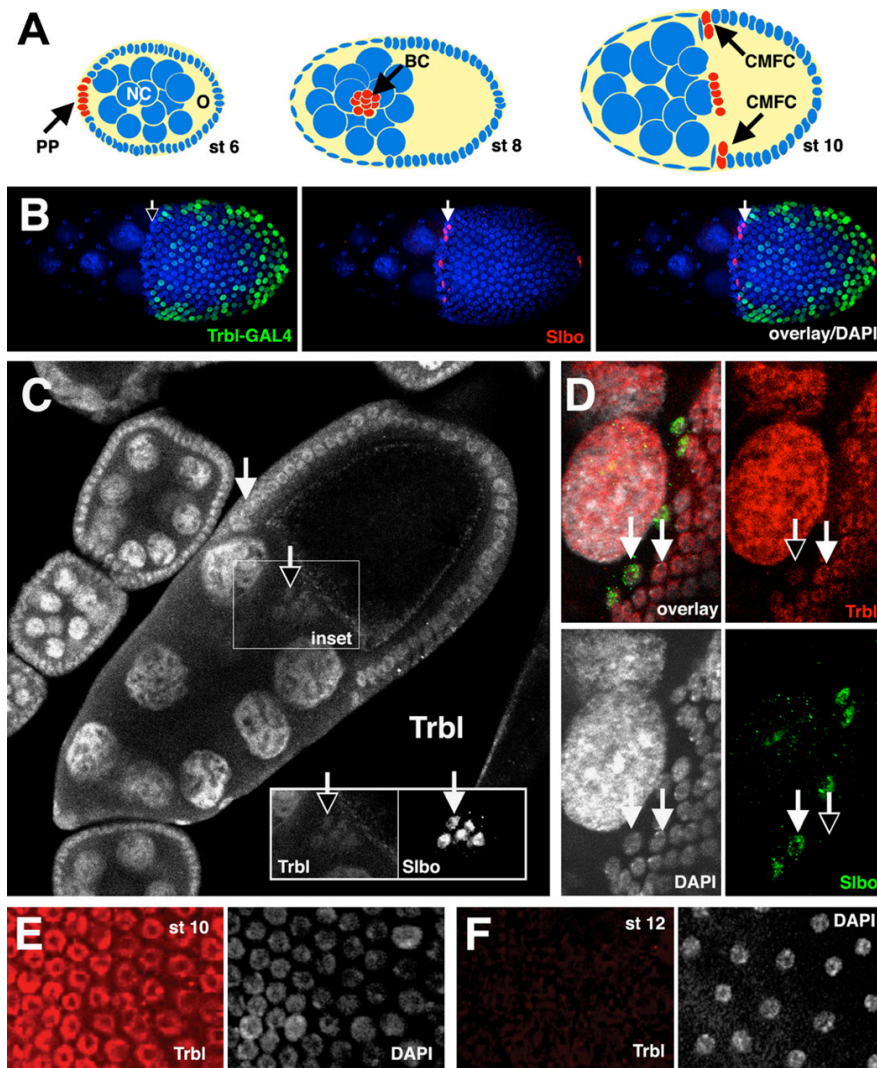


Figure.2.1 *Trbl* accumulates in the nuclei of non-migratory FC groups

(A) Outline of migratory cell types during oogenesis. At stage 9, posterior pole FC (PP) delaminate to form the border cell cluster (BC) which migrate through the nurse cells (NC) to reach the oocyte (O) at stage 10, when the centripetal FC (CMFC) migrate between the NC/O boundary. (B) *Trbl-Gal4* enhancer trap (*trbl*^{P{GawB}NP3530}) expresses UAS-GFP (green) in the main body FC with low levels in the centripetal FC (empty arrow) that express *Slbo* (red) (C) At stage 10B, *Trbl* accumulates at high levels in the nuclei of the main body FC. Lower levels of *Trbl* occur in the border cells (black arrow) at stage 10B. Inset contrasts high *Slbo* protein levels in the border cells (white arrow, right) with low levels of *Trbl* (left, empty arrow) (D) Low levels of *Trbl* (red) accumulate in the centripetal FC that express *Slbo* (green). DAPI reveals the location of all nuclei in the cell sheet (E) At stage 10, *Trbl* levels are high and nuclear (F) At stage 12 *Trbl* levels are low and non-nuclear.

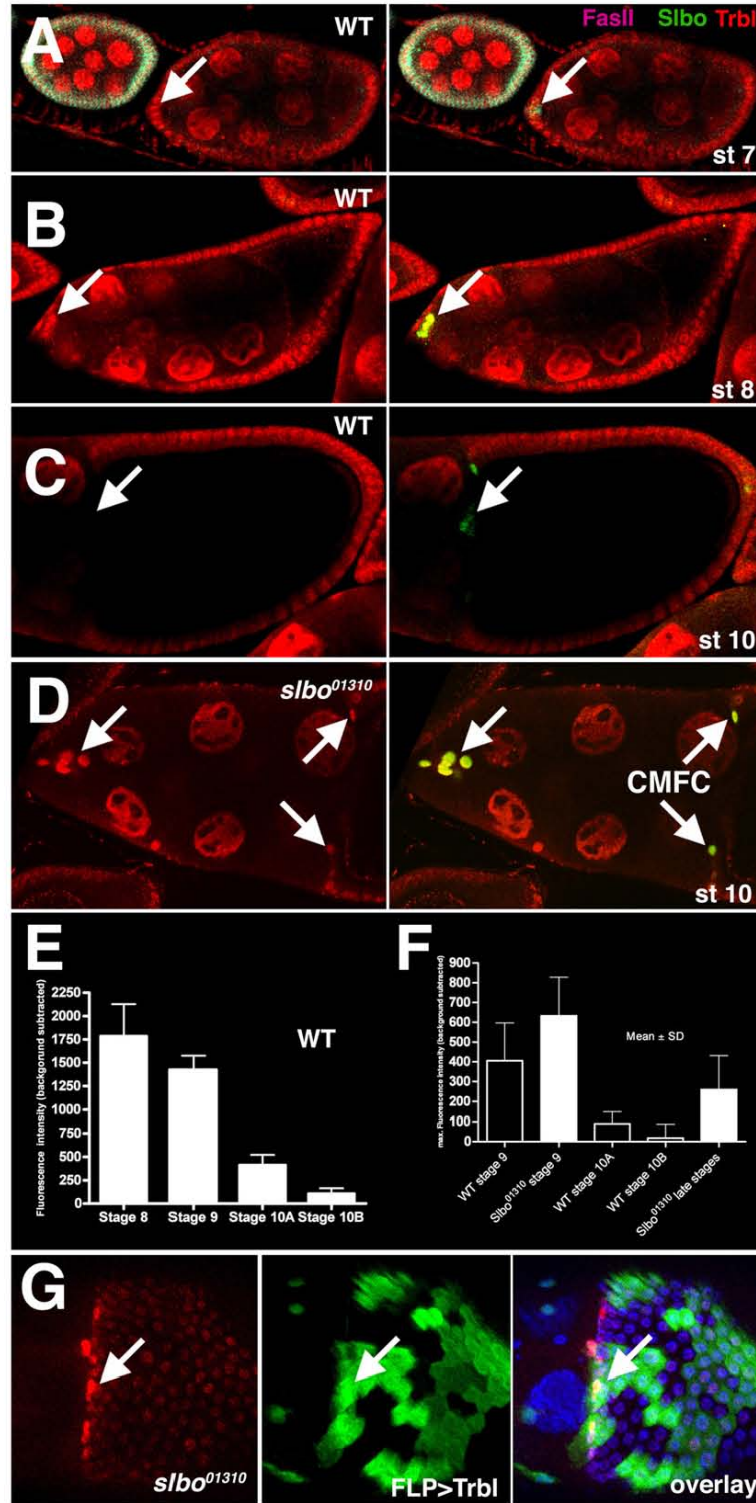
misexpression of *Slbo* has no effect on *Trbl* expression in the main body FC (Figure 2.3A, B). It has been shown that mouse Trib3 protein acts as a transcriptional cofactor to repress transcription (Ohoka et al., 2005; Takahashi et al., 2008), so we sought to test if *Trbl* misexpression could repress *slbo-lacZ*, an in vivo reporter of *slbo* transcription. As shown in Figure 2.2G, Flp-out *Actin-Gal4* misexpression of *Trbl* in the centripetal FC was insufficient to reduce *slbo* reporter gene expression. Thus *Slbo* is necessary but not sufficient to repress *Trbl* expression in the egg chamber while *Trbl* is neither necessary nor sufficient to repress *slbo* transcription.

Trbl is necessary to direct *Slbo* turnover

In flies and mouse cell lines, Trib family members are necessary to direct turnover of C/EBP proteins (Keeshan et al., 2010; Rorth et al., 2000). Because existing *trbl* alleles are not protein null and may retain *Trbl* activity, we sought to create a deletion in *trbl* coding sequence. To accomplish this, we used a regimen of hsFLP induction to sponsor FRT-mediated recombination in males transheterozygous for two FRT-bearing P-elements, $\{PXP\}trbl^{d07751}$ and $\{PXP\}trbl^{d03251}$ inserted at sites flanking the *trbl* gene and marked by a single mini-white marker (Figure 2.4A). Recombinants that deleted the *trbl* gene could be detected fortuitously by the presence of two mini-white markers in the hybrid transposon, and two resulting *trbl* deletions (designated *trbl*^{D13} and *trbl*^{D3}) were confirmed by PCR to remove sequences (from proximal to distal, respectively) 498,698 base pairs (bp) downstream from the 3' end of the gene to 28 bp downstream from the start site of transcription.

Figure. 2.2 *slbo* and *trbl* have opposing effects in migratory FC groups

(A). Prior to delamination at stage 8, *Trbl* (red) accumulates at high levels in the border cells nuclei (arrow, counterstained with *Fas2* in magenta) (B). At stage 9, *Trbl* levels remain high as border cell migration begins (C). By stage 10, only low levels of *Trbl* occur in the border cells at the nurse cell/oocyte boundary (arrow) (D). In the *slbo* mutant *slbo*⁰¹³¹⁰, *Trbl* levels remain high at stage 10 in the border cells (anterior arrow) and in the centripetal migrating FC (CMFC) (E). *Trbl* expression in WT egg chambers, measured as fluorescence intensity (see materials and methods) showing the decrease in *Trbl* expression as BC migration progresses from stages 8-10B. Error bars represent mean ± SD. The difference between groups is statistically significant (P value for one way ANOVA test <0.0001, Student's T test between each group < 0.05) (F). *Trbl* expression, measured as fluorescence intensity, in WT egg chambers (genotype *slbo*⁰¹³¹⁰/*CyO*) is lower when compared to mutant egg chambers (genotype *slbo*⁰¹³¹⁰/*slbo*⁰¹³¹⁰) both at stage 9 and stage 10A/B. Error bars represent mean ± SD. The difference between groups is statistically significant (P value for one way ANOVA test <0.0001, Student's T test value between each group < 0.5, except WT stage 10A and 10B, where the value is >0.05) (G). Misexpression of *UAS-Trbl* using the *Flp-out* actin driver can be detected in FC clones located in the centripetal FC (arrow) by GFP expression (green, arrow center panel) and have no effect on levels of *slbo-lacZ* (red). Genotype: *hsFLP1; slbo*⁰¹³¹⁰/*P{w+(mC)=AyGal4}25 P{w+(mC)=UAS-GFP.S65T}T2; UAS-Trbl*. Failure to repress *slbo-lacZ* was observed in 10/10 clones located in the centripetal FC.



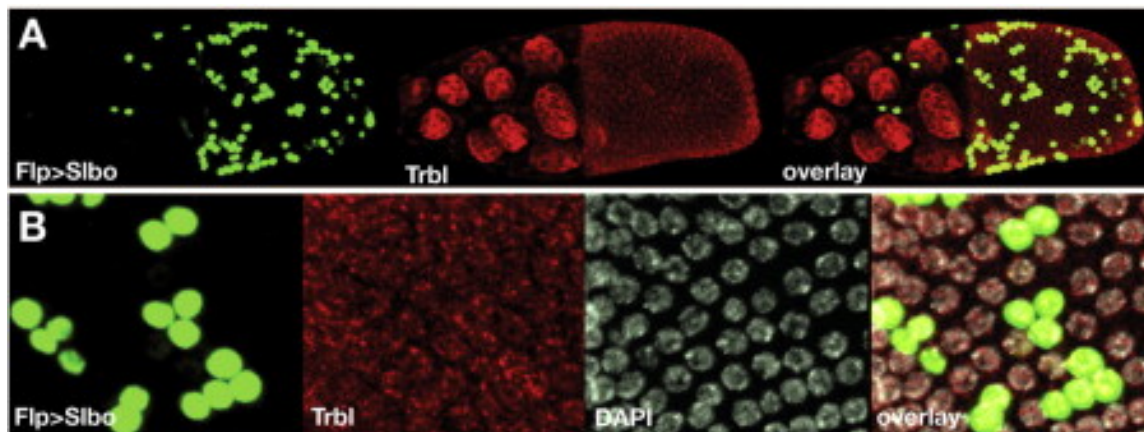


Figure 2.3 Slbo is not sufficient to repress Trbl expression

(A) Flp-out misexpression of Slbo in the main body FC, detected by UAS-GFP expression (green) had no effect on Trbl levels (red). Genotype in A and B: *hsFLP1; UAS-Slbo/P{w+(mC)=AyGal4}25 P{w+(mC)=UAS-GFP.S65T}T2*. (B) Another example of a Flp-out *slbo* clone at higher magnification shows no effect on Trbl levels.

The *trbl*^{D13} allele recombined onto an FRT80 chromosome showed reduced antisera staining in main body FC clones (Figure 2.4B) similar to reduced antisera staining seen in clones of *trbl*^{EP1119} (Figure 2.5A); indicating that *trbl*^{D13} and *trbl*^{D3} are bonafide *trbl* deletion alleles.

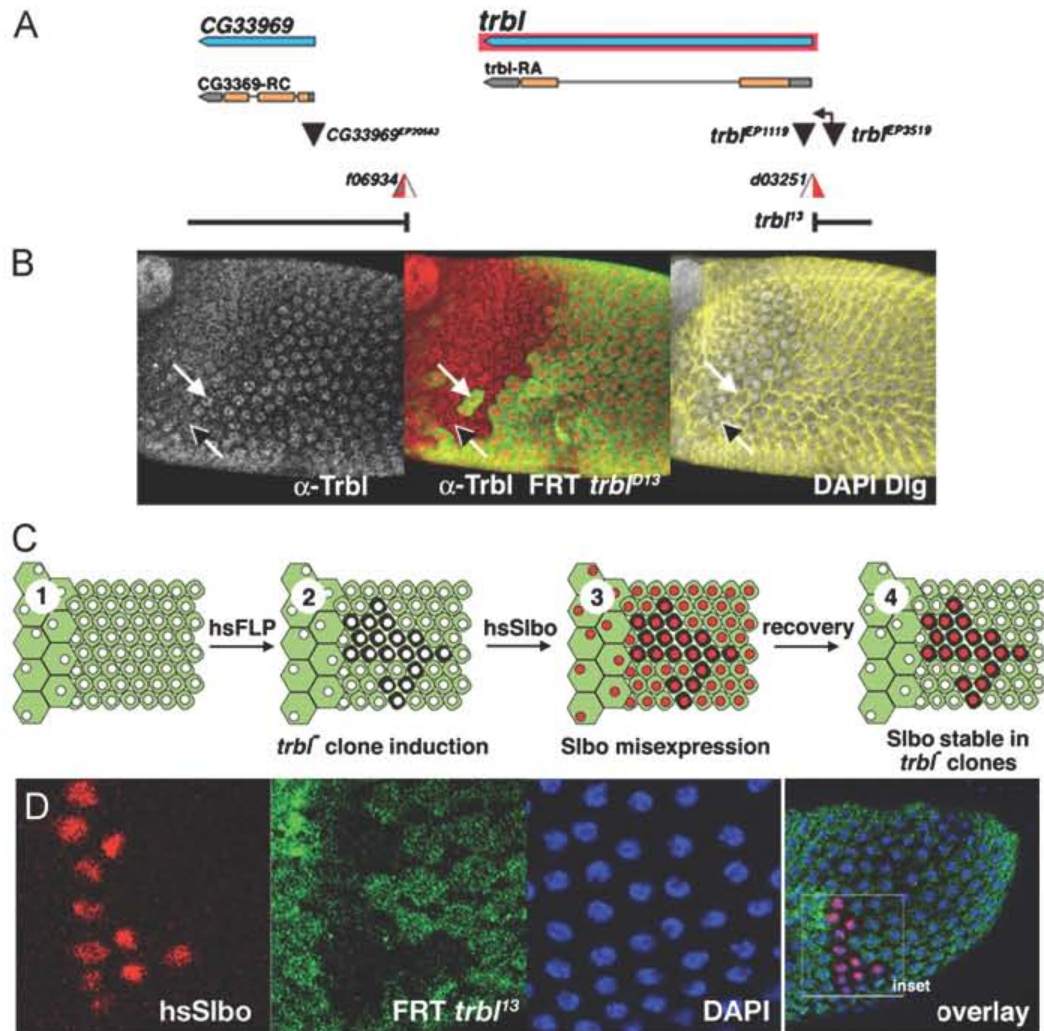
We used the *trbl*^{D13}FRT80 chromosome to test the requirement for Trbl in Slbo turnover in the main body FC (where Trbl levels are high) using a scheme outlined in Figure 2.4C. We produced FLP-FRT *trbl*^{D13} mutant clones in females bearing a hs-Slbo inducible transgene (genotype *hsFLP; hs-Slbo; UbiGFPFRT80/trbl*^{D13} FRT80) and three hours following recovery from a 30 minutes heat shock to induce ubiquitous *slbo* expression, we used Slbo antisera (Szafranski and Goode 2004) to compare Slbo turnover in WT cells to turnover in *trbl*^{D13} mutant clones. As shown in Figure 2.4D, Slbo levels are noticeably more stable in main body FC that are mutant for *trbl*^{D13}, indicating that Trbl is necessary for Slbo turnover in this tissue.

In the border cells, Slbo and Trbl have opposing effects on each other's expressions, so we examined their genetic interactions during the progress of BC migration (Table 1). While strong allelic combinations (*trbl*^{EP3519}/*trbl*^{D13}) led to ¹

¹ Some portion of this page is left blank intentionally to fit a table on page 30.

Figure. 2.4 Construction of a *trbl* null allele

(A). Map of the *trbl* gene region showing the location of Trbl (blue) and adjacent gene CG33969 (genes at top and respective transcripts below, with introns indicated as thin lines and coding regions as orange boxes). Insertion sites of alleles used are shown as black, inverted triangles (*CG33969*^{EP20583}, *trbl*^{EP119}, *trbl*^{EP3519}). Below these, the insertion sites of FRT-bearing transposons *P{XP}trbl*^{d07751} and *P{XP}trbl*^{d03251} are shown; each transposon contains the mini-white gene (represented by red half triangle) and the hybrid element (*trbl*^{D13}) deletes the intervening region (20888086-20394680 of chromosome 3L) and includes both mini-white genes (conceptually, a fusion of the two red half triangles). (B). Mutant clones of *trbl*^{D13} (absence of GFP, center panel) show reduction in nuclear staining of Trbl using the Trbl antisera (red and black and white, left panel). As well, these clones have uncharacterized defects in cell size and Dlg localization (right panel). White arrows indicate the location of two wild type cells positive for GFP (center panel) that express strong levels of nuclear Trbl (left panel); adjacent mutant cells (filled arrows) show (1) low levels of Trbl (left panel), (2) nuclear size defects (DAPI, right panel) and (3) reduced expression of Dlg (yellow, right panel). (C). Scheme for examining Slbo turnover in *trbl* mutant cells. Panel 1 shows the FC epithelium in a female of the genotype *hsFLP1; hs-Slbo; P(Ubi-GFP(S65T)nls)3L P(neoFRT)80B/ trbl*^{D13} *P(neoFRT)80B*. After FLP induction, *trbl*^{D13} clones can be detected by the absence of GFP, in panel 2. After 30 min heat shock induction of hs-Slbo, high levels of nuclear Slbo can be detected throughout the FC epithelium (red) in panel 3. Three hours after recovery, Slbo turnover in *trbl*^{D13} mutant cells (black) can be compared to WT cells (green) in panel 4. (D). In stage 10 egg chambers, *trbl*^{D13} mutant cells (no GFP) show higher levels of Slbo, three hours after hs-Slbo induction. This was at 3 hours after heat shock recovery in 28/32 clones detected in the main body FC.



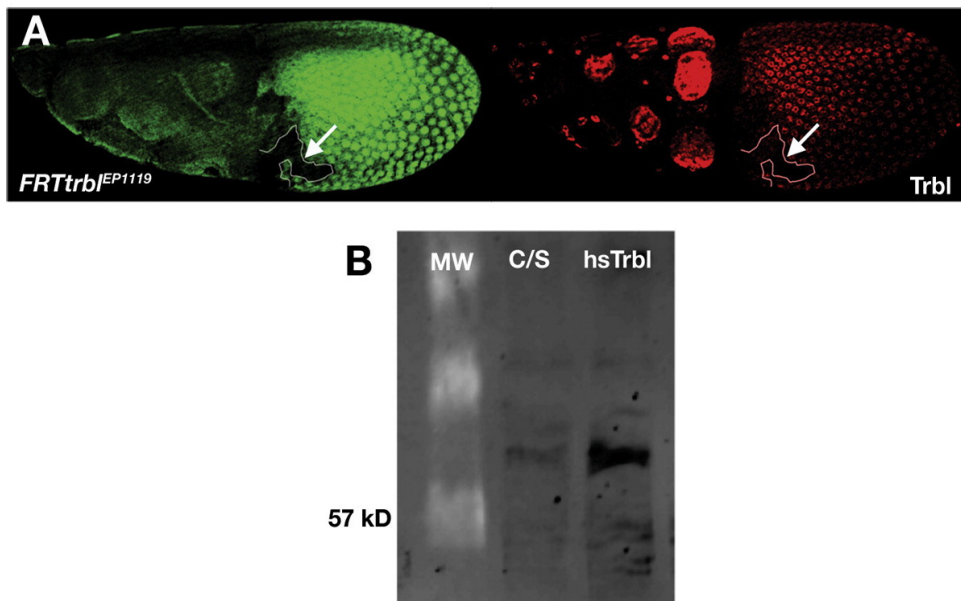


Figure.2.5 Characterization of Trbl antisera

(A) *FRTtrbl*^{EP1119} clones (no GFP, left panel) lead to reduction in Trbl antisera staining (arrow, left panel). (B) Western blotting of protein extracts prepared from ovaries detects a 65 kDa protein (MW=molecular weight markers) in WT (C/S) whose levels increase following heat shock Trbl misexpression in *hsGal4>UAS-Trbl* animals (hsTrbl).

rudimentary, undeveloped ovaries that lacked late stage egg chambers (Table 1), RNAi knockdown of Trbl activity specifically at late stages in the border cells (*Slbo2.6Gal4;UAS-Trbl IR²²¹¹⁴*; Table 1) partially blocked BC migration. Weaker mutant allelic combinations (*trbl^{EP1119}/trbl^{EP1119}*) had no effect on BC migration but did effectively suppress defects seen in *slbo⁰¹³¹⁰* females (Montell et al., 1992), resulting in an increased frequency of partial and complete BC migration (Table 1). We conclude that opposing activities of Trbl and Slbo contribute to the progress of BC migration, which is consistent with previous work (Rorth et al., 2000).

Trbl kinase domain is required for border cell migration

BC migration is blocked by Trbl misexpression (Rorth et al., 2000), so we used this sensitive migration phenotype to conduct a structure-function analysis of Trbl. We used site-directed mutagenesis to make three mutations in the Trbl kinase domain (Figure 2.6A): (1) FLCR/A was designed to disrupt a divergent sequence located in a region in conventional kinases (VAIK) predicted to bind ATP; (2) D/NLK was designed to disrupt the conserved DLK motif in the catalytic domain of the kinase region; and (3) SLE/G was designed to disrupt a conserved SLE motif predicted to coordinate Mg²⁺. Each of these mutations was made in a Flag-tagged Trbl transgene under UAS control, inserted into an attP vector (Bischof and Basler 2008) and injected to produce transgenic animals with insertions recombined into the second chromosome-landing site (attP40; 25C7 on 2L) or third chromosome-landing site (attP2; 68A4 on 3L). In this way, we could compare misexpression of mutant and WT transgenes while minimizing position effects.

Table 1 genetic interaction between *trbl* and *slbo* during BC migration.

Genotype	No Migration	Partial Migration	Full Migration
<i>Slbo2.6Gal4>UAS-Trbl RNAi</i> ²²¹¹⁴	5%	42%	53% (n=38)
<i>Slbo2.6Gal4>UAS-Trbl RNAi</i> ²²¹¹³	0%	2%	98% (n=54)
<i>trbl</i> ^{EP1119} / <i>trbl</i> ^{EP1119}	0%	1.7%	98.3% (n=291)
<i>trbl</i> ^{EP1119} / <i>trbl</i> ^{D13}	0%	0%	100% (n=145)
<i>trbl</i> ^{EP3519} / <i>trbl</i> ^{D13}	Reduced ovaries		
<i>slbo</i> ⁰¹³¹⁰ / <i>slbo</i> ⁰¹³¹⁰ ; <i>trbl</i> ^{EP1119} /+	58.3%	37.4%	4.2% (n=350)
<i>slbo</i> ⁰¹³¹⁰ / <i>slbo</i> ⁰¹³¹⁰ ; <i>trbl</i> ^{EP1119} / <i>trbl</i> ^{EP1119}	17.7%	61.5%	20.8% (n=96)

We tested the effect of misexpression of each transgene in the border cells using the *Slbo2.6Gal4* driver (Figure 2.6B), and the results are summarized in Figure 2.6 and Table 3. Following misexpression of Flag-tagged UAS-Trbl inserted at either attP2 on the third chromosome or attP40 on the second, we observed a significant block in BC migration (Table 2) that was comparable to the block caused

by misexpression of previously described transgenes UAS-Trbl or EP3519 (Rorth et al., 2000), which were tested in parallel. For each transgene, the block observed was more significant at 30°C, consistent with the temperature sensitivity of Gal4 activity.

As shown in Figure 2.6B-E and summarized in Table 2, misexpression of UAS-FlagTrbl transgenes bearing the FLCR/A (Figure 4C) or SLE/G mutation (Figure 2.6E) resulted in a strong block to BC migration, similar to WT UAS-FlagTrbl (Table 2). Thus these two kinase region mutations do not affect Trbl activity. In contrast, misexpression of the D/NLK mutation either at attP40 (Figure 2.6D) failed to block BC migration compared to WT UAS-FlagTrbl inserted at the respective landing site (Table 2).

Trbl kinase domain is required for Slbo binding and turnover

Previously, Trbl has been shown to bind Slbo in a pull down assay in S2 cells (Rorth et al., 2000), and we sought to test the strength of this interaction using a sensitive yeast two-hybrid assay. As shown in Figure 2.7, Trbl in a bait vector effectively interacts with Slbo in a prey vector to grow on histidine drop out plates in the presence of increasing amounts of 3-amino-1,2,4-triazol (3-AT). Surprisingly, Trbl in the bait vector is also able to interact with Trbl in the prey vector (Figure 2.7), but not as strongly as with Slbo in the prey vector (25mM 3-AT as compared to 100mM 3-AT, respectively). A β -galactosidase reporter gene assay confirmed that the relative strength of Trbl-Slbo interaction is 1400-fold greater than the Trbl-Trbl interaction (Table 3).

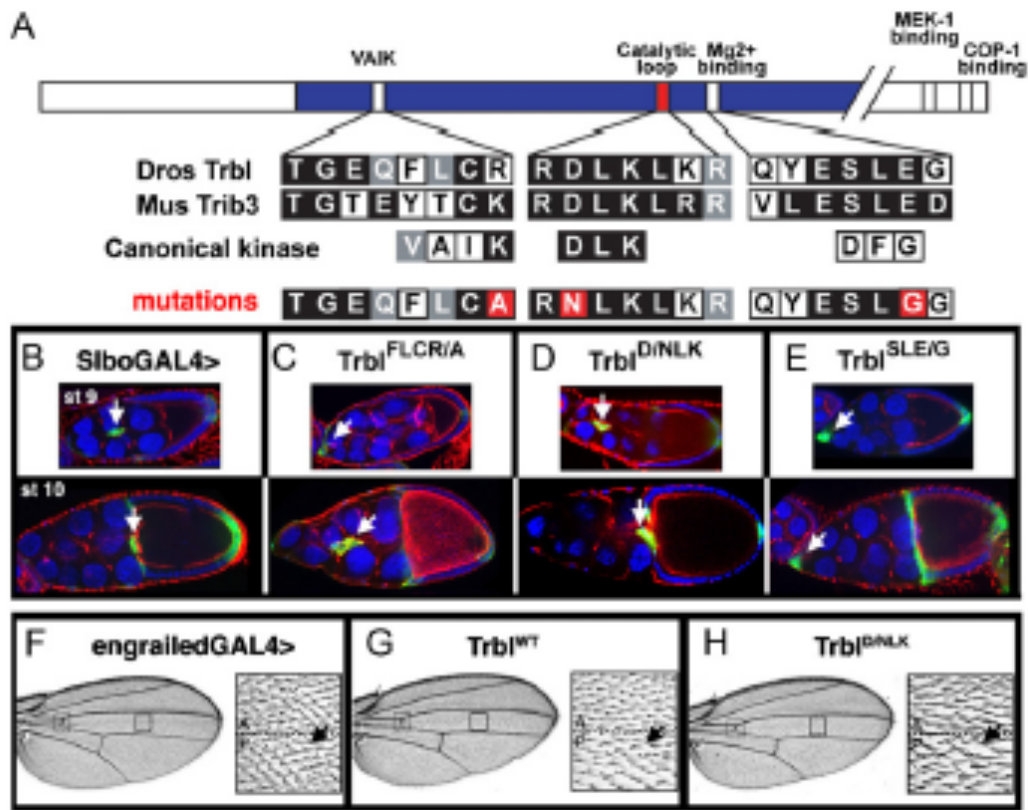


Figure. 2.6 Trbl kinase domain is required to block BC migration

(A). Map of the Trbl protein coding region shows the conserved central kinase region (blue) containing a degenerate VAIK motif, a conserved catalytic loop (red) and a putative Mg²⁺ binding domain. The *Drosophila* and mouse sequence is aligned below this and each of three site-specific mutations produced (red) in three respective motifs are show. (B-E). Panels show the effect of misexpressing GFP alone and each mutant Trbl protein. (B). *Slbo2.6Gal4*, *UAS-GFP* reveals that WT border cell migration shown at stage 9 and 10 progresses from the anterior of the egg chamber at stage 9 to a position at the border between nurse cells and oocyte by stage 10 (white arrow). (C-E). *Slbo2.6Gal4*> misexpression of the mutants Trbl^{FLCR/A} (C) or Trbl^{SLE/G} (E) resulted in a strong block to BC migration, similar to WT Trbl (not shown). In contrast, misexpression of D/NLK (D) failed to block BC migration. (F-H). Misexpression of WT Trbl in the posterior wing compartment (G) leads to cross vein defects (box) and increase in cell size (inset), when compared to the *engrailedGal4* driver alone (F). A similar cross vein defect and increase in cell size can be seen by misexpression of the D/NLK mutant in the posterior wing (H), suggests that it retains activity in this assay.

Table 2 Misexpression assay of UAS-Trbl, UAS-Trbl mutant transgenes and UAS-Trbl RNAi.

	No migration (%)	Partial migration (%)	Full migration (%)
<i>Slbo2.6Gal4</i>	0	0	100(n=110)
<i>Slbo2.6Gal4; UAS-FlagTrbl (III)</i>	57	28	15 (n=157)
<i>Slbo2.6Gal4; UAS-FlagTrbl^{D/NLK} (III)</i>	0	4	96 (n=140)
<i>Slbo2.6Gal4/UAS-FlagTrbl (II)</i>	24	41	35 (n=100)
<i>Slbo2.6Gal4/UAS-FlagTrbl^{D/NLK} (II)</i>	0	3	97 (n=59)
<i>Slbo2.6Gal4/UAS-FlagTrbl^{FLCR/A} (II)</i>	58	12	31 (n=121)
<i>Slbo2.6Gal4/UAS-FlagTrbl^{SLE/G} (II)</i>	70	16	14 (n=120)
<i>Slbo2.6Gal4; UAS-Trbl (Rorth)</i>	28	30	42 (n=71)
<i>Slbo2.6Gal4; UAS-Trbl^{EP3519}</i>	78	12	10 (n=51)

Because the D/NLK mutation abrogates Trbl function in the border cells, we used site-directed mutagenesis to make the same D/NLK mutation (Figure 2.6) in the central catalytic domain of the Trbl bait vector. When tested on histidine drop out plates in a two-hybrid assay, the D/NLK mutation exhibited significantly weaker interactions with both Slbo prey and Trbl prey (Figure 2.7). In the quantitative β -gal reporter gene assay, the D/NLK mutant resulted in a 16.5-fold reduction in Trbl binding while the very strong Slbo interaction was reduced to undetectable levels. We designed a second mutation to disrupt the C-terminal COP1 domain (Figure 2.6)

of the Trbl bait, a motif deemed critical for interaction with the proteasome. The COP1 mutant in the Trbl prey resulted in no reduction in binding to either prey Slbo or prey Trbl in both the plate growth and quantitative β -gal reporter gene assays (Table 3). Thus Trbl-Trbl and Trbl-Slbo interactions require an intact catalytic domain but not a COP1 binding site.

We compared the ability of WT Trbl and the D/NLK mutant to direct Slbo turnover in vivo in two ways. First, we misexpressed both transgenes in the border cells using the *Slbo2.6Gal4* driver. As shown in Figure 2.8A, WT Trbl misexpression led to reduced Slbo protein levels in the border cells, whereas *slbo-lacZ* reporter gene expression remained high, confirming previous observations that the transcription of *slbo* is unchanged in this tissue (Rorth et al., 2000). In contrast, Slbo protein levels were unaffected by misexpression of D/NLK (Figure 6B), consistent with the failure of this mutation to bind Slbo (Figure 2.7) and block BC migration (Figure 2.6C).

In a second approach, we misexpressed Trbl or D/NLK in the main body FC using a FLP-out driver in females bearing an inducible *hsSlbo* transgene (genotype: *hsFLP; hs-Slbo P{w+(mC) =AyGal4} 25 Pw+(mc)=UAS-GFP.S65T} T2/CyO; UAS-FlagTrbl*; scheme outlined in Figure 2.8C). Following 2.5-3 hours recovery from heat shock Slbo misexpression, clones misexpressing Trbl in the main body FC were detected by expression of UAS-GFP and revealed increased Slbo turnover compared to adjacent non-GFP, WT cells (Figure 2.8D). In contrast, GFP-positive clones misexpressing the D/NLK transgene resulted in no increase in Slbo turnover compared to adjacent WT cells (Figure 2.8E). Thus we interpret the strong

Table 3 Yeast Two hybrid interaction between Trbl and Trbl mutations with Slbo

Bait	Prey	-L-W-H	-L-W-H	-L-W-H	-L-W-H	-L-W-H	β -gal assay
		+10mM 3AT	+25mM 3AT	+50mM 3AT	+75mM 3AT	+100mM 3AT	
Trbl	Slbo	++	++	++	++	++	95
Slbo	Trbl	++	++	++	++	++	140
Trbl ^{FLCR/A}	Slbo	+	+	-	-	-	0.02
Trbl ^{D/NLK}	Slbo	+	-	-	-	-	0.03
Trbl ^{SLE/G}	Slbo	++	++	++	++	++	84
Trbl ^{MEK1}	Slbo	+	+	-	-	-	0.35
Trbl ^{COP1}	Slbo	++	++	++	++	+	90
Strong Control		++	++	++	++	++	18.4
Weak Control		++	++	+	+	+	0.40
Negative Control		+	-	-	-	-	0.013
No Plasmids		-	-	-	-	-	0

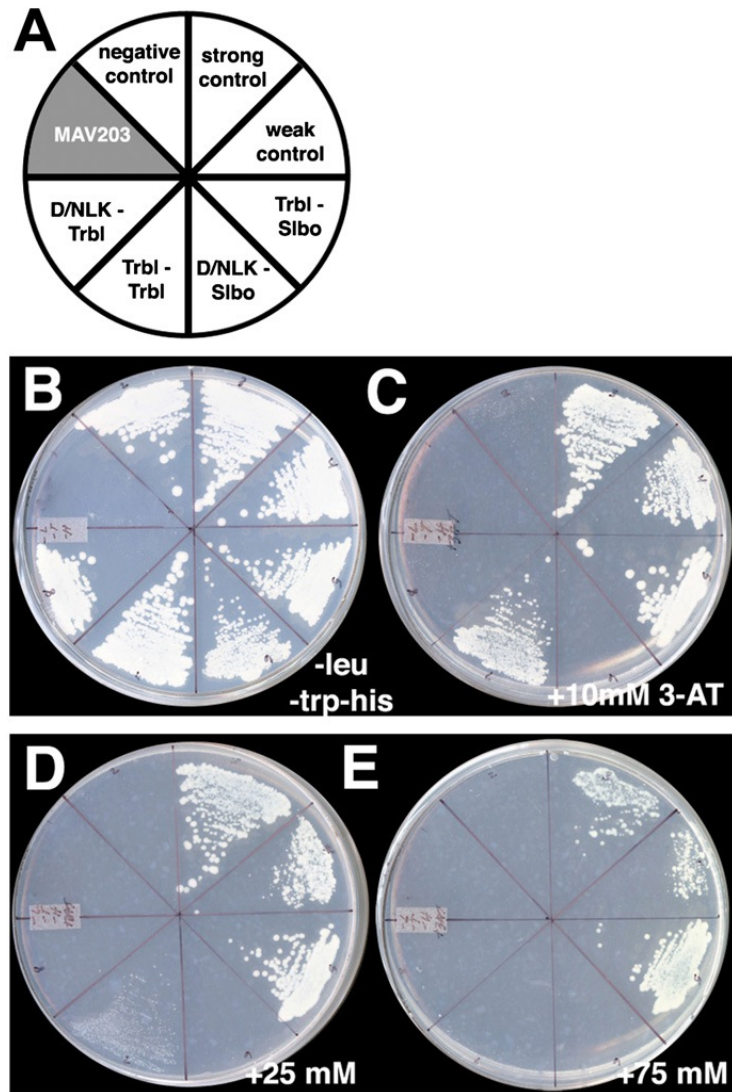


Figure. 2.7 Trbl kinase domain is required for Slbo binding in vitro (Y2H)

(A). Yeast strains harboring bait/prey combinations are spread on sectors of dropout YPD plates indicated. (B-E). Increasing amounts of 3-amino-1, 2,4-triazol (3-AT) reveal the following order in strength of interactions: Slbo-Trbl>Trbl-Trbl> Slbo-D/NLK \approx Trbl-D/NLK.

nuclear Slbo accumulation in D/NLK clone shown in (Figure 2.8D) as due to their larger size rather than due to an increase in Slbo stability. We conclude that the D/NLK catalytic motif mutation that disrupts Slbo binding in a yeast two-hybrid assay also abolishes the ability of Trbl to direct Slbo turnover in vivo.

Discussion

Mammalian Trib proteins have diverse functions including transcriptional co-activators and repressors in the nucleus and MAP kinase kinase inhibitors and proteasome adaptors in the cytoplasm (reviewed in Dobens and Bouyain, 2012). Tribs bind and direct the degradation of key regulatory proteins, in particular members of the C/EBP family- notably (1) C/EBP α , which is degraded by Trib1 to promote the formation of acute myelogenous leukemia (AML) tumors and by Trib2 during myeloid differentiation (Keeshan et al., 2006) and (2) C/EBP β , which is degraded by Trib2 during differentiation of 3T3-L1 preadipocytes (Naiki et al., 2007). As well, C/EBP β levels increase in Trib1 knockout mice (Keeshan et al., 2008; Yamamoto et al., 2007).

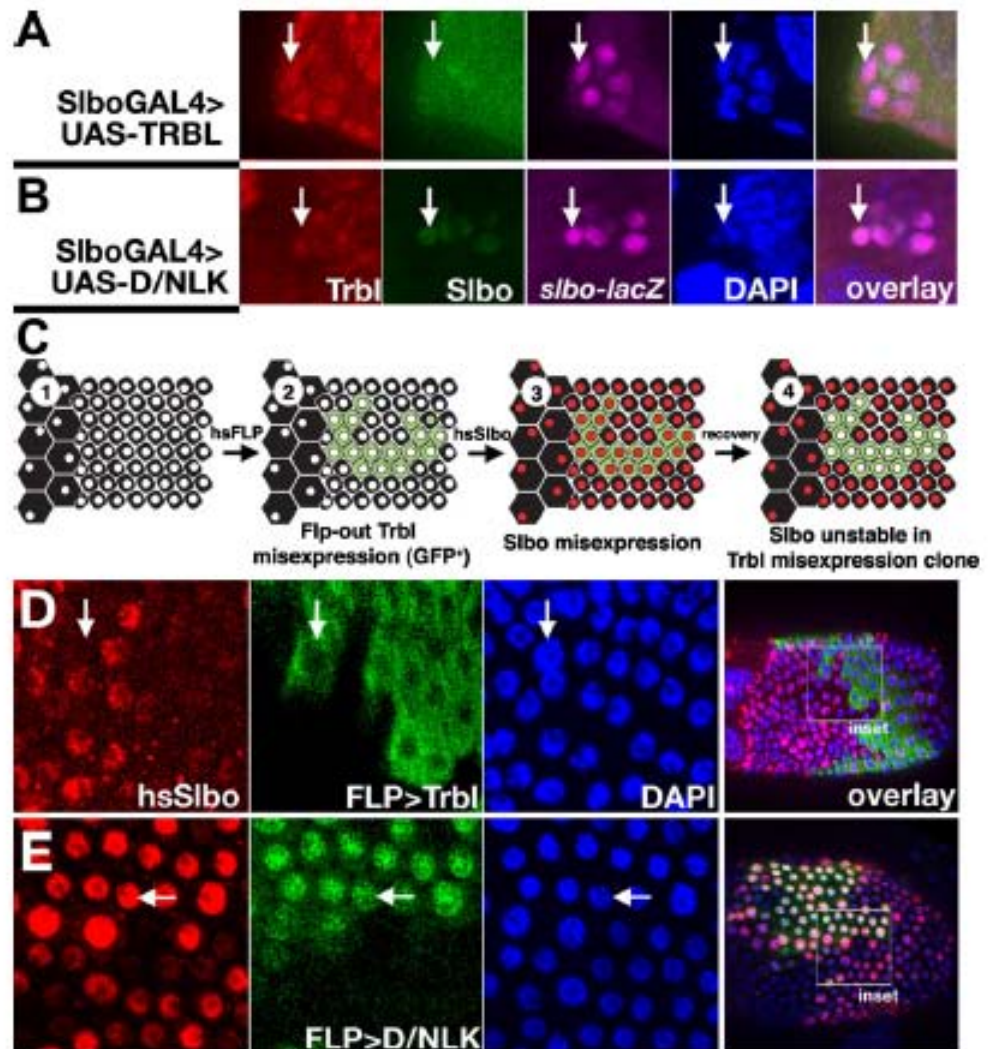
For Trib2, it has been demonstrated recently that a point mutation in the DLK catalytic loop motif disrupts its ability to direct turnover of C/EBP β and promote acute myelogenous leukemia (Keeshan et al., 2010), and here we demonstrate that the same DLK/R mutation in fly Trbl compromises its ability to direct Slbo turnover and block BC migration. We also show that an intact DLK catalytic motif is required for Trbl interactions both with Slbo and with Trbl, itself. These data support the notion that the conserved catalytic domain is critical for Trbl function.

The D/NLK Trbl mutant surprisingly retains WT activity when misexpressed in the posterior wing compartment, resulting in larger cells as measured by more widely spaced bristles when compared to the anterior compartment. We note that a similar mutation in Trbl located just C-terminal to DLK (DLKLK/R) also retains WT activity to block cell proliferation when injected into the blastoderm epithelium (Figure 7 of Grosshans and Wieschaus, 2000). Because WT Trbl is thought to block cell division by directing String/cdc25 turnover, our data suggest another domain outside the Trbl catalytic loop must be required for String degradation.

Several observations are worth noting regarding the *trbl* protein null allele and specific antisera that we have analyzed. The *trbl*^{D13} deletion allele described here (Figure 2.3A) is a stronger allele than those used previously (Rorth et al., 2000), but still yields a few escaper adults in combination with a deficiency of the locus (Table 1). Though *trbl* is not required for viability, we found that rare escaper animals hatch late and are infertile with vestigial ovaries; suggesting *trbl* has unexplored roles both in larval tissue growth and cell proliferation during early oogenesis. Antisera to Trbl revealed dynamic changes in subcellular localization during late oogenesis: Trbl accumulates in FC nuclei up to stage 11 after which nuclear levels drop and Trbl accumulates at low levels in the cytoplasm (Figure 2.1E,F). The notion that Trib localization is regulated and has functional importance is supported by observations that (1) GFP-tagged versions of Tribs are localized variously to the cytoplasm, nucleus and even the mitotic spindle (Saka and Smith, 2004), and (2) during BMP/TGF- β -signaling Tribs bind BMP receptors at the cell cortex, upon signaling are released into the cytoplasm to bind and degrade SMURFS, and subsequently

Figure 2.8 Trbl kinase domain is required for Slbo turnover in vivo

(A). Misexpression of UAS-Trbl in the border cells using the *Slbo2.6Gal4* driver reveals expression of the transgene using the Trbl antisera (red, arrow) and reduced levels of Slbo protein (green) while in the third panel, *slbo-lacZ* gene expression remains high (magenta). The fourth and fifth panels are DAPI staining (blue) and overlay, respectively (B). Misexpression of UAS-Trbl^{D/NLK} in the border cells using the *Slbo2.6Gal4* driver also detects transgene expression using Trbl antisera (red, arrow) and results in normal levels of Slbo protein (green) (C). Scheme for examining Slbo turnover in FC cells misexpressing Trbl. Panel 1 shows the FC epithelium in a female of the genotype *hsFLP1; hs-Slbo/P{w+(mC)=AyGal4}25 P{w+(mC)=UAS-GFP.S65T}T2; UAS-Trbl*. After Flp induction, clones misexpressing Trbl can be detected by the expression of GFP, in panel 2. After 30 min heat shock induction of hs-Slbo, high levels of nuclear Slbo can be detected throughout the FC epithelium (red) in panel 3. Three hours after recovery, Slbo turnover in Trbl-expressing cells (green) can be compared to WT cells (black) in panel 4 (D). Misexpression of UAS-Trbl in the main body FC (inset) using the Flp-out driver is detected by GFP (green, arrow) and correlates with lower levels of hs-Slbo (red) following heat shock recovery. Decreased hsSlbo was detected in 20/25 clones in the main body FC (E). Misexpression of UAS-D/NLK in the main body FC (inset) using the Flp-out driver is detected by GFP (green, arrow) and correlates with normal to increased levels of hsSlbo (red) following heat shock recovery. Increased hsSlbo was detected in 32/32 clones in the main body FC.



translocate to the nucleus to serve as Smad co-activators (Chan et al., 2007; Hegedus et al., 2006; 2007; Hua et al., 2011).

Trbl antisera also detected dynamic changes in Trbl levels during BC migration: Trbl is strongly expressed before delamination from the anterior epithelium and Trbl levels decrease during BC migration (Figure 2.2A-C). In *slbo* mutant egg chambers (Figure 2.2D,F) Trbl levels are significantly higher compared to WT at all stages examined, indicating that *slbo* is necessary to repress Trbl. However, Slbo misexpression alone is not sufficient to repress Trbl expression (Figure 2.3), suggesting that cofactors mediate Slbo repression of Trbl. Our observation that *slbo* represses Trbl stands at odds with previous work showing that Slbo turnover is reduced in *slbo* mutant egg chambers (Rorth et al., 2000). While further work must be done to reconcile these observations, it is possible that *slbo* both represses Trbl expression and activates an unidentified Trbl activator, whose existence is implied by work in embryos (Grosshans and Wieschaus 2000). In this way, while Trbl levels increase in a *slbo* mutant, its ability to direct Slbo turnover could be compromised. Together these data indicate that Slbo and Trbl are at the core of a negative feedback loop in which Slbo represses Trbl expression and conversely Trbl (via its catalytic loop) binds and degrades Slbo. Such a model is consistent with observations that in some instances protein kinase dimerization leads to autoinhibited complexes (Parrini et al., 2002).

Snail-related transcription factors, which direct E-cadherin-dependent cell migration in a wide range of normal and diseased tissues, are also regulated by protein turnover (Batlle et al., 2000; Cano et al., 2000; Herranz et al., 2008). Several

modifications affect Snail stability, including phosphorylation by GSK3 β , dephosphorylation by the small C-terminal domain phosphatase (SCP), and lysine oxidation by NFK β . In the latter case, NFK β prevents Snail phosphorylation by GSK3 β and subsequent degradation, whereas formation of a ternary complex between wild-type p53, the ubiquitin ligase Mdm2, and Snail2 promotes degradation (Wang et al., 2009). It is likely that during BC migration a similar level of complexity underlies Trbl effects on Slbo stability, and the proposed feedback between these genes results in oscillating levels of Slbo and corresponding fluctuating expression of Slbo target genes, notably DE-cadherin, whose turnover at the cell membrane has been demonstrated to promote proper BC migration (Mathieu et al., 2007). In mammals, Trib family members have been identified as tumor suppressors or oncogenes, depending on tissue context (Dobens and Bouyain 2012) and sorting out these conflicting data may be aided from a simpler *Drosophila* model. Conserved interactions between Trbl and C/EBP during cell differentiation in flies and mammals suggest the possibility that interactions between Trbl and the Cdc25 phosphatase String observed during cell division in fly tissue might be conserved in mammals as well. Conversely, mammalian work holds the promise to illuminate and direct further tests of Trbl function in *Drosophila*, notably documented interactions between mouse Trib3 and ATF4, another member of the B-Zip class of transcription factors active during pancreas β -cell differentiation (Liew et al., 2010). Synergies between these parallel lines of investigation will shed light on the diverse roles of Trb family members in cell growth, proliferation and differentiation.

CHAPTER 3

DROSOPHILA TRIBBLES ANTAGONIZES INSULIN SIGNALING-MEDIATED GROWTH AND METABOLISM VIA INTERACTIONS WITH AKT KINASE

Introduction

The insulin/insulin-like growth factor (IGF) signaling (IIS) pathway is conserved throughout the metazoan lineage and functions to sense local and systemic nutrient levels and connect this information to the control of cellular and organismal metabolism (Edgar 2006). Insulin signaling regulates tissue homeostasis, longevity and diverse developmental processes including body size and sexual maturation (Koyama et al., 2013). Insulin and insulin-like peptides act in an endocrine manner to bind insulin receptors (InR) in responsive tissue (Brogiolo et al., 2001; Chen et al., 1996; Ikeya et al., 2002). This triggers a phosphorylation cascade from the insulin receptor substrate (IRS) to phosphoinositide-3 kinase [PI3K (Carpenter et al., 1990)], which promotes the conversion of phosphatidylinositol 4, 5-bisphosphate (PIP2) to phosphatidylinositol 3, 4, 5-triphosphate (PIP3) in the cell membrane (Auger et al., 1989). PIP3 recruits phosphoinositide-dependent protein kinase 1 [PDK1 (Mora et al., 2004)] and Akt/PKB kinase (Coffer et al., 1998; Downward 1998). Akt is activated by phosphorylation at Thr308 and Ser473 (latter one is equivalent to *Drosophila* Ser505) and Akt in turn phosphorylates myriad substrates to promote cellular anabolism, including: (1) the Rheb-specific GTPase activating protein (GAP) Tsc2 to promote TOR Complex 1 (TORC1) signaling and protein synthesis (Garami et al., 2003a; Miron et al., 2003; Montagne et al., 1999)(2)

GSK-3 β to block glucose production and stabilize MYC to boost anabolic gene expression (Parisi et al., 2011; Teleman et al., 2008) ; and (3) the transcription factor FoxO to block its nuclear localization and reduce expression of catabolic genes (Junger et al., 2003).

The strength and duration of insulin signaling is controlled by phosphatases (Taguchi and White 2008) and feedback phosphorylation (Puig et al., 2003; Puig and Tjian 2005; Saltiel and Pessin 2002). Recently, mammalian Trib3 and Trib2 have been demonstrated to bind Akt and block its activation without lowering Akt levels, resulting in impaired insulin signaling in hepatocytes, adipocytes, skeletal muscle, liver, fat and pancreas (Du et al., 2003; Koh et al., 2006; Liu et al., 2010; Qi et al., 2006). Consistent with a role in reducing insulin outputs, increased Trib3 expression occurs (1) following either starvation or exercise in mice, (2) in db/db diabetic mice (Matsushima et al., 2006) and (3) following experimental treatments such as high-fructose feeding or chronic ethanol consumption that lead to impaired insulin responses (Bi et al., 2008; He et al., 2006). Aberrantly high Trib3 levels are detected in insulin-resistant humans (Liu et al., 2010; Oberkofler et al., 2010; Prudente et al., 2009) and a population variant Trib3Q/R84 associated with predisposition to metabolic disease dominantly blocks insulin signaling (Andreozzi et al., 2008; Prudente et al., 2005; Prudente et al., 2013).

Evidence shows that Tribs influence metabolism via effects on lipogenesis, as well: (1) Trib3 binds and degrades acetyl coA carboxylase 1 (Acc1, the rate limiting enzyme of fatty acid biosynthesis) to reverse fatty acid deposition (Qi et al., 2006); (2) Trib1 modulates hepatic lipogenesis (Burkhardt et al., 2010) (3) sequence

variations in humans Trib1 are associated with increased plasma lipoproteins and the risk of coronary artery disease (Chambers et al., 2011; Kathiresan et al., 2008; Varbo et al., 2011) ; and (4) Tribs block adipocyte differentiation and triglyceride accumulation by inhibiting the transcriptional activity of three master regulators of fat cell differentiation – PPAR γ (inhibited by Trib1), MLXIPL (MLX-Interacting Protein-Like, inhibited by Trib1) and C/EBP α (inhibited by Tribs 1, 2 and 3) (Angyal and Kiss-Toth 2012; Ishizuka et al., 2014; Naiki et al., 2007; Takahashi et al., 2008).

The notion that Trib3 binds Akt to 'dial-down' the insulin response in peripheral tissues is contradicted by genetic analysis showing that a rat Trib3 knockdown has no effect on Akt activity (Weismann et al., 2011) and mouse Trib3 knockout has no effect on metabolism at all (Okamoto et al., 2007). This lack of phenotype may be caused by overlapping functions with Trib1 and Trib2.

Drosophila presents a model system to test how insulin and insulin-like growth factor signaling (IIS) regulate tissue growth, glucose homeostasis, lipid metabolism, fecundity and longevity (Teleman 2010). Genes and tissue interactions comprising the fly insulin pathway have strong sequence, structural and functional homology to members of the vertebrate pathway (Teleman 2010). Mutations in fly IIS pathway components result in reduced cell, organ and body size with little effect on cell fate and differentiation. Similarly, ablation of the fly insulin producing cells in the brain, analogous to the pancreatic beta cells, leads to decreased animal size and increased sugar concentrations, modeling dwarfism and type 1 diabetes, respectively (Rulifson et al., 2002). In addition, many of the insulin target tissues in *Drosophila* are

functionally equivalent with adipose, liver, brain, kidney and skeletal muscle, all known to be important in type 2 diabetes (DiAngelo and Birnbaum 2009; Lee and Park 2004b). The parallels between flies and vertebrates extend to diet so that flies raised on high sugar diets feature the hallmarks of insulin resistance, including hyperglycemia and increased fat (Musselman et al., 2011; Na et al., 2013; Pasco and Leopold 2012). In this chapter, I demonstrate that *Drosophila* Trbl negatively regulates insulin signaling during tissue growth by binding and blocking the phosphorylation-dependent activation of Akt, underscoring the putative function of Trib proteins as central nodes in multiple signaling pathways regulating cell growth, proliferation and differentiation, and raising the intriguing possibility that Tribs may have a conserved role in coordinating nutrient-dependent growth in development and disease.

Materials and methods

Drosophila strains

(1) $p\{UAS-FLAG-trbl.WT\}$ (UAS-FlagTrbl) and (2) $p\{UAS-FLAG-trbl.DNLK\}$ (UAS-FlagTrbl D/NLK) have been described previously (Masoner et al., 2013). (3) $P\{w[+mC]=Gal4-Mef2.R\}^3$ (Mef2-Gal4) was a gift from Erika Geisbrecht and (4) $P\{Ppl-Gal4.P\}$ was a generous gift from John B. Thomas of Salk Institute. We obtained the following stocks from the Indiana Stock Center, (5) $P\{en2.4-Gal4\}e16E$ (*engrailed*Gal4, enGal4), (6) $P\{GawB\}ap[md544]$ (*apterous*-Gal4, ap-Gal4), (7) $P\{longGMR-Gal4\}^3$ (8) $y[1] w[1118]$; $P\{w[+mC]=UAS-Akt1.Exel\}^2$, (9) $P\{(UAS-Pi3K92E.Exel\}^2$, (10) $P\{UAS-S6k.STDE\}^3$, (11) $P\{UAS-foxo.P\}^2$; (12) $P\{TRiP.JF01859\}attP2$; from the Vienna stock center, (13) $w[1118]$;

P{GD11640}v22114, (14) *P{KK108667}* (106774); and from the Harvard stock center (15) *P{TRiP.HMS02198}* (41665).

Yeast two-hybrid screen

Yeast two-hybrid analysis and construction of bait vectors FLAGTrbl, FLAGTrbl^{D/NLK} was performed as described in chapter 2. To construct prey plasmid Akt1 cDNA was amplified using PCR to add flanking attB1 and attB2 sites. Forward and reverse primers were:

GGGACAAGTTTGTACAAAAAGCAGGCTTCATGTCAATAAACACAACCTTTCG
ACCTCAGCTC and

GGGACCACTTTGTACAAGAAAGCTGGGTCCTATTGCATCGATGCGAGACTTG
TG (attB1 and attB2 sequences in bold). The PCR product was cloned into the donor vector pDONR-21 and then into either pDEST32 (bait vector) or pDEST22 (prey vector). All constructs were confirmed by DNA sequencing.

Quantification of metabolites and lipids

Flies were reared on “Cornmeal, Molasses and Yeast Medium” (Bloomington Stock Center recipe). Measurements of the glucose and trehalose concentration in the hemolymph and triglyceride content of larval extracts were performed as described in (Musselman et al., 2011). For total triglyceride quantification, ~15 age matched larvae/group were washed three times in PBS, then wiped briefly on Kimwipe. Larvae were transferred to a 1.5 ml Eppendorf tube and homogenized on ice in 40µl of ice cold PBST (0.1% Tween20)/larva with a hand held homogenizer on ice. Homogenates were then heated at 65⁰C for ~5 minutes to deactivate lipases. 20µl of the homogenate was added to tube containing 680µl of triglyceride reagent

(Thermo Infinity™ Triglycerides Reagent), incubated at 37°C for 15 minutes. Samples were then centrifuged briefly to remove suspended particles and then measured on a plate reader at 540 nm in biological triplicate. For Nile red stains, larvae were dissected on a glass slide in 0.001% Nile Red (Sigma), 75% glycerol and incubated for 10 minutes before mounting. For Oil red O assay, dissected fat body was incubated with a working solution of 0.5 % Oil Red O dye in 6 ml isopropanol+ 4 ml H₂O (prepared freshly and filtered through a 0.45µm filter), incubated for 30 minutes at room temperature, washed three times in MilliQ H₂O and then the tissue bound dye was extracted with 100% isopropanol. O.D. was measured at 510 nm.

Western blots and immunostaining

Age matched larval fat body was homogenized in 2x sample buffer and equal amounts of homogenate were loaded onto SDS-PAGE gels and blotted according to standard protocol. Blots were probed with the following antibodies (all at 1:2000 dilution): (1) phospho-*Drosophila* Akt (Ser505) Antibody (Cell Signaling #4054), (2) Total anti Akt Rabbit mAb (Cell Signaling #4691), (3) anti Phospho-FoxO1 (Ser256) (Cell Signaling #9461), (4) anti-total FoxO (a generous gift from Marc Tartar), (5) anti- αTubulin (Developmental Studies Hybridoma Bank #12G10). Four experiments were done and multiple exposures taken, Western blot quantification was done on lightly exposed blots using Licor Image analysis software. Blots were stripped and re-probed using mild stripping protocol of Abcam (<http://www.abcam.com/ps/pdf/protocols/stripping%20for%20reprobing.pdf>). Primary antibodies were used in the following order - pAkt, pFoxO, total Akt, total FoxO, α-

Tubulin. Secondary antibodies conjugated to HRP (Genescript) were used, and the signals were detected by chemiluminescence using the Enhanced ECL kit (Biorad).

For whole-mount immunostaining of larval body wall muscles, age matched samples were collected and washed three times with PBS in an Eppendorf tube. Then they were incubated with 65°C PBS for 30 seconds. After that, the hot PBS was replaced with ice cold PBS and the tube was placed on ice. This technique straightens the larvae and makes dissected muscle flat. The larvae were laid in ice cold PBS on their dorsal side and dissected along the anterior-posterior axis. Fat body and other tissues were removed before the samples were fixed for 20 minutes in PBS with 4% paraformaldehyde. After washing three times in PBS+0.1%Tween 20 (PBST), samples were incubated for 30 minutes with Phalloidin (1:2000, Sigma), washed three times in PBST (15 minutes each time) and then mounted on 50% glycerol with DAPI (1:1000, Roche). Image analysis was done with ImageJ and Photoshop. Micrographs were collected using an Olympus confocal laser-scanning microscope and figures prepared using Photoshop. Wing preps were made as described in (Dobens and Dobens 2013). Wing curvature was documented on thoracic shish kebabs photographed using a Nikon dissection scope and attached Nikon D100 camera. Cell size and nuclear size was documented using the tools in Fijiwings. For wing analysis, crosses were reared at 30°C and female wings were selected and mounted. For Fijiwings analysis, we used FijiwingsEZ and calculated wing size in kilo pixels and trichome density in “per kilo pixel.”

Whole Body weight analysis

For analysis of body weight, age matched groups of mid L3 larvae were weighed on a precision Kahn microbalance (model 4400). More than ten age matched larvae/group were washed three times in PBS, dried on Kimwipe and weighed in triplicate and the average body weight calculated.

Larval fat body analysis

Approximately ten age matched mid third instar female larvae were collected in ice cold PBS and dissected partially in PBS to open up the body cavity and then fixed in 4% paraformaldehyde in PBS for 20 minutes. Fixed tissue was washed for three times in PBST (PBS+0.1% Triton X100, 10 minutes each time) and incubated with blocking reagent (PBST+ 10% normal goat serum) for two hours at room temperature with rocking. Then the samples were washed three times in PBST (5 minutes) and incubated with 1° antibody (1:1000 chicken anti-Trbl in PBST+ 2.5% BSA) overnight at 4°C with rocking. Then the tissue was washed three times in PBST (10 minutes) and incubated with 2° antibody (goat anti chicken Alexa Fluor488 conjugated IgG) in PBST+2.5% BSA) for two hours at room temperature with rocking. Tissue was washed three times in PBST (10 minutes) and once with PBS. Then a single strip of fat body from the ventral mid-section of each larva was collected and mounted on 75% glycerol to visualize the fluorescent staining.

For actin and DAPI staining, tissue was fixed and blocked as described above and washed for three times in PBST (5 minutes) and incubated with 1:500 TRITC conjugated Phalloidin (from Roche) in PBST+ 2.5% BSA for 20 minutes at room temperature with rocking. Then the samples were washed three times in PBST (15

minutes) and once with PBS. Then a single strip of fat body from the ventral mid-section of each larva was collected and mounted on 75% glycerol+ 20 μ M DAPI (Roche, 10236276001) to visualize fluorescent staining. A single image was taken from each fat body strip (hence each larva) and multiple images were used for the quantification.

Larval age synchronization and pupation time assay

~ 40 virgin (two-five days old) and male flies were reared on “Cornmeal, Molasses and Yeast Medium” (Bloomington Stock Center recipe) supplemented with dry yeast for three days. Food was changed every day. On day four, flies were transferred to a fresh vial for 30 min to get rid of any held eggs. After that, flies were again flipped to a new vial with regular food (no yeast supplement) and kept for two hours. Females laid ~20 eggs during that time. After 18 hours, all unhatched eggs were removed from the vial. Larvae were collected from that vial at proper developmental time for assays. Mid third instar larvae were selected from food and presence of food in the gut was checked. For pupation assay, ~30 first instar larvae were plated in triplicate on regular fly food at 30⁰C or 25⁰C. Pupae formed were counted in every four-eight hours over the course of six-seven days. After seven days, total number of pupae was counted and assigned as 100%. The fraction of the larvae pupariated during different time was calculated from total pupariated.

Experiment was done in biological triplicate.

For the eclosion assay, ~30 synchronized wandering third instar larvae were collected and transferred to the wall of a new vial. The numbers of pupae hatched were counted in every few hours. After seven days, total number of pupae counted

and assigned as 100%. The fraction of the male/female animals hatched during different time was calculated from total animals hatched. Experiment was done in biological triplicate.

Statistical Analysis

Statistical analysis was performed with Graph Pad Prism (v 5.0) and all data are presented as mean \pm SD and analyzed using one way ANOVA and/or unpaired, 2-tailed Student's t test (as detailed in Supplemental Table 1). A P-value of less than 0.05 is considered significant.

Results

Akt interacts with Trbl in a wing misexpression screen

Trbl misexpression blocks cell proliferation in the embryo and wing, consistent with its ability to bind String/Twine cdc42 phosphatase and block entry into mitosis (Grosshans and Wieschaus 2000; Mata et al., 2000). Consequently, misexpression of Trbl in the posterior wing compartment using the *engrailedGal4* (*enGal4*) driver results in an increase in cell size (detectable as a decrease in the density of trichomes, which mark individual wing cells; Figure 3.1B, E, J) and a decrease in overall wing size (Figure 3.1E, H, K). We performed a wing co-misexpression screen for genes that modify these divergent Trbl misexpression phenotypes and identified Akt1, which suppressed Trbl phenotypes when co-misexpressed with Trbl, effectively decreasing cell size and increasing tissue size to generate a wing structure that appeared nearly wild type (Figure 3.1C,F, I-K).

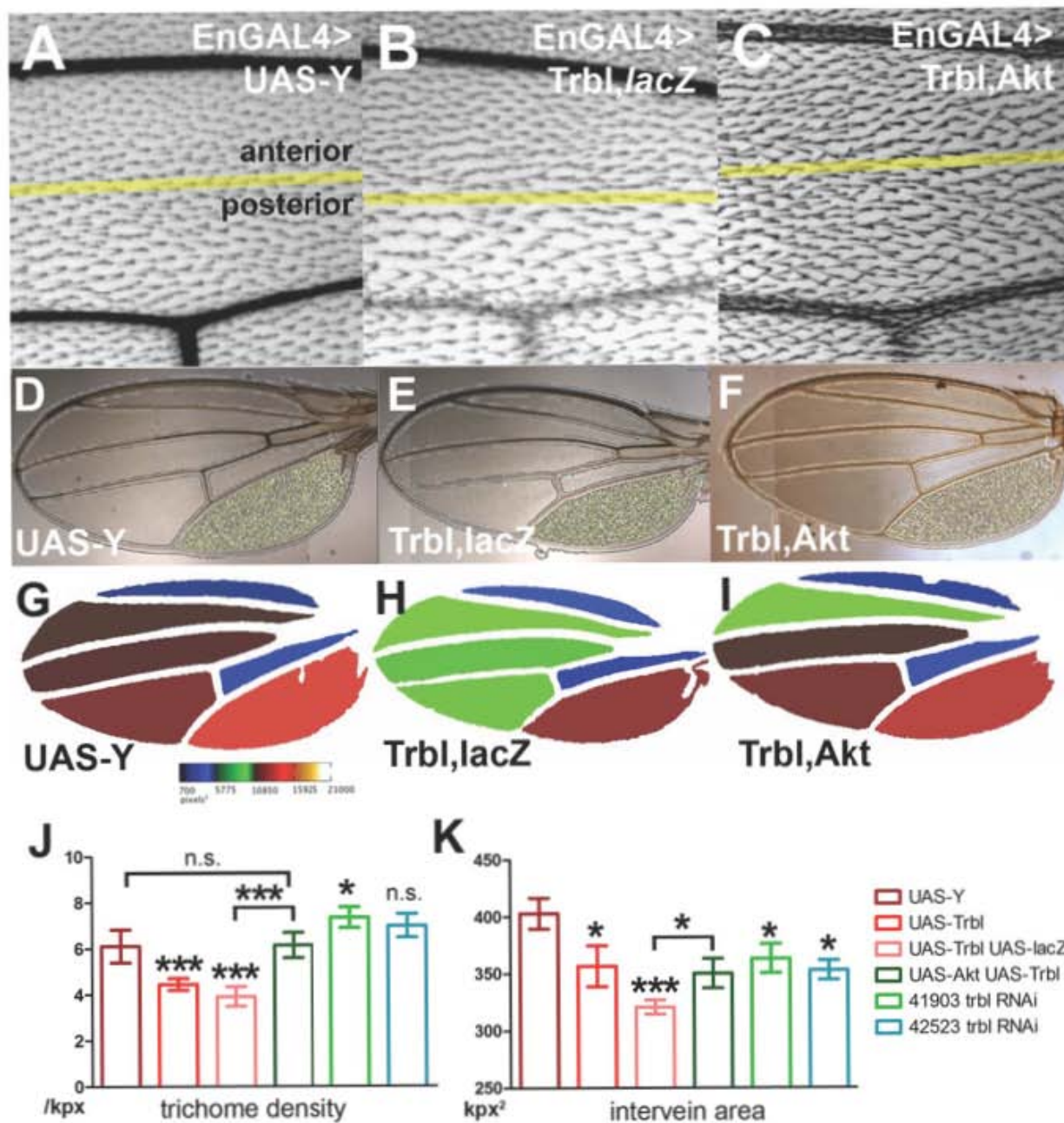
To precisely document the interaction between Trbl and Akt, we used Fijiwings (Dobens and Dobens 2013). Because trichomes are produced by individual wing epithelial cells, trichome density is an inverse measure of cell size. In WT wings, trichome density was 6.1 trichomes/square kilopixels (kpx^2 ; averaged from at least three WT wings) while Trbl misexpression reduced trichome density in the posterior intervein region to 4.5 trichomes/ kpx^2 . The strength of this phenotype was not diluted by co-misexpression of UAS-lacZ ($3.5/\text{kpx}^2$; Figure 3.1J), whereas co-misexpression of Trbl with Akt increased the density to 6.1, a significant increase resulting in a trichome density similar to WT (Figure 3.1J). With respect to tissue size, WT wings had an average area of 402 kpx^2 in the posterior intervein region, and Trbl,lacZ misexpression reduced this to 320.8 kpx^2 while co-misexpression of Trbl with Akt resulted in an area of 350.2 kpx^2 , a significant increase in size (Figure 3.1K).

Trbl antagonizes cell growth in larval tissue

Akt1 is a key mediator of insulin signaling, so I focused on the requirement for Trbl in the larval fat body, an insulin responsive tissue (Colombani et al., 2005). Specific antisera revealed fat body expression of Trbl localized to the nucleus and more diffuse in the cytoplasm (Figure 3.2A), and I confirmed the specificity of the Trbl antisera by overexpressing UAS-Trbl using the fat body-specific *PumplessGal4* (PplGal4) driver, which resulted in a strong increase in detectable nuclear and cytoplasmic Trbl staining compared to controls (Figure 3.2A,B) while these lines had weight (Figure 3.2C) and fat body cell size (Figure 3.2H–K) decreases relative to control tissue.

Figure 3.1. Akt is a Trbl interacting gene in a wing misexpression screen.

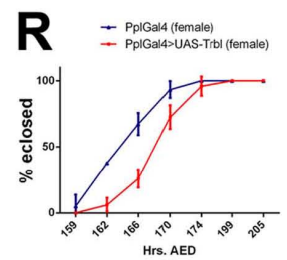
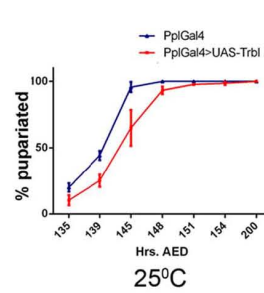
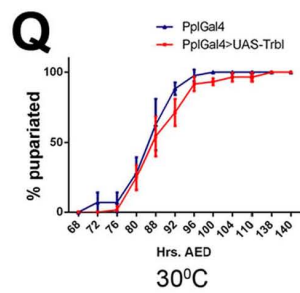
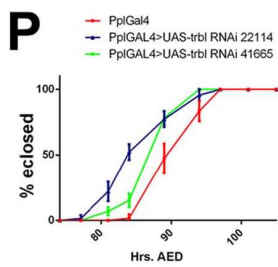
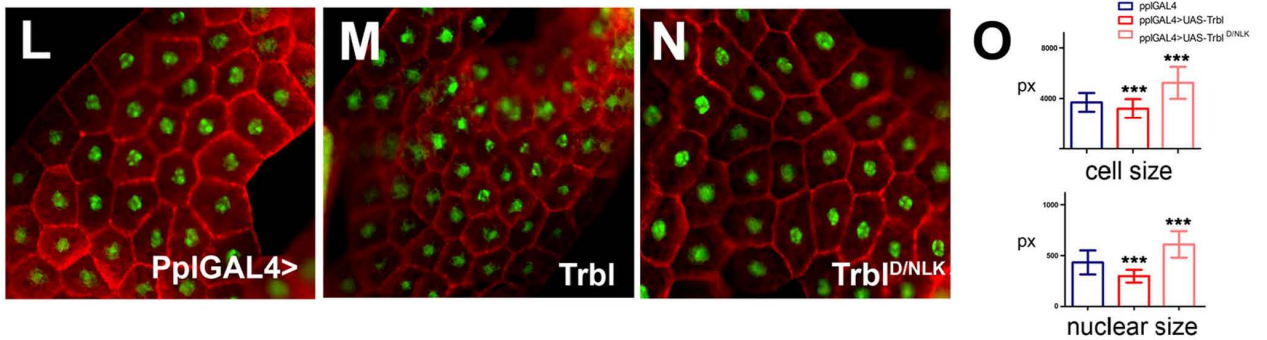
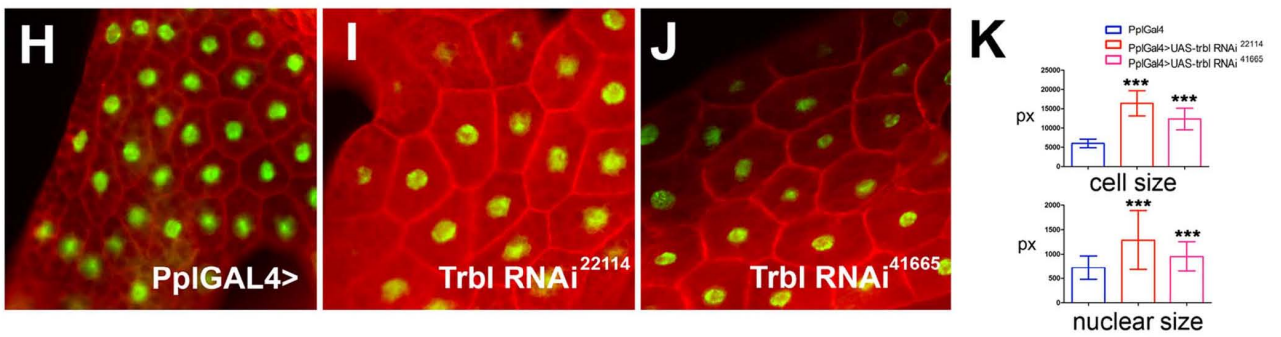
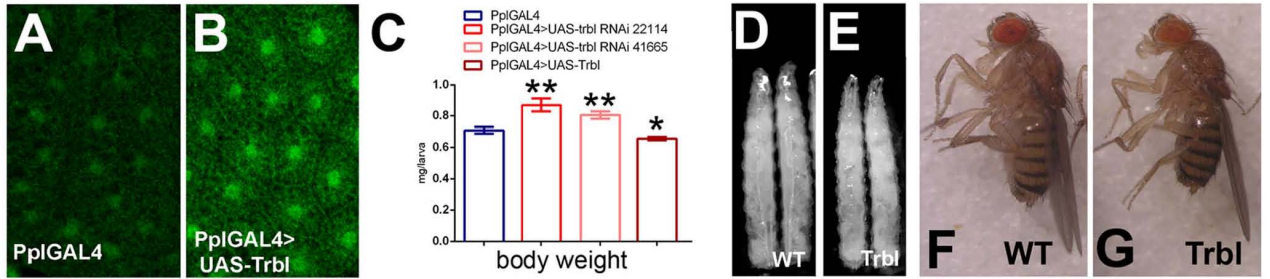
(A) *engrailedGal4 >UAS-Y* control wing shows normal size and trichome distribution in both the anterior and posterior compartments. (B) *engrailedGal4 >UAS-Trbl* misexpression in the posterior compartment shows a reduced trichome density relative to WT (genotype *enGal4>UAS-lacZ, UAS-Trbl*). (C) The Trbl misexpression trichome phenotype is suppressed by co-misexpression of Akt, restoring the normal distribution of trichomes (genotype *enGal4>UAS-Akt, UAS-Trbl*). (D-K). Fijiwings analysis of Trbl and Akt misexpression in wing. (D–F) Detection of trichomes for representative wings. (G–I) Heat map analysis of intervein areas for representative wings. Note that third posterior intervein region in WT is red; brown in Trbl misexpressing wing and the same area is reddish brown following co-expression of Akt. (J) Measurement of trichome density (in trichomes per kilopixel) is the result of the average of at least four wings for each genotype. Trbl misexpression in posterior wing compartment resulted in an 18.3% decrease in trichome density, an effect that was not lessened by co-misexpression of a *UAS-lacZ* transgene, indicating UAS-transgene dosage did not modify Trbl phenotypes, and this reduction was antagonized by co-misexpression of *UAS-Akt*. For J and K, for average trichome densities, n = 8 for UAS-Y and UAS-Trbl, 10 for UAS-Trbl; UAS-lacZ and *UAS-Akt; UAS-Trbl*, 6 and 4 for 41903 and 42523 RNAis respectively. P values calculated from one-way ANOVA (for the entire group) and from two-tailed t test (between two genotypes where indicated) (n.s. = not significant; *P<0.05; **P<0.01; ***P<0.001), and all error bars are SD. (K) Measurement of area (kpx^2 , in kilopixels of third posterior intervein region) is the average of at least three wings for each genotype. Trbl misexpression in posterior wing compartment resulted in a 12% decrease in intervein tissue size, an effect that was not suppressed by co-misexpression of a *UAS-lacZ* transgene, indicating UAS transgene dosage did not modify Trbl phenotypes and this reduction was effectively antagonized by co-misexpression of *UAS-Akt*. For areas, n = 3 for all cases except for 42523 RNAi line where n = 2.



Because larval size and weight thresholds trigger pupariation and eclosion, I measured the timing of these events and observed an advance in the timing of pupariation in *trbl RNAi*-overexpressing larva compared to WT controls (Figure 3.2P, panel 1), consistent with this increase in weight. Compared to WT larva, PplGal4 misexpression of Trbl in the fat body reduced significantly body weight in age-matched larvae (Figure 3.2C), and reduced overall size of both age-matched larvae (Figure 3.2D,E) and two-day old adult females (Figure 3.2F,G). Direct examination of the larval fat body tissue confirmed that UAS-Trbl overexpression reduced cell and nuclear size significantly compared to WT (Figure 3.2L, M, O). Misexpression of a Trbl transgene bearing a site directed mutation in the conserved ATP binding motif in the divergent kinase domain (D/NLK) increased cell size significantly compared to WT (Figure 3.2N), as measured by cell circumference or nuclear size (Figure 3.2O). These comparisons (Figure 3.2L–O) were made at 25°C because Trbl D/NLK caused lethality when misexpressed at 30°C. Overexpression of Trbl in the larval fat body delayed the timing of pupariation compared to a wild type control cohort (Figure 3.2Q, panel 1). This delay was more marked at 25°C where growth periods are longer (Figure 3.2Q, panel 2). These changes in the timing of pupariation following Trbl overexpression suggest larvae feed an extended period to reach critical weight before pupa formation, and consistent with this, overexpression of Trbl at 30°C led to a delay in eclosion, to a greater extent in females than males (Figure 3.2R).

Figure 3.2. Larval fat body specific overexpression of *Trbl* suppresses growth and delays development.

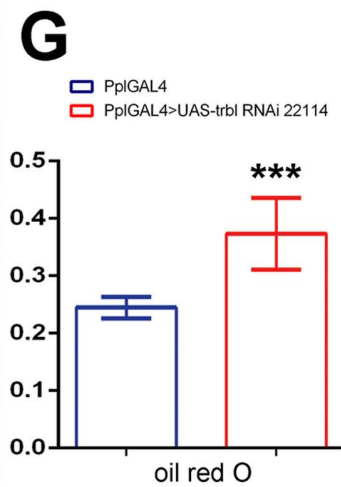
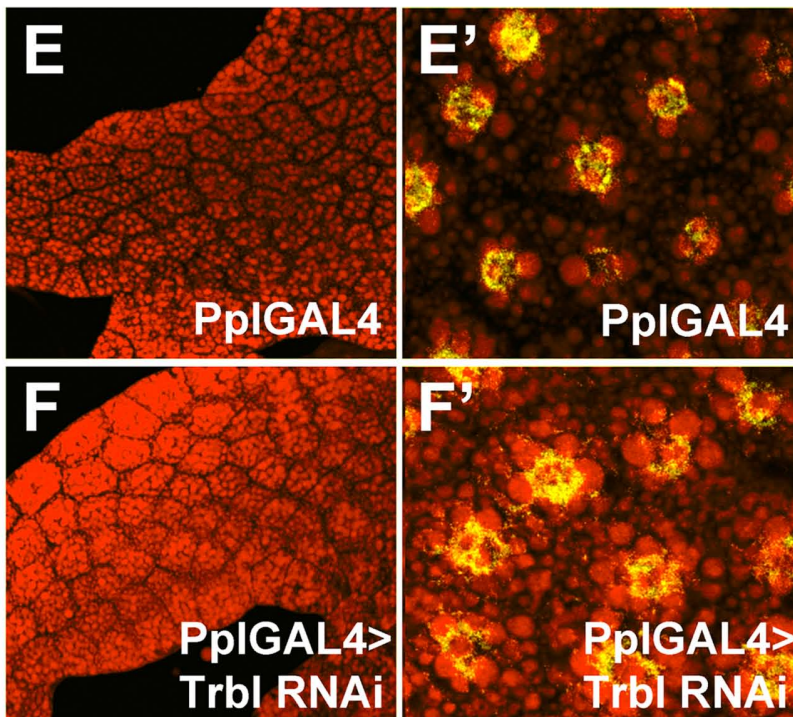
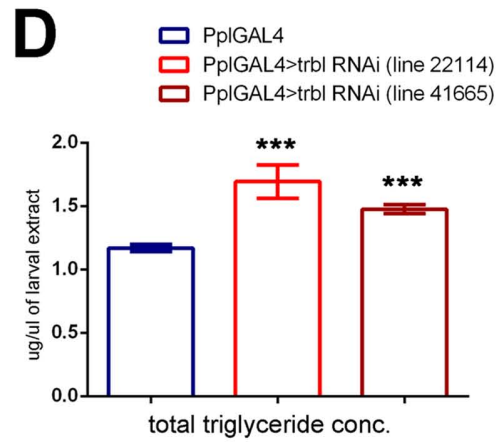
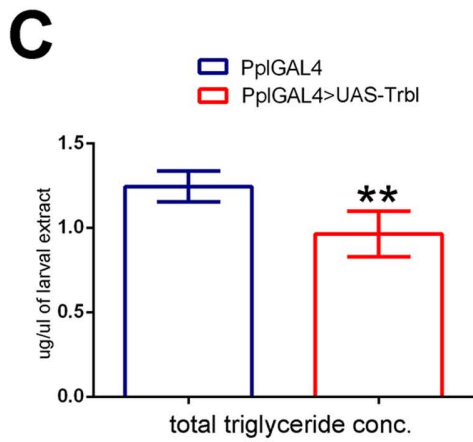
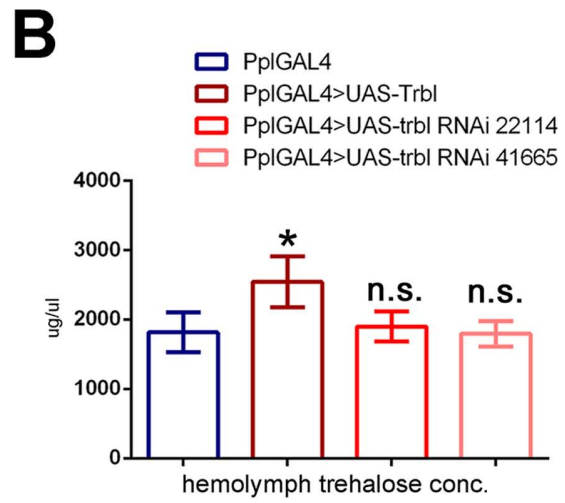
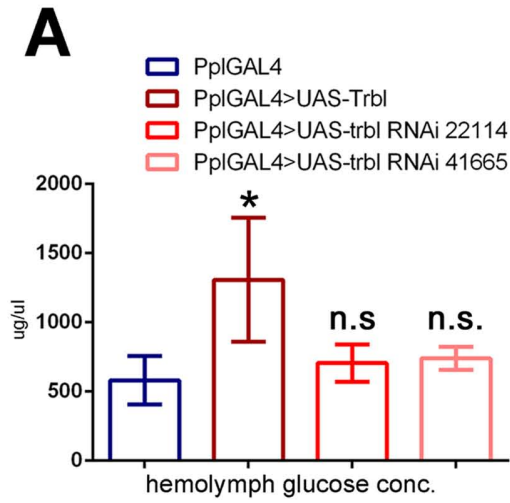
(A,B). *Trbl* antisera detects a cytosolic and nuclear antigen in mid-third instar larval fat body (A) whose levels increase in *PplGal4>UAS Trbl* larvae (B); note that images in A and B were taken under identical fixation and microscopy conditions). (C). Body weight measurement of age matched mid-third instar larvae of indicated genotypes. Compared to the control, misexpression of *trbl* RNAi line 22114 increased body weight by <25% and *trbl* RNAi line 41665 increased body weight by <14% (in triplicate, n = 16/genotype) whereas *Trbl* overexpression in fat body reduced larval weight by <7%. (D,E). Age matched mid third instar control *PplGal4* larvae (D, designated WT) are larger than *PplGal4>UAS Trbl* larvae (E). (F,G). Adult body size comparison of two day-old females is shown. *PplGal4>UAS Trbl* female adults (F) are smaller than *PplGal4* control (G, designated WT). (H–J). Size analysis of micrographs of fat body cells from age-matched mid-third instar larvae is shown. *PplGal4* control (H) and two RNAi lines (I,J) are shown. Tissues were stained with phalloidin (red) to reveal actin at cell periphery and DAPI (green) to reveal nuclear size. Note that Fig 2H–J and 2L–N are taken under the same magnification, collectively. (K). Measurement of cell size (top) and nuclear size (bottom) of fat body cells expressing *trbl* RNAi. Quantification of size is made in pixels. For K, n= 50 for cell size and n =90 for nuclear size. P values from T test are indicated (n.s.= not significant; *P<0.05; **P<0.01; ***P<0.001) and all error bars are \pm SD. (L–N). Size analysis of micrographs of fat body cells from age-matched mid-third instar larvae is shown. *PplGal4* control (L), *Trbl* (M) and *Trbl D/NLK* (N) are shown. Tissues were stained with phalloidin (red) to reveal actin at cell periphery and DAPI (green) to reveal nuclear size. Note that these experiments were performed at 25°C because *PplGal4>UAS-D/NLK* is lethal at 30°C. (O). Measurement of cell size (top) and nuclear size (bottom) of fat body cells expressing *Trbl* or *D/NLK*. n=100 for cell size and ~100 for nuclear size except for *UAS-Trbl* where n = 52. (P). Misexpression of both *trbl*-RNAi lines 22114 and 41665 advanced pupariation compared to a *PplGal4* age matched control. For P-R, all error bars are \pm S.D. (Q). Pupariation, measured by eversion of spiracles in wandering larva, is delayed in *Trbl* overexpressing larvae compared to age-matched control *PplGal4* larvae reared at 30°C (panel 1) and this difference is accentuated when development is slowed at 25°C (panel 2; each performed in triplicate, n<25/genotype). (R). Eclosion of *PplGal4.UAS Trbl* females is delayed relative to an age matched control (performed in triplicate, n~10/genotype).



I next examined the effect of manipulating *Trbl* levels on metabolites (Figure 3.3). Compared to WT larva, *Trbl* overexpression in the fat body led to a significant increase in circulating levels of both glucose (Figure 3.3A) and glucose disaccharide trehalose, the main circulatory sugar in *Drosophila* (Figure 3.3B), secreted from the fat body. In contrast, *trbl* RNAi misexpression had little effect on levels of either compared to control animals (Figure 3.3A, B). *Trbl* overexpression led to a significant decrease in total triglyceride levels (Figure 3.3C), the main form of stored fat in larva, while *trbl* RNAi misexpression in the fat body resulted in a significant increase in triglyceride levels compared to control animals (Figure 3.3D). Consistent with increased triglycerides, *trbl* RNAi misexpression in the fat body resulted in a noticeable increase in the number and size of lipid drops as revealed by fluorescence from Nile Red staining (Figure 3.3 E, F). To measure precisely this increase, we isolated fat body tissue expressing *trbl* RNAi and compared the extent of Oil Red-O binding to control tissue. As shown in Figure 3.3G, *trbl* RNAi 22114 line showed a significant increase in absorbance at 510nm compared to controls corresponding to the increased dye bound to lipid in this tissue. These data are consistent with previous reports showing that reduced insulin signaling leads to hypoglycemia and decreased accumulation of fat (Musselman et al., 2011) and point to a conserved role for *Trbl* in blocking insulin signaling to reduce growth and increase catabolic pathway activity.

Figure. 3.3. Trbl affects circulatory sugar and total lipid level

(A). Compared to controls, Trbl overexpression in fat body increases hemolymph glucose level by ~110% whereas *trbl* RNAi knock down does not alter glucose level significantly (in triplicate, n=30/genotype). For panels A-D and G, P values from student's t test are indicated (n.s. = not significant; *P< 0.05; **P < 0.01; ***P < 0.001) (B). Compared to controls, hemolymph trehalose levels were significantly increased in larvae overexpressing Trbl in fat body but did not change significantly in *trbl* RNAi knock down larvae. (in duplicate, n=30/genotype). (C). Compared to controls, overexpression of Trbl reduces total triglyceride level significantly by ≈22%. (D). Compared to controls, misexpression of *trbl* RNAi line 22114 increased significantly total triglyceride level by ~44% and for *trbl* RNAi line 41665 triglyceride levels were increased significantly by ~25%. (E,F) *Trbl* RNAi misexpression increases lipid accumulation. Nile red staining of dissected WT tissue (E, E', DAPI in yellow) shows reduced lipid accumulation compared to fat body misexpressing Trbl RNAi (F, F', line 21114). (G) Fat body from *PplGal4* flies driving expression of Trbl RNAi (line 22114) shows a significant increase in Oil Red O binding (in arbitrary units) compared to fat body tissue dissected from control *PplGal4* flies.



Trbl suppresses Akt-mediated larval growth phenotypes

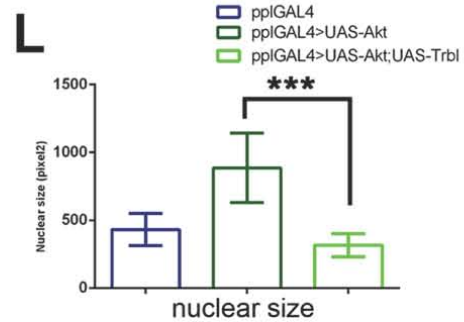
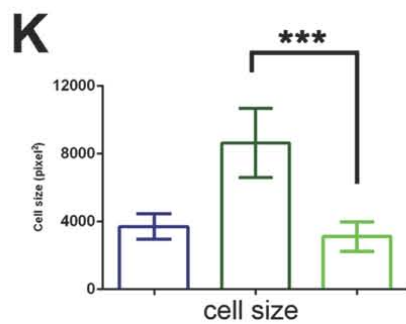
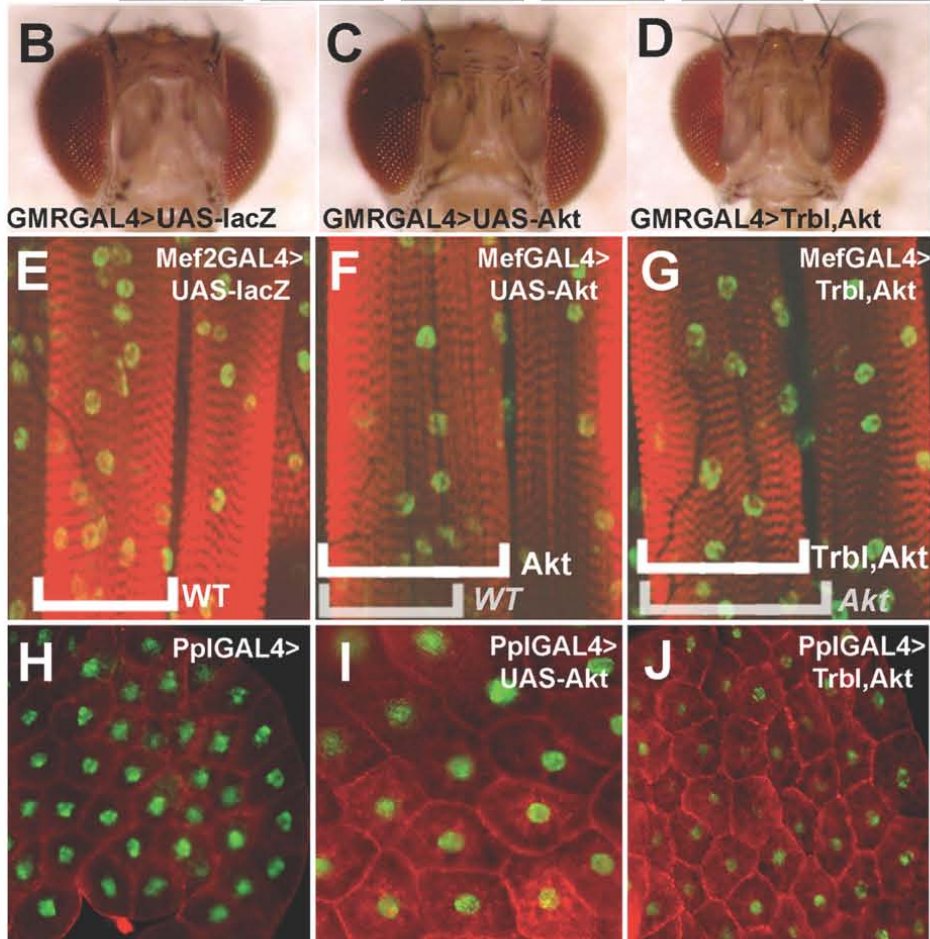
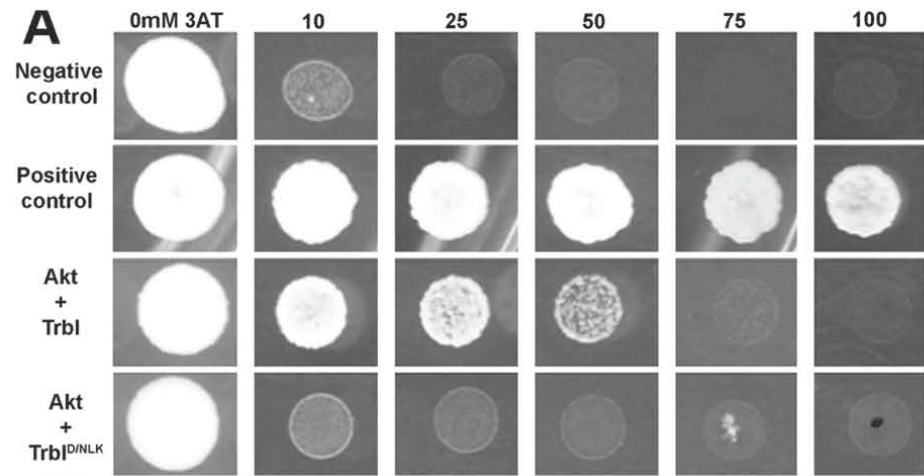
To understand the molecular nature of Trbl's interaction with Akt, I performed a yeast two-hybrid assay, expressing Trbl in the bait vector and Akt1 in the prey vector. As shown in Figure 3.4A, Trbl interacts with Akt1, resulting in detectable growth under stringent conditions (up to 50mM 3-Amino-1, 2, 4-triazole on histidine dropout plates). A mutation in the conserved kinase domain (Trbl D/NLK) reduced growth to levels comparable to a negative control, consistent with a disruption in this interaction (Figure 3.4A).

I next examined Trbl interactions with Akt during growth and patterning of different larval tissues (Figure 3.4B-L). Akt1 misexpression in the eye and head using the *GMRGal4* driver increased head size compared to WT (Figure 3.4B, C). Co-misexpression of Trbl and Akt effectively suppressed this Akt large head phenotype (cf. Figure 3.4C, D). In the larval muscle (Figure 3.4E), *Mef2Gal4* misexpression of Akt at 25°C led to an increase in the breadth of muscle fibers (Figure 3.4F) that was reduced by co-misexpression of Trbl (Figure 3.4G). Finally, in the fat body (Figure 3.4H), *PplGal4* misexpression of Akt1 resulted in a large cell phenotype (Figure 3.4I), which was suppressed by co-misexpression of Trbl (Figure 3.4J). Akt-mediated increases in fat body cell and nuclear size were significantly reduced by Trbl co-misexpression (Figure 3.4K and L, respectively). Thus, Trbl can effectively inhibit Akt activity in different types of larval tissue, i.e. mitotic and endoreplicating tissues.

Next, I examined the effect of Trbl overexpression on the activation of Akt and total Akt level using specific antisera. I performed Western blot analysis of protein

Figure. 3.4. Trbl binds Akt and suppresses Akt-mediated growth phenotypes

(A). the ability of yeast cells to grow on increasing concentrations of 3AT growth inhibitor depends on the strength of the protein-protein interaction. Yeast cells co-expressing Akt prey and WT Trbl bait are able to grow in presence of up to 50 mM 3AT whereas yeast cells co-expressing Akt and Trbl D/NLK bait are unable to grow in presence of 10 mM 3AT, similar to negative controls. (B-D). Akt misexpression in head capsule by the *GMRGal4* driver results in increased head size (C), which is effectively suppressed by Trbl co-misexpression (D). Genotypes: (B) *GMRGal4*, (C) *GMRGal4>UAS-Akt1*, (D) *GMRGal4>UAS-Akt1, UAS-Trbl*. (E-G). Akt misexpression in the larval muscle using the *MefGal4* driver results in an increase in muscle size (Fig E, F) while Trbl effectively suppresses this (G). Genotypes: (E) *Mef2Gal4*, (F) *Mef2Gal4>UAS-Akt1*, (G) *Mef2Gal4>UAS-Akt1, UAS-Trbl*. (H-J). Age matched mid-third instar larval fat body cells from *PplGal4>UAS-Akt* (I) are detectably larger than WT (H). This Akt-mediated increase in cell size is noticeably suppressed in fat body cells co-expressing Trbl and Akt (J). Tissues were stained with Phalloidin (red) to reveal cell boundary and DAPI (green) to reveal nucleus. Note that Fig 4B-D, E-G, H-J are taken under the same magnification, respectively. (K). Quantification of fat body cell size in pixels (n~100 cells/genotype; for K and L, P values from two-tailed T test data are indicated (n.s.= not significant; *P< 0.05; **P < 0.01; ***P < 0.001) (L). Quantification of fat body nuclear size in pixels (n~100 nuclei/genotype).



extracts collected from dissected fat bodies, and measured protein levels from scanned blots of at least three independent experiments (Figure 3.5).

Representative blots presented in Figure 3.5A and summarized in Figure 3.5B, C. These results show that *Pp/Gal4* driving *Trbl* led to a significant reduction of phospho-Akt levels compared to control animals; in contrast, levels of total Akt were not significantly different from control animals when corrected for levels of tubulin, which were consistently reduced in *Trbl*-misexpressing larva, likely due to the overall reduction in animal size (Figure 3.5A, C). In contrast, misexpression of the kinase dead mutation *Trbl D/NLK* resulted in an increase in phospho-Akt levels compared to control animals without affecting total Akt levels (Figure 3.5A-C), perhaps due to dominant negative interactions with endogenous *Trbl* (see discussion). As expected, ectopic Akt led to a strong increase in both phospho-Akt and total Akt, confirming the specificity of these antisera (Figure 3.5A-C). *Trbl* co-misexpression with Akt was sufficient to significantly inhibit phosphorylation-dependent activation of Akt, resulting in a 6.5-fold decrease compared to Akt misexpression alone (Figure 3.5A, B). As expected, *Trbl* had no effect on the high levels of total Akt produced by Akt co-misexpression (Figure 3.5A, C). We note that *Trbl* co-misexpression also did not affect the levels of total Akt seen by misexpression of Akt alone (Figure 3.5C), confirming that UAS-transgene dosage does not titrate *Pp/Gal4*. As shown in Figure 3.5D-F, misexpression of three independent *trbl* RNAi lines led to a significant increase in endogenous phospho-Akt levels with no significant change in total Akt levels in two of three RNAi lines used (Figure 3.5D-F).

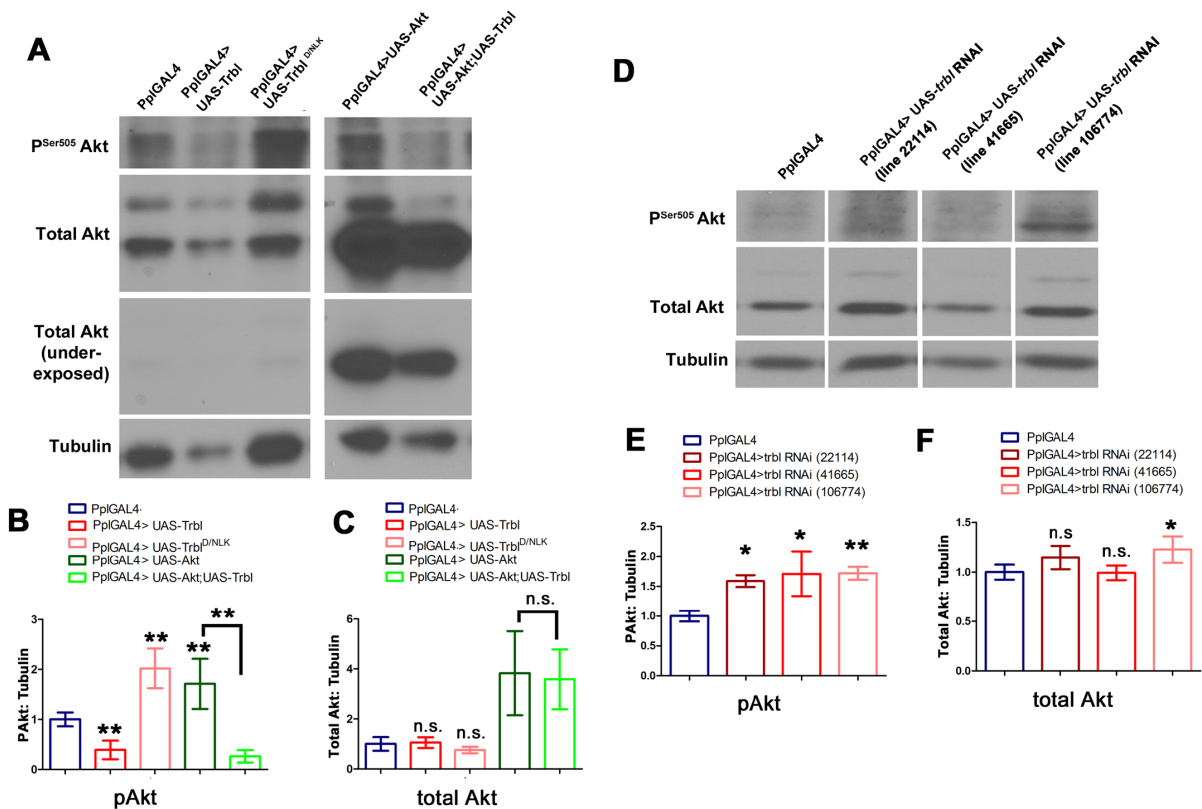


Figure. 3.5. The Trbl kinase domain is required to block Akt activation

(A). Representative Western blot of fat body from age matched third instar larvae driving transgene expression by *PpGal4*. In panels A and D, fat body extract from identical numbers of larva was loaded in each lane. (B, C) Quantification of Western blots of fat body extracts from four independent ($n=4$) experiments showing the effect of Trbl and Trbl^{D/NLK} on Akt activation and total Akt levels. For quantification of panels B, C, E and F, α -Tubulin band was used as loading control and results were normalized to *PpGal4*; P values from two-tailed t test data are indicated (n.s.= not significant; * $P < 0.05$; ** $P < 0.01$; *** $P < 0.001$) Table 1 and all error bars are \pm SD (B). P^{Ser505} Akt. (C). Total Akt. (D). Representative Western blot of fat body extract from age matched third instar larvae driving transgene expression by *PpGal4*. (E, F). Quantification of western blots of fat body extracts from four independent experiments showing the effect of *trbl* RNAi knockdown on Akt activation. (E). pSer⁵⁰⁵ Akt. (F). Total Akt.

Trbl blocks insulin signaling upstream but not downstream of Akt

Because the insulin signaling pathway is highly conserved in *Drosophila*, we tested the epistatic relationships between Trbl and components of insulin signaling lying upstream and downstream of Akt using the misexpression of transgenes in the wing (Figure 3.6). As shown previously in Figure 3.1, *engrailedGal4* misexpression of Trbl in the posterior compartment of the wing resulted in a decrease in trichome density, which I focused on for analysis here. *EnGal4* misexpression of an RNAi targeting Pten, an upstream inhibitor of insulin signaling (Gao et al., 2000), increased trichome density as shown previously (Dobens and Dobens 2013), and this phenotype was suppressed by Trbl co-expression (Figure 3.6B,C and J). Similarly, Trbl mediated reduction in trichome density was not masked by PI3 kinase, when co-misexpressed in the posterior wing (Figure 3.6E, F and J). In contrast, *enGal4* misexpression of a wild type copy of S6 kinase, which lies downstream of Akt, effectively suppressed the Trbl large cell phenotype, resulting in an average trichome density not significantly different from S6 kinase expression alone (Figure 3.6H, I and J).

It has been shown previously that *apterous-Gal4* (*apGal4*) misexpression of insulin signaling components results in dorsal compartment overgrowth leading to a characteristic bending of the wing (Montagne et al., 1999), and the tissue specificity of this driver allowed us to test Trbl interaction with several Akt targets that were lethal in combination with *enGal4*. *apterous-Gal4* misexpression of Trbl caused the wing to bend up, consistent with the notion that Trbl blocks cell division and growth when misexpressed in the dorsal wing compartment (Figure 3.6K,L; 4). In contrast,

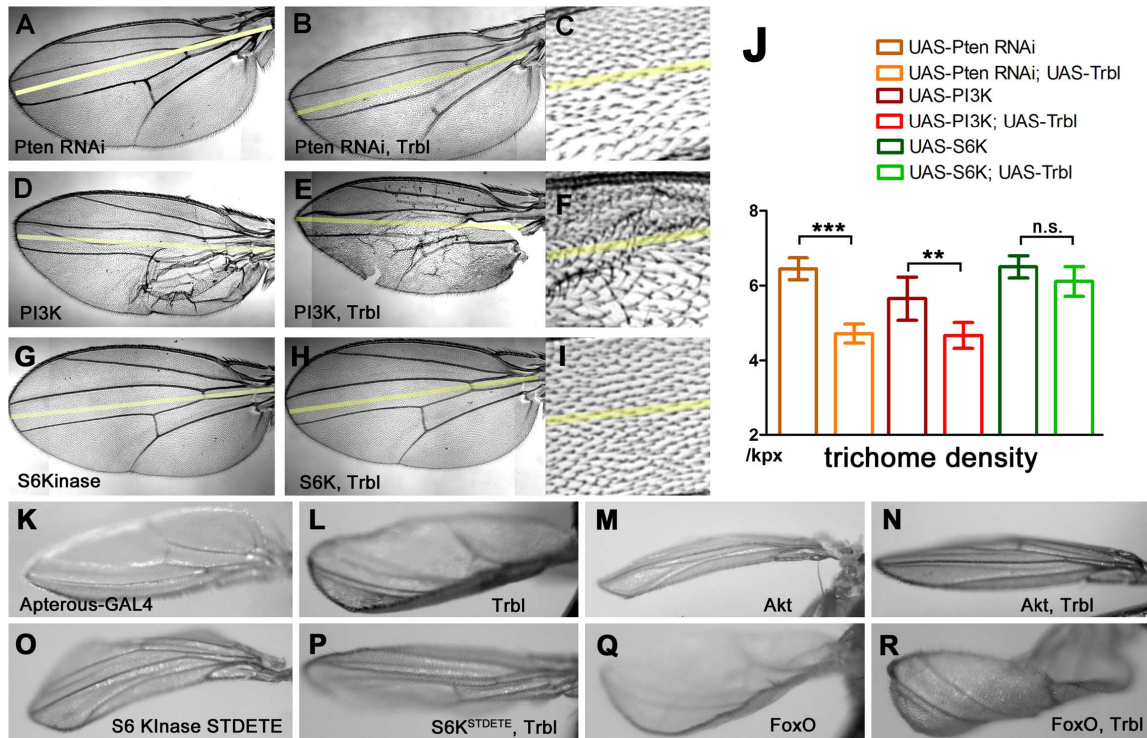


Figure. 3.6 Trbl blocks insulin signaling

(A) *enGal4>UAS-PtenRNAi* misexpression. (B,C) *enGal4>UAS-PtenRNAi, UAS-Trbl* co-misexpression results in the Trbl large cell phenotype. (D) *enGal4>UAS-PI3K* misexpression results in posterior wing patterning defects. (E, F) *enGal4>UAS-PI3K, UAS-Trbl* co-misexpression results in the Trbl large cell phenotype. (G) *enGal4>UAS-S6Kinase*. (H, I) *enGal4>UAS-S6Kinase, UAS-Trbl* co-misexpression effectively suppresses the Trbl large cell phenotype. (J) Trichome densities from genetic interactions shown in A-I. Average trichome densities from n=six wings; P values from one-way ANOVA and t tests between two genotypes where (n.s. = not significant; *P < 0.05; **P < 0.01; ***P < 0.001) and all error bars are \pm SD. (K) *apGal4* control wing shows flat wing blade. (L) *apGal4> UAS-Trbl* causes upturned wings, (M) *apGal4>UAS-Akt* results in downturned wings, (N) *apGal4>UAS-Akt, UAS-Trbl* results in a flat wing blade. (O) *apGal4>UAS-S6K^{STEDE}* results in downturned wings. (P) *apGal4>UAS-S6K^{STEDE}, UAS-Trbl* suppresses the activated S6kinase effect on the wing, resulting in a flat wing blade. (Q) *apGal4> UAS-FoxO* results in upturned wing. (R) *apGal4>UAS-FoxO, UAS-Trbl* results in strongly upturned wings.

apGal4 misexpression of Akt caused the wing to bend downward (Figure 3.6M). This Akt overgrowth phenotype was suppressed by co-misexpression of *Trbl*, resulting in a nearly flat wing blade (Figure 3.6N).

We next tested interactions between *Trbl* and two Akt targets. *apGal4* misexpression of an activated version of the *Drosophila* homolog of the Akt target S6 kinase 1 [dS6KSTDE; (Barcelo and Stewart 2002)] resulted in a bending downward of the wing blade (Figure 3.6N), an overgrowth phenotype that was effectively suppressed by *Trbl* co-expression (Figure 3.6O), consistent with combinatorial, opposing interaction between these genes. Misexpression of FoxO, a target of Akt phosphorylation-dependent inhibition, led to a curved upward wing (Figure 3.6P), a phenotype that was noticeably enhanced by *Trbl* co-misexpression (Figure 3.6Q), suggesting an additive interaction between *Trbl* and FoxO to block growth. To examine this directly, we used specific antisera to detect Akt phosphorylation-inactivation of FoxO, which occurs at Ser 256. I probed Western blots of fat body extracts from age matched *Trbl*-overexpressing larvae using antibodies to phospho-FoxO and total-FoxO to simultaneously detect effects on phospho-FoxO and total FoxO levels. As before, I performed at least three experiments. As shown in representative Westerns presented in Figure 3.7A-C, *Trbl* overexpression in the fat body led to a significant reduction in phospho-FoxO levels compared to controls (Figure 3.7A,B), while total FoxO levels were unaffected when corrected for total protein levels as measured by α -Tubulin, which was consistently reduced in *Trbl*-misexpressing animals (Figure 3.7A,C). Akt misexpression led to a significant

increase in phospho-FoxO, indicating that the antisera can reliably detect Akt-dependent phosphorylation-dependent inactivation of FoxO (Figure 3.7A, B). Trbl co-misexpression effectively blocked this Akt-dependent increase in phospho-FoxO levels. Unexpectedly co-misexpression of Trbl and Akt in the fat body led to a significant reduction in total FoxO levels (Figure 3.7A, C), suggesting that Trbl and Akt might act in combinatorial manner to direct FoxO turnover. Finally, I detected a reproducible and significant increase in phospho-FoxO levels following misexpression of Trbl D/NLK (Figure 3.7A, B), an increase that parallels the increase in phospho-Akt levels associated with misexpression of Trbl D/NLK (Figure 3.5E-G). Despite this increase in phospho-FoxO levels, Trbl D/NLK misexpression led to a significant decrease in total FoxO levels (Figure 3.7A,C), an unexpected effect that, again, may be due to dominant effects on endogenous Trbl as discussed in the following section.

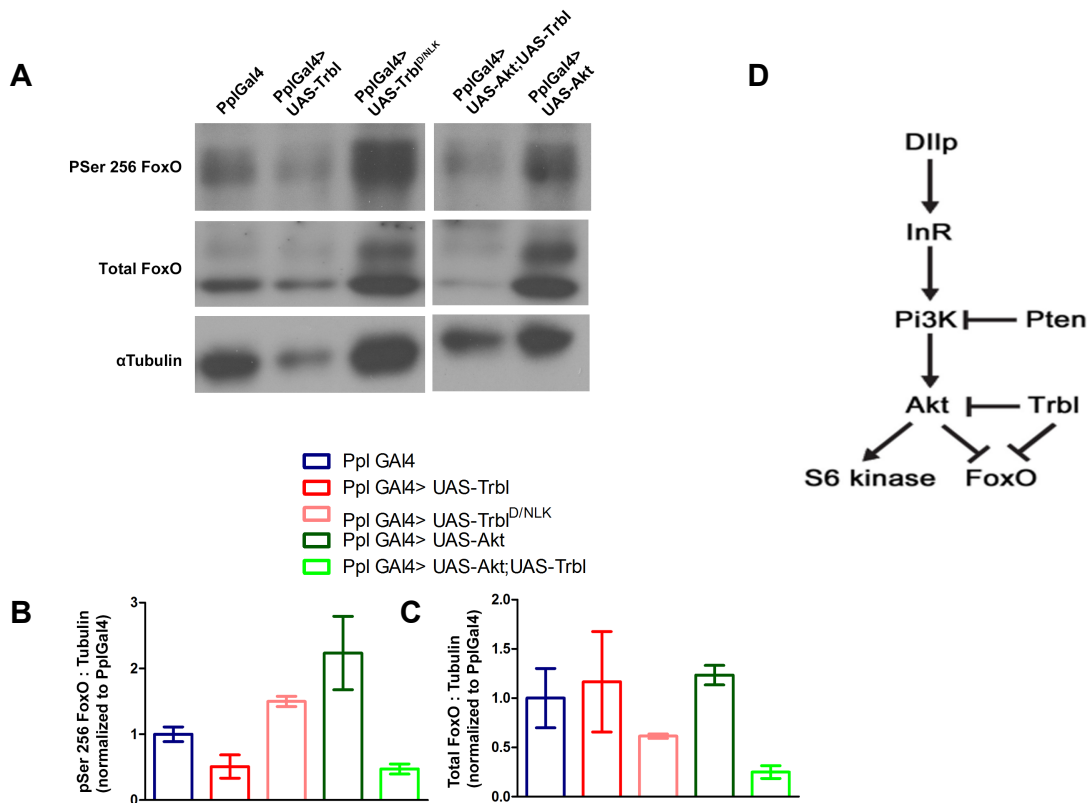


Figure. 3.7 Trbl reduces FoxO phosphorylation; a model for Trbl action

(A). Representative Western blot of fat body extract from age matched third instar larvae driving transgene expression by *PplGal4*. Equal amount of fat body extract was loaded in each lane. Tubulin blot picture is same as Fig. 3.5A because the same blot was stripped and reprobbed as described in materials and methods (B,C). Quantification of western blots of fat body extracts from four independent experiments (n=4) showing the effect of Trbl and Trbl^{D/NLK} on FoxO phosphorylation and total FoxO levels. For all quantification, α-Tubulin was used as loading control and results were normalized to *PplGal4*; P values from two-tailed t test data are indicated (n.s.= not significant; *P < 0.05; **P < 0.01; ***P < 0.001) and all error bars are ± SD. (B). P-Ser²⁵⁶ FoxO. (C). Total FoxO. (D). Model for Trbl regulation of Akt and FoxO.

Discussion

In this chapter, I show that *Drosophila* Trbl binds Akt to block its phosphorylation-dependent activation and does so without affecting Akt levels (model in Figure 7D). By this mechanism, Trbl blunts insulin signaling responses to regulate anabolic and catabolic pathways affecting circulating and stored metabolites with influences on body size, weight and the timing of both pupariation and eclosion. Previously, Trbl has been shown to regulate activities of the *Drosophila* C/EBP homolog Slbo during cell migration and in separate work, Trbl has been shown to regulate activity of String/Twine during cell proliferation (Grosshans and Wieschaus 2000; Mata et al., 2000; Rorth et al., 2000), in both cases by binding the respective proteins but – quite distinct from its interaction with Akt – by directing their proteasome-dependent degradation.

My demonstration that a mutation in the kinase domain of Trbl (D/NLK) reduces the ability of Trbl to bind Akt and block Akt-mediated cell growth is consistent with previous work showing that this mutation disrupts the ability of Trbl to block Slbo dependent cell migration and direct Slbo turnover (Masoner et al., 2013). Despite the requirement for the kinase domain in mediating Trbl function, several of my observations indicate that Trbl D/NLK retains effects on metabolic activity: (1) misexpression of Trbl D/NLK led to an increase in fat body cell size; (2) Trbl D/NLK misexpression increased Akt and FoxO phosphorylation; and (3) under conditions of increased *Pp/Gal4* activity, Trbl D/NLK was lethal. While it is possible that Trbl D/NLK interferes with endogenous Trbl to promote Akt activity, our yeast two hybrid (Y2H) data shows that both Trbl-Trbl and Trbl-Akt interactions are disrupted by the

D/NLK mutation [here and (Masoner et al., 2013)]. Thus, dominant effects of Trbl D/NLK occur in a manner that is indirect or requires endogenous factor(s) absent in the Y2H assay.

Misexpression studies show that WT Trbl effectively blocks insulin signaling both upstream and at the level of Akt. Downstream from Akt, S6 kinase co-misexpression suppressed the Trbl curved-wing phenotype and FoxO co-misexpression enhanced it. When I examined FoxO protein, I found Trbl reduced FoxO phosphorylation without an effect on total FoxO levels, an outcome that is expected if Trbl blocks Akt activation. Co-misexpression of Trbl and Akt reduced FoxO phosphorylation as well, but unexpectedly significantly reduced total FoxO levels relative to misexpression of either transgene alone (Figure 3.7C). This outcome is reproducible and suggests that Akt and Trbl act synergistically to direct FoxO degradation (model, Figure 3.7D). Another puzzling result came from examining the effect of TrblD/NLK misexpression on FoxO: while an increase in FoxO phosphorylation occurred, which is expected given that Trbl D/NLK increases Akt activity, D/NLK potentially reduced total FoxO levels. This result makes the increase in phospho-FoxO following Trbl D/NLK misexpression even more striking in light of the significant decrease in total FoxO levels that occur simultaneously. In humans, Trib2 has been identified as a repressor of FoxO in malignant melanomas (Zanella et al., 2010) and complementarily, FoxO represses Trib3 expression to de-repress Akt and enhance insulin sensitivity in hepatocytes (Matsumoto et al., 2006). Thus, there is good reason to expect significant cross-regulation among insulin, Akt, FoxO, and Tribbles.

My demonstration that Trbl binds and blocks Akt activation without affecting Akt levels indicates functional conservation with Trib3, which was identified in a yeast two hybrid screen of Akt1 interactors and was shown to block phosphorylation-dependent activation of Akt, in a manner that required the conserved kinase domain (Du et al., 2003; He et al., 2006). Though some evidence contradicted these early findings (Iynedjian 2005), the notion that Trib3 regulates insulin signaling was bolstered by the identification of a Q84R single nucleotide polymorphism in Trib3 associated with insulin resistance and type 2 diabetes. When this population variant was introduced into a Trib3 transgene and misexpressed in cell culture, Q84R was shown to reduce Akt phosphorylation more potently, possibly by enhancing the binding between Trib3 and Akt (Andreozzi et al., 2008; Prudente et al., 2005).

The Trib family of proteins mediates a highly complex network of molecular and cellular interactions, yet how Tribs link these diverse pathways to allow proper cell function is poorly understood. In mice, Trib3 regulates lipogenesis by triggering the degradation of acetyl-CoA carboxylase 1 via association with an E3 ubiquitin ligase (Qi et al., 2006) and mediates the cellular endoplasmic reticulum stress response (Eder et al., 2008a; Ohoka et al., 2005; Shang et al., 2009; Yamamoto et al., 2007), suggesting this family of proteins integrates metabolic and inflammatory pathways in various tissues. In mice and humans, Trib3 levels are regulated by nutrient availability in skeletal muscle cells, β cells, adipocytes, and tumor cells, highlighting a possible role in the regulation of metabolic flux in insulin-sensitive tissues (Ding et al., 2008; Du and Ding 2009; Liew et al., 2010; Liu et al., 2010; Yacoub Wasef et al., 2006).

Since Tribs likely act as adaptor proteins to regulate multiple cell signaling pathways and key cell cycle components, it is unsurprising that they been associated with colorectal cancers (Miyoshi et al., 2009), breast cancer (Wennemers et al., 2011), melanoma (Zanella et al., 2010), acute myeloid leukemias (Dedhia et al., 2010; Gilby et al., 2010), esophageal carcinogenesis (Duggan et al., 2010) and chronic lymphocyte leukemia (Johansson et al., 2010). Despite a growing body of work featuring Trib protein's roles in cancer and metabolic disorders, a mechanistic understanding of the pathway disruptions underlying disease physiology is far from complete. That my data strongly support a role for Trbl in blocking Akt activity should serve to dispel confusion generated by contradictory data obtained from mammalian systems, and substantiate *Drosophila* as a well-equipped model organism to dissect Trib function in normal biology and disease due to the absence of Trib paralogs and presence of highly conserved pathways regulating metabolism and growth.

CHAPTER 4

EVOLUTIONARILY CONSERVED ARGININE 141 OF *DROSOPHILA* TRIBBLES PLAYS CRUCIAL ROLES IN THE REGULATION OF THE INSULIN- SIGNALING PATHWAY

Introduction

Insulin signaling pathway is an evolutionarily conserved cellular signaling system that maintains organismal nutrient homeostasis and diverse developmental processes including body size and sexual maturation in metazoan animals (Koyama et al., 2013). The binding of insulin (insulin-like peptides in insects) to insulin receptors on the surface of responsive tissues triggers a phosphorylation cascade to activate phosphoinositide-3 kinase (PI3K) (Carpenter et al., 1990). PI3K converts membrane phosphatidylinositol 4, 5-bisphosphate (PIP₂) to phosphatidylinositol 3,4,5-triphosphate (PIP₃) (Auger et al., 1989), leading to the recruitment of the Akt kinase to plasma membrane (Coffer et al., 1998; Downward 1998), where it is phosphorylated at Thr308 by phosphoinositide-dependent protein kinase 1 (PDK1) (Mora et al., 2004). PI3K also mediates activation of Mammalian Target of Rapamycin Complex 2 (mTORC2) (Zinzalla et al., 2011) that phosphorylates Akt at Ser473 (Sarbasov et al., 2006). Phosphorylation at these two sites activates the catalytic function of Akt. Akt is a central node in the insulin signaling pathway [reviewed in (Manning and Cantley 2007)]. It phosphorylates many substrates to promote anabolism and survival including: (1) the Rheb-specific GTPase activating protein (GAP) Tsc2 to induce Target of Rapamycin complex 1 (TORC1) signaling which promotes protein and lipid biosynthesis (Garami et al., 2003b; Miron et al.,

2003; Montagne et al., 1999; Porstmann et al., 2008) (2) GSK-3 β to inhibit gluconeogenesis and stabilize MYC to boost anabolic gene expression (Parisi et al., 2011; Teleman et al., 2008) (3) the pro-apoptotic protein BAD to inhibit apoptosis (Datta et al., 1997); and (4) the transcription factor FoxO to block its nuclear localization and reduce expression of catabolic and apoptotic FoxO target genes [reviewed in (Junger et al., 2003)]. Given the extremely important role that Akt plays in insulin signal transduction, it is not surprising that aberrant alteration of Akt function underlies the pathophysiological properties of insulin resistance syndrome, the precursor to the development of type 2 diabetes mellitus (T2DM) [reviewed in (Zdychova and Komers 2005)]

Drosophila Tribbles (Trbl) is a member of the Trib family of evolutionarily conserved protein kinases that play multiple roles in development, tissue homeostasis and diseases [reviewed in (Dobens and Bouyain 2012; Kiss-Toth 2011)]. Mammalian Tribbles homolog Trib3 has been identified as a key regulator of tissue growth and homeostasis. A major function of Trib3 is to inhibit insulin signaling by directly binding and inhibiting the activation-phosphorylation of Akt, leading to impaired insulin signaling in various insulin responsive tissues (Du et al., 2003; Koh et al., 2006; Koo et al., 2004; Liu et al., 2010) [reviewed in (Prudente et al., 2012)]. Akt inhibitory activity has also been attributed to Trib2 (Du et al., 2003). In addition, we recently identified the *Drosophila* Trbl (the only Trib protein in *Drosophila*) as an inhibitor of Akt activation and insulin signaling (Das et al., 2014), indicating that the function of Trib proteins in insulin signaling pathway is evolutionarily conserved.

A single nucleotide polymorphism (dsSNP ID: rs2295490) of human Trib3 associated with insulin resistance has recently been described. This non-synonymous polymorphism changes amino acid Glutamine (Q) at position 84 to arginine (R). Carriers of the R84 allele are predisposed to develop insulin resistance and early onset Type 2 Diabetes (T2DM) in different human populations (Gong et al., 2009; Prudente et al., 2010; Prudente et al., 2005). Cell culture studies indicate that 84R is a stronger inhibitor of Akt activation than the more prevalent Q84 allele (Andreozzi et al., 2008; Prudente et al., 2005). All Trib proteins share an extensive sequence homology at their central kinase domain (Hegedus et al., 2006) that is associated with binding and preventing Akt activation (Das et al., 2014; Du et al., 2003). This encouraged me to check if Q84 is conserved in other Trib proteins as well. We performed an extensive sequence alignment between *Drosophila* Trbl and all mammalian Trib proteins. Very surprisingly, I observed that R and not Q actually occupies the position corresponding to Trib3 84 in almost all Trib proteins; it is conserved in *Drosophila* Trbl (position R141) and all mammalian Trib1 and Trib2s (Figure 4.1A). Additionally, R but not Q was found in most other mammalian Trib3s (including chimpanzee Trib3); only Human and Neanderthal Trib3 contain Q at this position. I sought to determine if this extremely conserved R residue plays an important role in insulin signaling pathway and the function of Trbl in general. Therefore, I generated a mutant Trbl carrying Q at that site (changing R with Q; R141Q, referred as 141Q hereafter) and compared its activity with WT Trbl in relevant fly tissues.

I show here that 141Q is indeed a less potent inhibitor of Akt activation in adipose tissue: misexpression of 141Q did not prevent activating phosphorylation of dAkt (the only Akt in *Drosophila*) to the same extent as WT Trbl did and consequently, 141Q acted as a weaker inhibitor of insulin action, as demonstrated by effects of misexpression on developmental timing and various metabolite contents. I also observed that R141 is specifically involved with the regulation of insulin signaling, as misexpression of 141Q does not change WT Trbl's regulatory action on other cellular processes such as cell migration and division. Using in vivo and in vitro methods I show that 141Q increases Trbl's physical interaction strength with Akt but not with C/EBP transcription factor, a known binding partner of Trbl (Masoner et al., 2013), confirming that the 141Q mutation has effects specific for metabolism. I further confirmed the conserved role of R141 by showing that mouse Trib3 containing R at the conserved position was not only able to prevent Akt activation when introduced in the *Drosophila* adipose tissue, but also it did so with a potency similar to WT Trbl and significantly higher than that of 141Q. Taken together, the data presented here indicate that Trib3 Q84 appeared late during the course of evolution and suggest that this human and Neanderthal Trib3 variant conferred more avid interaction strength with Akt kinase, but reduced the potency of Akt inhibition, compared to related Trib3s.

Materials and methods

Drosophila strains

(1) *P{UAS-FLAG-trbl.WT}* (WT Trbl) (2) *P{UAS-FLAG-trbl.^{R141Q}}* (141Q) and (3) *P{UAS-FLAG- mouseTrib3}* are described below (3) *y1 w**; *P{r4-GAL4}3* was a generous gift from Laura Musselman. We obtained the following stocks from the Indiana Stock Center, (4) *P{en2.4-GAL4}e16E* (engrailed-GAL4, en-GAL4), (5) *y[1] w[1118]*; *P{w[+mC]=UAS-Akt1.Exel}2* (6) *w1118*; *P{GD11640}v22114*; from the Vienna stock center, (7) *{GAL4-slbo.2.6}1206 P{UAS-GFP.S65T}T2/CyO* (Slbo2.6-Gal4) was a generous gift from Pernille Rorth (8) *w[1118]*.

Construction of *UAS-FLAG-trbl WT* and *UAS-FLAG- mouse trib3*

The complete ORF of *trbl* and mouse *trib3* was amplified from cDNA using the oligonucleotides

ATGGATTACAAGGATGACGACGATAAGATGGATAACAGTAGCGGTC and
TCAGCCCATGTCCACATCCGTATCGGGTTC (for *trbl*) and

ATGGATTACAAGGATGACGACGATAAGATGCGAGCTACACCTCTG and
TCAGCCGTACAGCCCCACCTCCCCTTC (for *trib3*) to generate a N-terminal FLAG fusion (FLAG sequence in bold), cloned into pSTBlue-1 (AccepTor Vector kit, Novagen) and confirmed by DNA sequencing. An *EcoRI* fragment containing the full-length FLAGTrbl and FLAGTrib3 was then cloned into pUASTattB and again confirmed by DNA sequencing.

Construction of *UAS-FLAG-trbl^{R141Q}*

Mutated version of Trbl was generated from *pSTBlue-1+FLAGTrbl* using the QuikChange II XL Site-Directed Mutagenesis Kit (Stratagene) and oligonucleotide were designed as described therein. Following primers were used- 5'-CTAACCGCCTCCAATCTG**GAAT**GCGTGGACATCTTCACC-3' and 5'-GGTGAAGATGTCCACGC**ATTCC**AGATTGGAGGCGGTTAG-3'. Site-directed mutation were confirmed by DNA sequencing. Each of these transgenes were inserted into an attP vector (Bischof and Basler 2008) and injected to produce transgenic animals with insertions recombined into the second chromosome landing site (attP40; 25C7 on 2L) or third chromosome landing site (attP2; 68A4 on 3L). In this way, we could compare misexpression of mutant and WT transgenes while minimizing position effects. Embryo injections were performed as a fee-for-service (Genetic Services, Inc., Cambridge, MA), and transgenic lines established were confirmed for the presence of the WT or mutant transgene by sequencing of PCR product.

Yeast two-hybrid screen

The ProQuest Two-Hybrid System (Invitrogen) was used to perform yeast two-hybrid interaction tests. Plasmid DNA transformations of *Saccharomyces cerevisiae* strain MaV203 were performed as outlined in the kit manual and grown on SC media lacking both tryptophan and leucine to confirm the presence of both the bait and prey plasmids. Equal number of transformed cells (determined by O.D.₆₀₀ and accordingly diluting the stock) was then transferred to a series of plates to test for interactions: SC-Leu-Trp-His, SC-Leu-Trp-His+3AT (at various concentrations). Plate images were taken after 3-4 days of growth at 30°C. To

construct bait and prey plasmids *FLAGTrbl WT*, *FLAGTRBLR141Q* and *slbo*, cDNAs were amplified using PCR to add flanking *attB1* and *attB2* sites. Forward and reverse primers for *FLAGTrbl WT* and *FLAGTRBL^{R141Q}* were, respectively: 5'-

GGGGACAAGTTTGTACAAAAAAGCAGGCTTCATGGATTACAAGGATGACGAC

GATAAG -3'; and for *Slbo*, respectively, 5'-

GGGGACAAGTTTGTACAAAAAAGCAGGCTTCATGCTGAACATGGAGTCGCCG

CAG-3', 5'-

GGGGACCACTTTGTACAAGAAAGCTGGGTCCTACAGCGAGTGTTTCGTTGGTG

TTG-3'. To construct prey plasmid *Akt1* cDNA was amplified using PCR to add flanking *attB1* and *attB2* sites. Forward and reverse primers were:

GGGGACAAGTTTGTACAAAAAAGCAGGCTTCATGTCAATAAACACAACCTTTTCG

ACCTCAGCTC and

GGGGACCACTTTGTACAAGAAAGCTGGGTCCTATTGCATCGATGCGAGACTTG

TG (*attB1* and *attB2* sequences in bold). The PCR product was cloned into the donor vector pDONR-21 and then into either pDEST32 (bait vector) or pDEST22 (prey vector). All constructs were confirmed by DNA sequencing.

Protein sequence alignment

The amino acid sequence of *Trbl* was obtained from flybase.org (FBgn0028978). All other protein sequences were obtained from flybase. The Neanderthal Trib sequences were obtained from 'The Neanderthal genome project (<http://neandertal.ensemblgenomes.org>). Sequence alignment was performed with 'Clustal Omega' online alignment software (Sievers et al., 2011).

Fly husbandry

Fly stocks were maintained at 25°C on standard “Cornmeal, Molasses and Yeast Medium (CMYM)” recommended by Bloomington stock center. All the crosses were performed at 30°C and progeny animals were reared at 30°C.

Larval developmental stage synchronization

All experiments involving *Drosophila* larvae were performed with age-matched female larvae. To do this, ~ 150 virgin driver flies (2-5 days old) and UAS-transgene carrying male flies were reared in mini embryo collection cage (FLYSTUFF, catalog no. 59-105) on CMYM supplemented with yeast paste for two days. Food was changed every day. On day three, flies were transferred to a fresh food plate for 30 minutes to get rid of any held eggs. After that, flies were again flipped to a new food plate with regular food and allowed to lay eggs for 2-3 hours. After 18 hours, first instar larvae were collected and transferred to a fresh food plate and allowed to grow until they reach mid-third instar (~ 72 hours after egg deposition, determined by their size and branched anterior spiracle morphology). All experiments described in this report were performed with mid-third instar female larvae, which could be distinguished from male larvae by the considerably smaller size of female gonads. Control larvae for each experiment were obtained from crossing the driver line with W^{1118} males.

Larvae preparation for experiments

Third instar larvae containing food were transferred on a nylon mesh and thoroughly washed under slow flowing tap water to remove as much food particles as possible. Then the larvae were transferred to PBS and washed once more with

PBS. Fifteen female larvae were isolated and wiped briefly on kimwipe to remove residual PBS. Those larvae were used for experiments and all experiments were done in biological triplicate.

For analysis of body weight, larvae were weighed on a precision Kahn microbalance (model 4400).

For the pupation assay, ~30 synchronized mid-third instar larvae were collected and transferred to a new vial. The number of pupae formed (anterior spiracle eversion was used as a marker for pupation) were counted in every couple of hours. After 7 days, total number of pupae counted and assigned as 100%. The fraction of pupation was then plotted against time.

Quantification of metabolites

For total triglyceride quantification, larvae were homogenized on ice in 20 μ l of PBST (0.5% Tween20)/larva with a hand held homogenizer. Homogenates were then heated at 65⁰C for ~5 minutes to deactivate lipases and 20 μ l of homogenate was added to tube containing 680 μ l of Thermo Infinity™ Triglycerides Reagent, incubated at 37⁰C for 15 minutes followed by centrifugation at 10000g for 3 minutes to remove any suspending material and then the O.D. was measured on a plate reader at 540 nm. Triglyceride standards (Supelco triglyceride mix, cat. no. 17811-1AMP, from Sigma) ranging from 1-10 mg/ml were used to generate a standard curve. Triglyceride content was normalized to protein content from the same samples.

For glycogen quantification, larvae were homogenized on ice in 20 μ l of PBST (0.1% Tween20)/larva with a hand held homogenizer. Homogenates were then

heated at 65⁰C for ~5 minutes to deactivate glycogen breaking enzymes and 50µl of each homogenate was added to tube containing 450µl of Thermo Infinity™ glucose reagent+ Amyloglucosidase from Roche (Cat. no. 10 102 857 001) (5µl/ml of glucose reagent), incubated at 37⁰C for 2hours, followed by centrifugation at 10000g for 3 minutes to remove any suspending material and then the O.D. was measured on a plate reader at 340nm. Exactly same experiment was performed without any added amyloglucosidase to determine free glucose concentration in tissue and it was subtracted from the values from corresponding amyloglucosidase containing samples. Glycogen standards (Sigma, cat. no. G8751-5G) ranging from 0.1-2 mg/ml was used to generate standard curve. Glycogen content was normalized to the protein content of the same samples.

For protein quantification, larvae were homogenized on ice in 20µl of PBST (0.1% Tween20)/larva with a hand held homogenizer. Homogenates were then centrifuged (at 4^oc) at 10000g for five minutes and sup was collected. Protein concentration was determined from the sup using Pierce BCA protein assay kit according to manufacturer's protocol.

For hemolymph glucose and trehalose estimation, 15 female larvae were placed on a piece of parafilm. Then larval bodies were pierced with a fine tungsten needle near the mouthpart. Upon body wall piercing, hemolymph oozes out from the larvae. From 15 larvae, ~4µl of hemolymph was collected and immediately stored on ice. 2µl of hemolymph was diluted 10 fold in ice cold PBS and 5 µl of this diluted sample was mixed with 100µl pre-chilled Thermo Infinity™ glucose reagent for glucose assay. Then the samples were incubated at 37^oc for five minutes and the

O.D. was measured at 340 nm. For trehalose assay, porcine kidney trehalase (Sigma T8778) was added in 1 µl/ml of glucose reagent and the samples were incubated at 37°C overnight. Then the O.D. was measured at 340 nm. Free glucose concentration was subtracted from trehalase treated samples to determine only trehalose concentration. Glucose and trehalose standards ranging from 0.08-2 mg/ml and 0.08-5 mg/ml respectively were used to generate standard curve.

Western blots and Co-IP

Fat body was dissected from 30 age matched female larvae in PBS on ice and then transferred to homogenization buffer (10 µl/larva). After homogenization on ice, 20 µl was removed for protein assay. The rest of the sample was mixed with equal amount of 2x sample buffer and heated at 100°C for five minutes. Then the samples were centrifuged at 10000g for 5 minutes and supernatants containing equal amount of protein were loaded onto 10% SDS-PAGE gels. SDS-PAGE resolved bands were then transferred to Amersham Hybond PVDF membrane and western blotting was done according to standard protocol (Cell Signaling Technology). Blots were probed with the following antibodies (all at 1:2000 dilution): (1) phospho-*Drosophila* Akt (Ser505) Antibody (Cell Signaling #4054), (2) Akt (pan) (C67E7) Rabbit mAb (Cell Signaling #4691), (3) anti-alpha-tubulin (#12G10 Developmental Studies Hybridoma Bank). Blots were stripped and re-probed using mild stripping protocol of Abcam. Primary antibodies were used in the following order: pAkt, pan Akt, α Tubulin. Secondary antibodies conjugated to HRP (GeneScript) were used, and the signals were detected on X ray films by chemiluminescence using the Enhanced ECL kit (Biorad). Experiments were done in biological triplicate and at

least four unsaturated bands were used for quantification using Licor Image analysis software.

The entire co-IP experiment was performed at 4°C. On day 1, antibody conjugated PrecipHen (Goat anti-chicken conjugated sepharose beads, Aves lab) was prepared by washing PrecipHen three times with co-IP buffer, and then anti-Trbl antibody (in 1:20 ratio) was added to the beads and incubated overnight with agitation. Next day, unbound antibodies were removed by washing three times with co-IP buffer. Larval fat body was collected from ~100 larvae in ice-cold co-IP buffer (125mM Tris-Cl pH 7.6, 150mM NaCl, 2.5mM MgCl₂, 0.5mM EDTA, 0.5% NP-40, 5mM β-glycerophosphate, 1mM Sodium orthovanadate, 5mM sodium fluoride, 5% glycerol, protease inhibitors and freshly added 1mM PMSF). Then the samples were homogenized and the final volume was made up to ~500 µl by adding fresh co-IP buffer. Samples were then centrifuged at 10000g for 10 minutes to remove cellular debris. Protein concentration was determined by BCA assay and equal amount of protein was used for co-IP. For pre-wash, the sup was mixed with 50µl of PrecipHen and incubated for 30 minutes with agitation. Then the beads were removed by centrifugation at 2000g for three minutes and the sup was incubated with 100µl anti-Trbl antibody bound PrecipHen for three hours with mild agitation. After the incubation period, samples were washed three times with co-IP buffer and antibody bound protein complexes were eluted using glycine elution buffer and the pH was immediately normalized by adding Tris-Cl pH 8. Then the eluate was mixed with 4X SDS-PAGE sample buffer and subjected to SDS PAGE followed by western blotting as described in previous section. To detect Trbl, a nitrocellulose membrane instead

of PVDF was used because PVDF is not suitable for chicken antibody. Chicken anti-Trbl antibody was used at 1:1000 dilution and BlockHen (in 1:10 dilution in PBS) was used as blocking agent. Special HRP conjugated 2° antibody (Pierce Clean-Blot™ IP Detection Kit- HRP, doesn't bind to denatured 1° antibody present in co-IP eluate) was used to detect bands on western blot.

Fat body immunostaining

Approximately 15-20 larvae were dissected partially in PBS to open up the body cavity and expose the fat body, and then fixed in 4% paraformaldehyde in PBS for 20 minutes. Fixed tissue was washed for three times in PBST (PBS+0.1% TritonX100) and incubated with blocking reagent (PBST+ 2% normal goat serum+ 10% BlockHen) for two hours at room temperature with agitation. Then the samples were washed three times in PBST to remove excess blocking agent and incubated with 1° antibody (1:1000 chicken anti-Trbl, 1:500 rabbit anti Akt in PBST+ 2.5% BSA) overnight at 4°C with agitation. Tissue was washed three times in PBST. For the first wash, PBST was supplemented with 1:500 TRITC conjugated phalloidin and incubated for 15 minutes. After three washes, tissues were incubated with 2° antibody (Alexa Fluor conjugated IgG) in PBST+2.5% BSA for two hours at room temperature with agitation. After washing three times in PBST and once with PBS, a single strip of fat body from the ventral mid-section of each larva was collected and mounted on 75% glycerol to visualize the fluorescent staining. Micrographs were collected using an Olympus confocal laser-scanning microscope and figures prepared using imageJ.

Wing analysis

For wing analysis, crosses were reared at 30°C and progeny female wings were selected and mounted (one wing per female was used). For Fijiwings analysis, we used FijiwingsEZ and calculated wing size in kilo pixels and trichome density in “per kilo pixel²”.

Border cell migration assay

Crosses were reared at 30°C and progeny females were fed on CMYM supplemented with dry yeast for 2 days to boost egg production. On the third day, ovaries were dissected from ~20 females and stained for GFP (*Sibo* gene expression reporter, marks border cells). Migration status of BCs from stage 10 egg chambers were determined by randomly selecting ~50 egg chambers and observing the position of BCs. BCs at the nurse cell-oocyte boundary was considered to have completed the migration and positions away from nurse cell-oocyte boundary were considered as incomplete migration. Experiment was done in biological triplicate.

Statistical Analysis

Statistical analysis was performed using Graph Pad Prism (v 6.0) and one way ANOVA followed by either unpaired, two-tailed Student's T test (for analysis of 2-3 groups) or Tukey's post hoc analysis of significance (for more than 3 groups) were done. All data are presented as mean \pm SEM. A p value of less than 0.05 was considered significant.

Results

141Q is a less potent inhibitor of dAkt activation

During the active feeding stage of *Drosophila* larval development, fat body (equivalent to mammalian adipose tissue) stores nutrient in the form of lipid droplets and supplies the animal with essential nutrients during pupation or starvation (Butterworth FM 1965). Fat body is highly sensitive to insulin signaling and fat body specific alteration of insulin signaling exerts systemic effect on larval growth and maturation (Britton et al., 2002). Therefore, I used this established model system to study the R141Q mutation's effect on the activity of Trbl. In control fat body cells, endogenous Trbl can be detected localized to the cytoplasm, as revealed by Trbl specific antisera (Figure 4.1B, Top panel). Fat body specific driver *r4-Gal4* (Lee and Park 2004a) misexpression of a UAS-Trbl transgene resulted in prominent nuclear and membrane localization of Trbl (Figure 4.1B, middle panel). Misexpression of 141Q showed similar subcellular distribution (Figure 4.1B, bottom panel), indicating that R141 does not strongly affect sorting or localization of Trbl.

Next, I checked if the 141Q mutation compromises Trbl's ability to inhibit Akt activation. Cell culture evidences from human hepatocytes and vein endothelial cells suggest that the Trib3 R84 variant is a comparatively stronger inhibitor of Akt activation than the Trib3 Q84 variant (Andreozzi et al., 2008; Prudente et al., 2005). Accordingly, I predicted that the 141Q mutation would make Trbl a weaker inhibitor of dAkt activation. To test this hypothesis, I misexpressed WT Trbl or 141Q using *r4-Gal4* driver and performed western blot from fat body tissue extracts with anti-phospho Ser505 (equivalent to mammalian Ser 473) Akt and anti-pan Akt. Both WT Trbl and

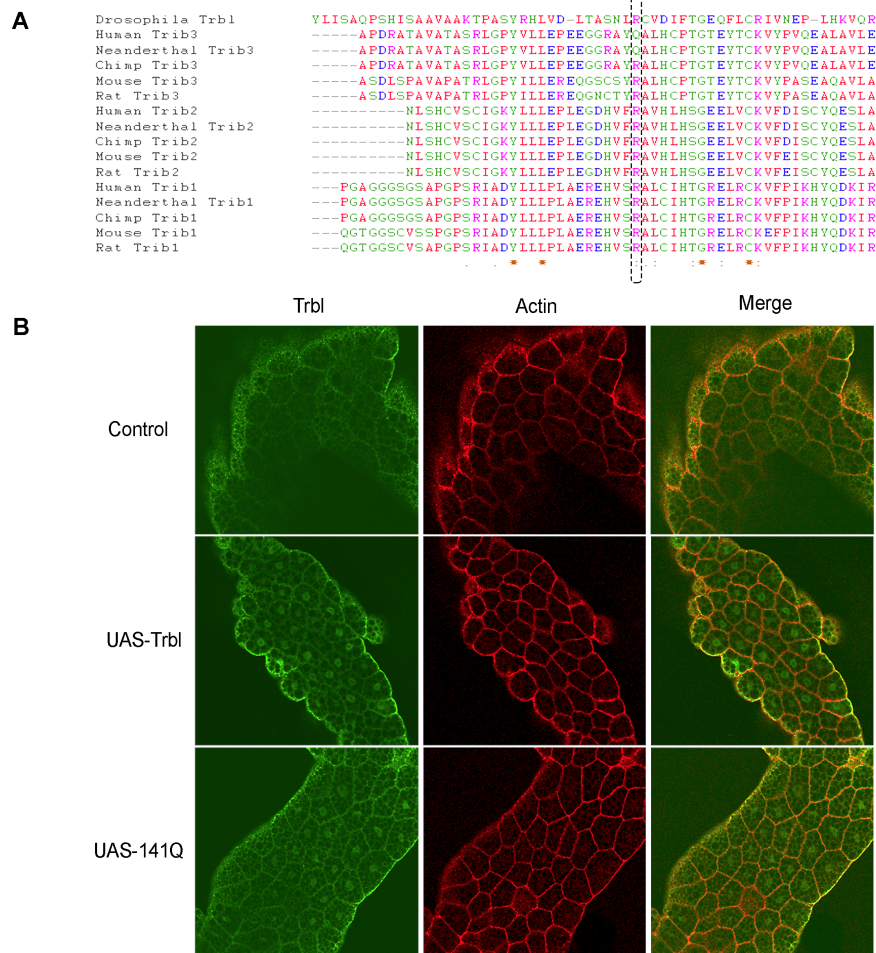


Figure 4.1- Human Trib3 Q84 position is highly conserved and contains R in most Trib proteins.

(A) Sequence alignment of Drosophila Trbl with mouse, chimpanzee, neanderthal and human Trib proteins. Positions corresponding to human Trib3 Q84 are highlighted with yellow
 (B) 141Q mutation does not alter Trbl’s subcellular localization. Genotype: Control- *r4-Gal4/+*, UAS-Trbl- *UAS-Trbl/+; r4-Gal4/+*, UAS-141Q- *UAS-Trbl^{R141Q}/+; r4-Gal4/+*. Note that all images were taken with identical confocal parameters.

141Q misexpression reduced pSer505 Akt level in comparison to control (Figure 4.2A, left panel), and quantification from multiple western blots revealed that both reductions were statistically significant (Figure 4.2C). However, WT Trbl-mediated inhibition was much more prominent; the extent of Akt Ser505 phosphorylation was ~70% lower in WT Trbl misexpression compared to that of 141Q. These observations clearly show the important role in Akt activation of the arginine residue at this conserved position in Trbl, leading me to test the effect of mouse Trib3 that contains R in the position corresponding to human Trib3 Q84 (Figure 4.1A). As shown in Figure 4.2A, mouse Trib3 misexpression resulted in a decrease in pSer505 level similar to that observed with WT Trbl but significantly lower than 141Q. In agreement with several previous observations (Das et al., 2014; Du et al., 2003; Prudente et al., 2005), none of the misexpressed transgenes significantly changed total Akt level (Figure 4.2C). In a complementary experiment, I knocked down Trbl in fat body using RNAi, and observed highly increased level in pSer505 without any change in total Akt level (Figure 4.2D) showing that Trbl plays a physiologically relevant role in Akt regulation in *Drosophila*.

141Q is a weaker inhibitor of insulin signaling

Third instar larva stop feeding and wander away from the food to start pupae formation when nutrient storage reaches a critical threshold necessary to sustain metabolic need during pupation phase and the timing of the pupa formation is regulated by insulin signaling (Shingleton et al., 2005). Trbl misexpression in the fat body delayed the timing of pupation. In contrast, 141Q misexpressing larvae pupariated normally (Figure 4.3A), consistent with the notion that 141Q is a weaker

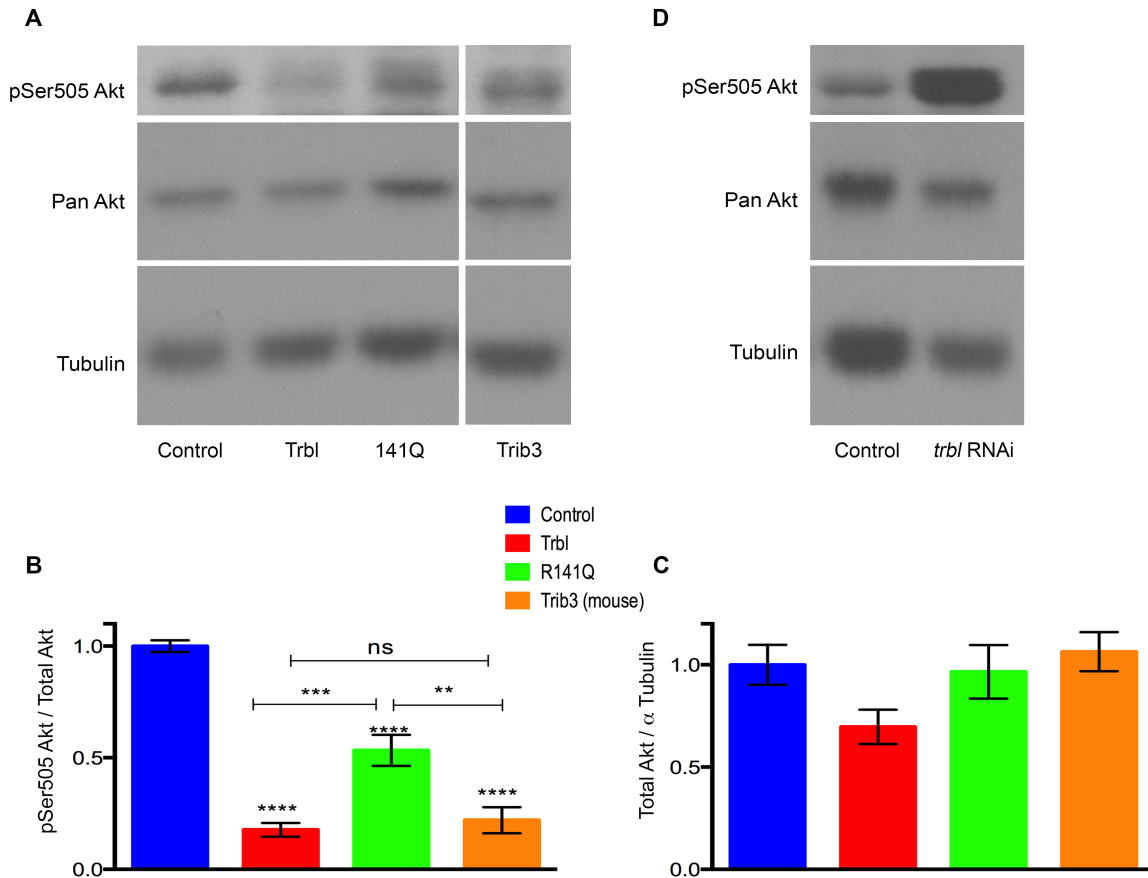


Figure 4.2: R141 plays crucial role in the inhibition of dAkt activation.

(A) Representative Western blot of fat body extracts from age matched mid-3rd instar larvae driving transgene expression by *r4-Gal4*. Genotype: Control- *r4-Gal4*/+, *Trbl*- *UAS-Trbl*/+; *r4-Gal4*/+, 141Q- *UAS-Trbl*^{R141Q}/+; *r4-Gal4*/+, *Trib3*- *UAS-mouseTrib3*/+; *r4-Gal4*/+.

(B and C) Quantification of Western blots of fat body extracts from three independent experiments (number of bands: 4-6) showing the effect of *Trbl*, 141Q and mouse *Trib3* on Akt activation and total Akt levels. α -Tubulin band was used as loading control and results were normalized to control. Genotypes are same as (A). P values from one-way ANOVA are “< 0.0001” for (B) and “non-significant” for (c). For (B), Tukey's multiple comparisons test was used to determine the significance (ns = not significant; *P<0.05; **P<0.01; ***P<0.001, ****P<0.0001). Error bars represent Mean \pm SEM.

(D) Representative western blot showing *trbl* knock down results in vast increase in pSer505Akt level (despite visibly lower level of Total Akt and α -Tubulin). Genotype: Control- *r4-Gal4*/+, *trbl*-RNAi- *r4-Gal4*/ *trbl* RNAi22114.

inhibitor of insulin signaling. *r4-Gal4* driven misexpression of either WT Trbl or R141Q significantly decreased larval body weight. R141Q misexpressing larva also weighed more than WT Trbl larva, though the difference was not statistically significant (Figure 4.3B). To see specific effects of 141Q mutation on metabolism, I next determined larval metabolite contents.

Consistent with its role in inhibiting the activation of Akt, a key inducer of the essential enzymes required for fatty acid biosynthesis (Porstmann et al., 2005; Porstmann et al., 2008), WT Trbl misexpression decreased larval triglyceride [constitute more than 90% of the stored fat in insects (Canavoso et al., 2001)] level by ~55%. In contrast, 141Q reduced triglyceride level by only ~40% (Figure 4.3C). Additionally, the triglyceride level in 141Q misexpressing larvae was significantly higher than that of WT Trbl (~30% increase), a difference that might explain the normal pupation rate seen following misexpression of 141Q.

In response to insulin, Akt acutely stimulates glucose uptake in adipose tissue (Kohn et al., 1996). Akt was found to be associated with GLUT4 glucose transporter containing vesicles upon insulin stimulation of mammalian adipocytes (Calera et al., 1998), and Akt activation results in GLUT4 translocation to the plasma membrane (Kohn et al., 1996). Hepatic Trib3 misexpression in mouse model system leads to hyperinsulinemia (Du et al., 2003; Matsushima et al., 2006) likely due to its ability to block Akt-mediated glucose uptake. Consistent with this, I showed previously that Trbl misexpression in the *Drosophila* fat body increases circulating sugar levels (Das et al., 2014). In humans, insulin sensitivity was found to be step-wise reduced from homozygous Q84Q to heterozygous Q84R to homozygous R84R

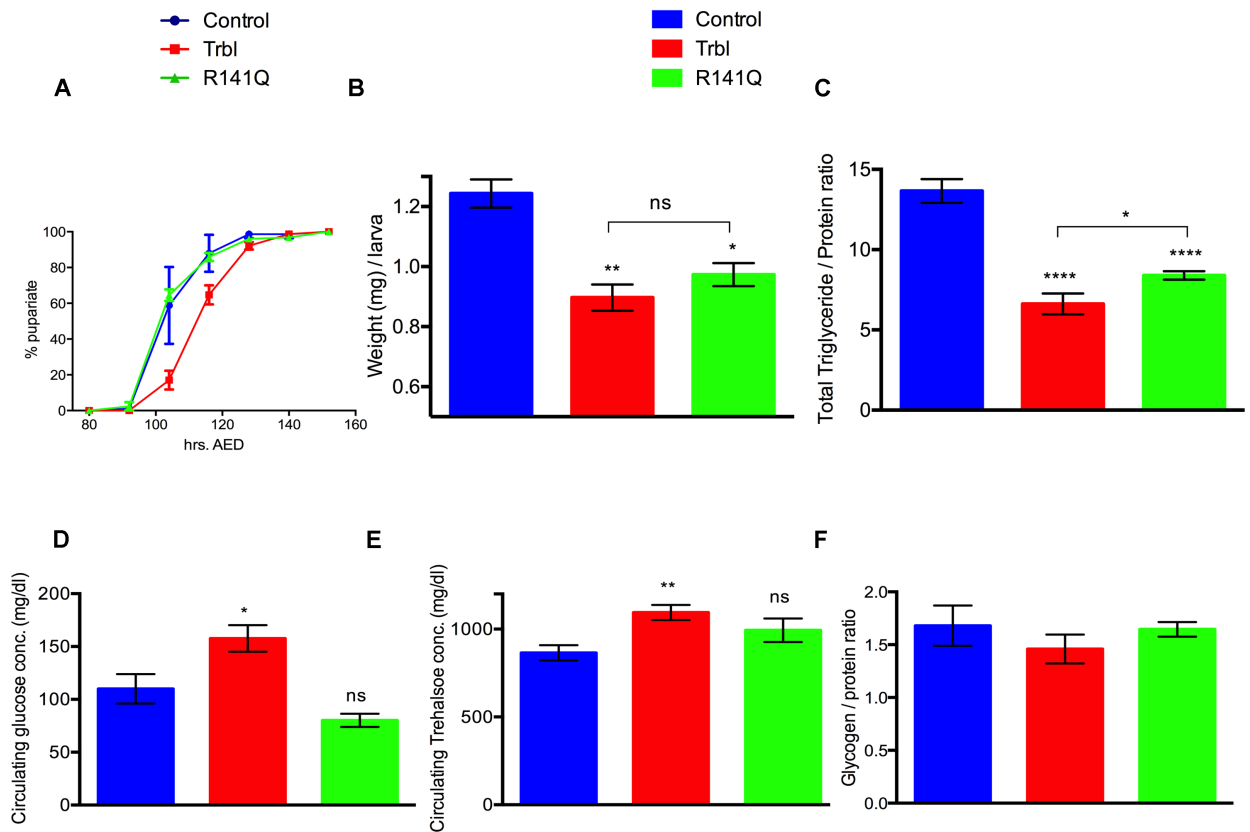


Figure 4 3: Trbl 141Q is a less potent inhibitor of larval growth and metabolism.

Genotype: Control- *r4-Gal4/+*, *UAS-Trbl- UAS-Trbl/+*; *r4-Gal4/+*, *UAS-141Q- UAS-Trbl^{R141Q}/+*; *r4-Gal4/+*. All experiments were done in biological triplicate. Error bars represent Mean \pm SEM.

(A) Fat body specific WT Trbl misexpression delays pupation compared to the control, whereas 141Q misexpressing larvae pupariate normally. Experiment was done in biological triplicate (AED - after egg deposit).

(B) Misexpression of both WT Trbl and 141Q reduces mid-3rd instar larval body weight significantly than WT Trbl. However, the weight differences between WT Trbl and 141Q is not significant.

(C-F) Comparison of metabolite contents of mid-third instar larvae misexpressing WT Trbl or 141Q in the fat body. (C) Stored triglyceride (D) circulating glucose (E) circulating trehalose and (F) stored glycogen. Note that triglyceride and glycogen contents are presented as relative to the protein content of the same sample (to normalize the weight difference between control and transgenes).

P values from one way ANOVA are " < 0.001 , < 0.0001 , 0.0012 , 0.02 and non-significant for B-F, respectively. Unpaired two-tailed T test was used to determine if the difference between two genotypes is significant (ns = not significant; * $P < 0.05$; ** $P < 0.01$; **** $P < 0.0001$).

individuals (Prudente et al., 2005). To determine the 141Q mutation's effect on circulating sugar levels, I collected hemolymph of larvae misexpressing either WT Trbl or 141Q in the fat body. Compared to control, misexpression of WT Trbl increased circulating glucose level by ~45%. In contrast, 141Q misexpression did not significantly alter circulating glucose concentration (Figure 4.3D). Because trehalose (a glucose disaccharide) constitutes the major form of circulating sugar in insects [reviewed in (Thompson 2003)], I measured circulating trehalose level as well in hemolymphs collected from WT Trbl and 141Q larvae. As expected, WT Trbl significantly increased circulating trehalose level (by~25%, compared to control) whereas 141Q misexpression did not show any significant change in trehalose levels (Figure 4.3E). This effect of the 141Q mutation on Trbl's activity could result from improved clearance of sugars from the hemolymph by body wall muscles that store sugars in the form of glycogen. To rule out this possibility, I measured larval glycogen content and found that neither WT Trbl nor 141Q misexpression in fat body alters larval glycogen level significantly (Figure 4.3F). It is important to note that body wall muscle is the major storage site of glycogen in *Drosophila* larvae (Ruaud et al., 2011). Taken together, these data indicate that the arginine 141 residue, corresponding to the conserved position Q84 in Trib3, is important for the function of Trbl-mediated regulation of metabolism.

141Q binds to Akt strongly than its WT counterpart

As 141Q is a weaker inhibitor of Akt activation, I assumed that 141Q would bind to Akt less strongly than its WT counterpart, allowing more phosphorylation of Akt at Ser505. To test this assumption, I performed yeast two hybrid (Y2H) assay by

expressing either WT Trbl or 141Q in the bait vector and dAkt in the prey vector. To my surprise, 141Q was found to interact with Akt1 more strongly, resulting in detectable growth in presence of up to 75 mM 3AT (3-Amino-1, 2,4-triazole) on His⁻ dropout plates, whereas WT Trbl could grow well only up to 50 mM of 3AT (Figure 4.4A). I sought to further investigate Trbl-Akt interaction in vivo by performing co-immunoprecipitation (co-IP) analysis from fat body extracts misexpressing dAkt and either WT Trbl or 141Q. Western blot analysis of eluates bound to Trbl antisera showed that while Akt co-immunoprecipitation occurs with both WT Trbl and 141Q, considerably more Akt was associated with the same amount of 141Q than WT Trbl (Figure 4.4B). Collectively, these results suggest that the Q variants – mouse Trib3 and 141Q here –are weaker inhibitors but stronger interaction partners of Akt, resulting in far reaching consequences for metabolism as described in the discussion section.

141Q mutation selectively affects insulin signaling and interaction with Akt

Other than Akt, Trib proteins have been reported to control the activity of several other key regulatory proteins by physically interacting with them. I wanted to see whether 141Q mutation only affects interaction with Akt or it is instrumental for other aspects of Trbl function. Therefore, I tested interaction with these proteins in vivo and in vitro with either WT Trbl or 141Q.

Drosophila C/EBP transcription factor homolog Slbo is a key regulator of border cell (BC) migration during oogenesis. Trbl promotes proteasomal degradation of Slbo required for proper BC migration (Rorth et al., 2000), consequently misexpression or knock down of Trbl inhibits border cell migration (Masoner et al.,

2013). Similarly, mammalian Trib3 and Trib2 also inhibit C/EBP activity (Bezy et al., 2007; Dedhia et al., 2010). To study the impact of 141Q mutation on Slbo activity, I misexpressed either WT Trbl or 141Q specifically in the BCs using *slbo2.6-Gal4* driver and compared the extent of BC migration inhibition in populations of egg chambers. As shown in Figure 4.4C, both WT Trbl and 141Q elicited similar inhibitory effect on BC migration (measured at developmental stage 10, when border cells finished migration). In addition, I tested interaction strength between Slbo and WT Trbl or 141Q using Y2H assay. Both interacted strongly with Slbo, manifested by the growth under very stringent conditions, i.e. in the presence of 100 mM 3AT (Figure 4.4D). Together these results indicate that 141Q does not alter either Slbo turnover or Slbo-Trbl interactions.

Trbl inhibits somatic cell division by binding and promoting degradation of String, a *Drosophila* homolog of CDC25 phosphatase. Trbl misexpression in the third posterior compartment of the wing imaginal disc (actively proliferating precursor of adult wing tissue) by the *en-Gal4* driver resulted in cell growth without cell division. As a result, trichome (single hair protrusion projecting out from each mature wing cell) density in third posterior compartment is reduced compared to the anterior wing compartment where Trbl is not misexpressed (Mata et al., 2000). We misexpressed either WT Trbl or 141Q in the third posterior compartment by *en-Gal4* and compared trichome density of the third posterior intervein region to that of marginal intervein region using FijiWings (Dobens and Dobens 2013). As shown in Figure 4.4E, misexpression of both transgenes resulted in a similar reduction in trichome density ratio of third posterior to that of marginal compartment.

Figure 4.4: R141 plays a crucial role only in Trbl's physical interaction with Akt and the regulation of insulin signaling.

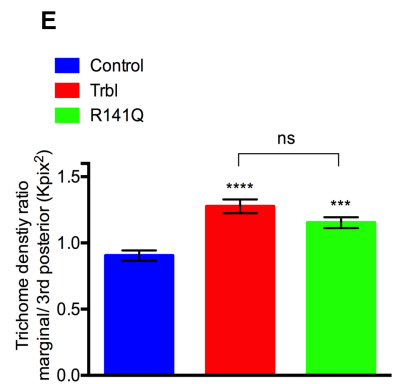
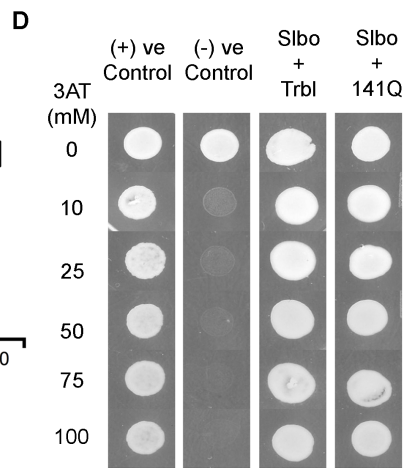
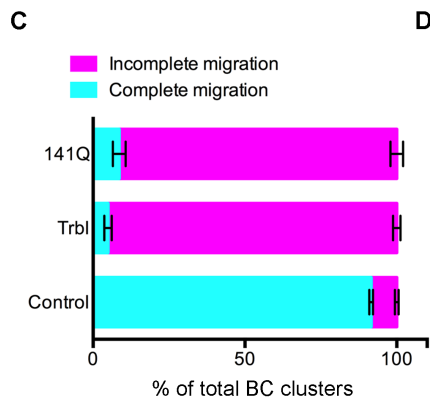
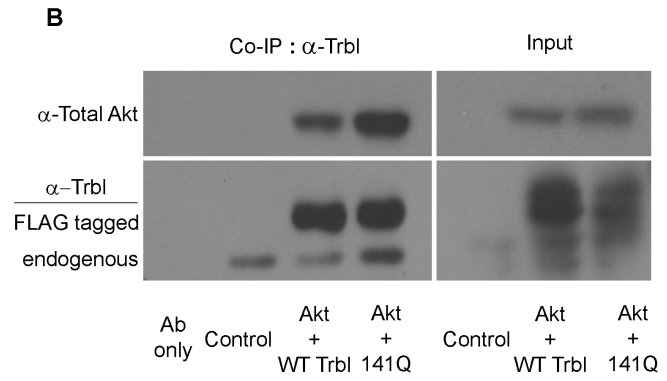
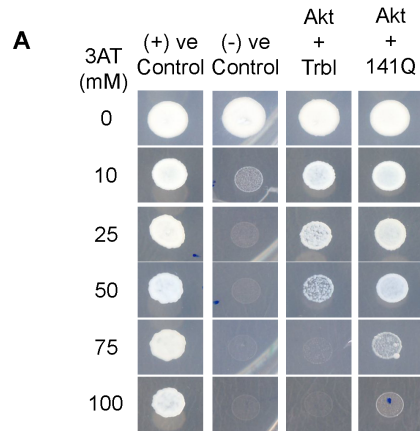
(A) Yeast 2 hybrid assay showing 141Q binds to Akt more strongly than WT Trbl in vitro. The ability of yeast cells to grow on increasing concentrations of 3AT growth inhibitor depends on the strength of the protein-protein interaction. Yeast cells co-expressing Akt prey and R141Q bait are able to grow well in the presence of up to 75 mM 3AT whereas cells co-expressing Akt and WT Trbl could only grow in presence of up to 50 mM 3AT. Note that equal numbers of transformed yeast cells were used to seed the plates used for assay.

(B) Co-IP from fat body extracts co-misexpressing Akt with Trbl and 141Q showing 141Q is a stronger binding partner of Akt than WT Trbl in vivo. A representative western blot is shown. Left panel shows the presence of more total Akt (α -Total akt bands) associated with 141Q than WT Trbl, although Akt level is same in the tissue extract used for co-IP (right panel, input). No Akt is visible in control bands. Also, Trbl level is similar in eluted samples (α -Trbl bands) as well as in inputs. Note that in addition to misexpressed Trbl/141Q, chicken anti-Trbl antibody could also detect endogenous Trbl. Ab only: Co-IP procedure was done with only co-IP antibody (without any tissue extract) alongside other samples. Serves as 2^o antibody control during western blot, Genotype: Control- *r4-Gal4/+*, UAS-Trbl- UAS-Trbl/UAS-Akt; *r4-Gal4/+*, UAS-141Q-UAS-Akt, UAS-Trbl^{R141Q}/+; *r4-Gal4/+*

(C) 141Q does not interfere with Trbl's ability to prevent Slbo mediated border cell (BC) migration. *Slbo2.6-Gal4* drives transgene expression in the BCs with the pattern of Slbo expression. Compared to control, Trbl and 141Q misexpression prevents BC migration to a similar extent (C). Genotype: Control- *Slbo2.6-Gal4/+*, Trbl- *Slbo2.6-Gal4/UAS-Trbl*, 141Q- *Slbo2.6-Gal4/UAS-Trbl^{R141Q}*. Error bars represent Mean \pm SEM.

(D) Yeast 2 hybrid assay showing that R141 is not required for physical interaction between Trbl and Slbo. Yeast cells co-expressing Slbo prey and WT Trbl or R141Q bait are able to grow well under very stringent condition i.e. in the presence of up to 100 mM 3AT. Note that equal number of transformed yeast cells was used to seed the plates used for assay.

(E) 141Q is not essential for Trbl's ability to inhibit cell division. *En-Gal4* mediated misexpression of WT Trbl and R141Q leads to similar degree of inhibition of cell division, resulting in decrease in trichome density in 3rd posterior compartment (normalized to marginal compartment) of the wing. Error bars represent Mean \pm SEM (n=10 for control, 7 for WT Trbl and 141Q). Genotype: Control- *en-Gal4/+*, Trbl- *en-Gal4/UAS-Trbl*, 141Q- *en-Gal4/UAS-Trbl^{R141Q}*. P value from one way ANOVA < 0.0001. Unpaired two-tailed T test was used to determine if the difference between two genotypes is significant (ns = not significant; ***P<0.001, ****P<0.0001).



Taken together, these results suggests that R141, which plays a crucial role in binding and preventing Akt activation, does not affect Trbl's interaction with other key regulators of cellular processes, and this aspect of Trbl function could be exploited potentially for the treatment of insulin resistance and diabetes (see details in discussion section).

Discussion

In this chapter, I show the importance of an arginine (R141) residue in the function of Trbl on insulin signaling. This R residue is evolutionarily conserved in almost all mammalian Trib proteins excluding human and Neanderthal Trib3s, where the prevalent residue is Glutamine (Q84) (supplementary document 1), indicating that Trib3 Q84 appeared late during mammalian evolution. In humans, a polymorphism where R replaces Q84 (Q84R) has been associated with insulin resistance and Type 2 diabetes (Prudente et al., 2005; Prudente et al., 2009). Human cell culture studies show that compared to the Q84 variant, R84 Trib3 is a stronger inhibitor of the activation of the Akt kinase, a key mediator of insulin action. Here I report that when the R141 of *Drosophila* Trbl is mutated to Q (141Q), it significantly decreases the ability of Trbl to prevent the activation of Akt (Figure 4.2), and consequently, does not inhibit larval growth and anabolism as effectively as WT Trbl (Figure 4.3). In addition, I observed that R141Q mutation increases Trbl's physical interaction strength with Akt both in vivo and in vitro (Figure 4.4). Collectively, these observations suggest that Trib Q variants bind to Akt more strongly but do not block Akt activation as potently as Trib R variants. In agreement with this notion, I found that when mouse Trib3 (a R variant Trib) is misexpressed in

Drosophila fat body, it inhibits Akt activation to an equivalent extent as *Drosophila* WT Trib1 and significantly more than 141Q mutant Trib1 (Figure 4.2A and B).

The presence of Q in human and Neanderthal Trib3 could have been instrumental for their remarkable capability of long distance running that originated in the genus *Homo* about 2 million years ago [reviewed in (Bramble and Lieberman 2004)]. Human long distance running is an energetically demanding practice (Taylor and Heglund 1982) requiring a constant supply of fuel for a long period of time and temporary inhibition of anabolic processes. At the same time, cells must endure the limiting nutrient conditions and not undergo starvation-induced apoptosis. Human cell culture studies demonstrated that Trib3 expression level is induced upon glucose and amino acid starvation (Schwarzer et al., 2006). Also, short-term nutrient deprivation causes an increase in *trib3* mRNA and protein levels in adipose tissue of rats (Liu et al., 2012). These observations imply that in general, mammalian Trib3 acts as a 'brake' on insulin signaling under limited nutrient conditions to temporarily prevent Akt mediated anabolism. In humans, however, during extreme physical activity such as endurance running, Trib3 additionally allows residual Akt activity to continue by lesser degree of inhibition and protecting Akt from other Trib proteins. This hypothesis is supported by observed overlapping expression of all Trib proteins, most noticeably in white adipose tissue (Okamoto et al., 2007) and Trib2's ability to bind and inhibit Akt activation (Du et al., 2003). Akt plays a central anti-apoptotic role [reviewed in (Franke et al., 2003; Zhang et al., 2011)], and Akt signaling allowed by human Trib3 under low nutrient conditions may promote cell survival. A strong support for this postulate comes from the observation in human cell culture, where

Trib3 has been shown to prevent starvation induced apoptosis (Schwarzer et al., 2006).

The R141 motif is located at the N terminus of the conserved kinase domain of Trib proteins. In the previous chapter I have reported the contribution of the kinase domain's DLK motif to Trbl's ability to inhibit Akt activation and physical interaction with Akt. The kinase domain of mouse Trib3 has also been attributed to the interaction with and inhibition of Akt (Du et al., 2003). However, the DLK motif is absolutely conserved in all Trib proteins and mutation in this motif completely abolishes Trbl-Akt physical interaction. The DLK motif is also required for Trib protein's interaction with C/EBP and mediating proteasomal degradation of C/EBPs (Keeshan et al., 2010; Masoner et al., 2013). In this respect, R141 is unique because it is only required for interaction with and inhibition of Akt and 141Q mutation does not interfere with Trbl's ability to inhibit cell division or interact and mediate proteasomal degradation of C/EBP (Figure 4). For these reasons, the R141 motif presents a good therapeutic target. A drug molecule that masks this surface would likely prevent Trib-Akt interactions without affecting functions of Trib proteins in other key cellular processes and could be useful to treat insulin resistance.

CHAPTER 5

APPENDIX

Trib2 inhibits Akt activation in *Drosophila* fat body

In previous chapter, I have demonstrated the evolutionarily conserved function of Trib proteins in Akt inhibition by showing that when introduced in the fat body, mouse Trib3 is capable of inhibiting endogenous dAkt activation (Figure 4.2). To further test this hypothesis, I misexpressed mouse Trib2 in larval adipose tissue in the similar manner as described in 'materials and methods' section of chapter 4. Western blot analysis from fat body extract indicates that compared to the control, phosphorylation level of the Akt Ser505 decreases significantly upon Trib2 misexpression (Figure 5.1), pointing to the extremely conserved nature of the regulation of insulin signaling by Trib proteins. Taken together with Figure 4.2, this result indicates that in the absence of an individual Trib homolog (for instance in a knockout animal), other Trib proteins may functionally compensate, resulting in normal physiology as observed in *trib2* or *trib3* knockout animals (Okamoto et al., 2007). These results also indicates that Trib homologs may have tissue specific functions controlled by non-conserved N and C terminal domains. These regions may bind to regulatory proteins present in specific tissues and mediate tissue specific function of Trib proteins.

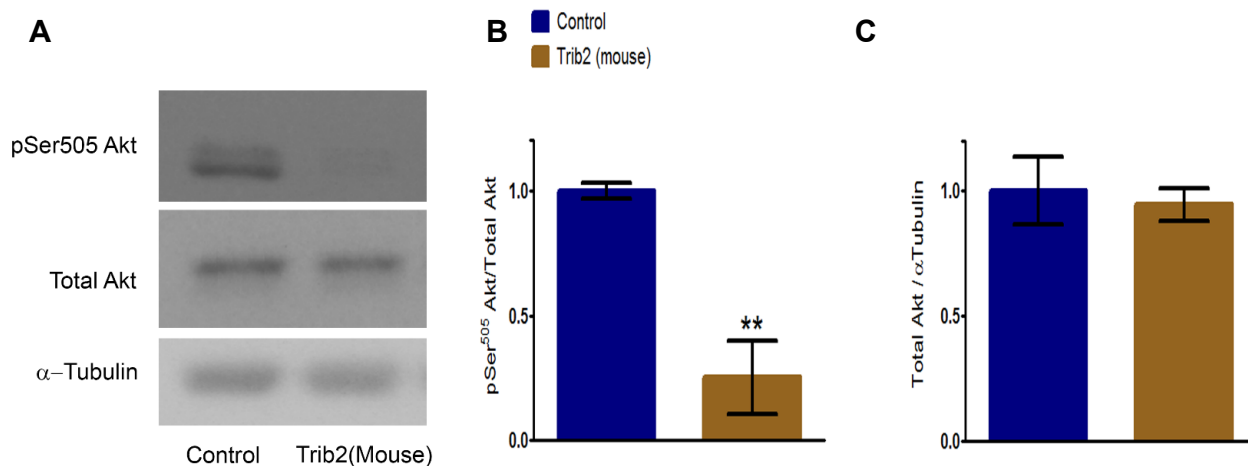


Figure 5.1: mouse Trib2 can inhibit endogenous dAkt activation in fat body.

(A) Representative Western blot of fat body extracts from age matched mid-3rd instar larvae driving transgene expression by *r4-Gal4*. Genotype: Control- *r4-Gal4/+*, Trib2- *UAS-Trib2/+; r4-Gal4/+*,

(B and C) Quantification of Western blots of fat body extracts from three independent experiments (number of bands: 3-4) showing the effect of mouse Trib2 on Akt activation and total Akt levels. α -Tubulin band was used as loading control and results were normalized to control. Student's T test was used to determine the significance (** $P < 0.01$). Error bars represent Mean \pm SEM.

CHAPTER 5

FUTURE DIRECTIONS

Molecular mechanism of Trbl-Akt interaction

In previous chapters, I have described the ability of WT Trbl and two mutant versions of Trbl to physically interact with Akt and prevent the Akt activation by phosphorylation at Ser505. The D/NLK mutation in the conserved catalytic loop of Trbl completely abolishes both the Trbl-Akt physical interaction and Akt activation. In contrast, the R141Q mutant is a comparatively weaker inhibitor of Akt activation than WT Trbl but it binds to Akt more strongly. Assuming the sole mode of the Akt inhibition by Trbl is by directly binding to Akt and blocking the access of TORC2 complex to Ser505 site, what could be the reason behind the observed inconsistency between Akt binding and Ser505 phosphorylation-inhibitory activity of 141Q mutant described in chapter four? One model that I have developed to fit all the observations regarding Trbl-Akt interactions invokes the novel notion that Akt phosphorylates and inactivates Trbl to boost anabolic processes, analogous to the Akt-mediated phosphorylation-inhibition of FoxO transcription factors. Upon insulin-stimulated activation, Akt binds to FoxO and phosphorylates three extremely conserved (from worms to humans) Akt phosphorylation sites [reviewed in (Tzivion et al., 2011)], resulting in nuclear exclusion of FoxO and subsequent suppression of FoxO target genes that promote catabolism. Genetic evidence that Akt blocks Trbl activity is seen in Figures 3.1, 3.4 B-D and 3.4 H-J where co-misexpression of Akt can inhibit Trbl's growth suppression phenotypes in different *Drosophila* tissues. While evidence that Akt directly phosphorylates Trbl is lacking, I note that threonine

147 of Trbl, located just downstream of R141 (Figure 4.1), is well conserved in all Trib proteins and resembles Akt consensus phosphorylation site (RxRxxS/T, where x represents any amino acid).

It has been reported that PRMT1 (Protein Arginine Methyl Transferase 1, a conserved enzyme that adds methyl group to the selective arginine residues on substrate proteins) methylates FoxO at Arg248 and Arg250 within a consensus motif for Akt phosphorylation, to block Akt binding and phosphorylation-inactivation (Yamagata et al., 2008). If similarly Akt interacts with Trbl via R141 motif and this interaction is required for the phosphorylation-inactivation of Trbl, my model predicts that methylation of Trbl at R141 by dART1 (the *Drosophila* homolog of PRMT1) will block this inhibition by reducing Akt affinity for this site; as a result, methylated 141R is resistant to Akt phosphorylation-inactivation and can effectively inhibit Akt activation.

According to my model, the 141Q mutant is not methylated and thus binds more readily to Akt (as shown in Figure 4.4A and B) and consequently 141Q is phosphorylated readily by Akt at Thr147, thus reducing Trbl's ability to inhibit Akt (as shown in Figure 4.2A and 4.3). If this prediction is correct, dART1 misexpression should enhance Trbl activity but it will have no effect on 141Q activity, which can be tested initially in several assays of Trbl activity in vivo. In the wing assay, co-misexpression of dART1 and Trbl would decrease trichome density to a greater extent than Trbl misexpressed alone. On the other hand, dART1 should not interact with 141Q and thus its co-misexpression with 141Q should have no effect on the reduction in trichome density caused by 141Q misexpression alone. In a

complementary manner, my model predicts that Akt would inhibit 141Q more strongly than WT Trbl, which can also be tested initially in the wing misexpression assay. As shown in Figure 3.1, co-misexpression of Akt by *en-Gal4* driver suppresses Trbl's ability to inhibit cell division. I predict that co-misexpression of Akt with 141Q mutant would result in even higher degree of inhibition of the Trbl activity, resulting in further increase in trichome density compared to Akt and WT Trbl co-misexpression. If preliminary results match with my prediction, this notion could be tested further by misexpressing Trbl in the larval fat body and identifying Trbl with methylated arginine 141 and phosphorylated threonine147 residues by specific custom-made antibodies on western blots. A second way to test the hypothesis would be to perform mass spectrometric analysis of the immunoprecipitation eluate of fat body extracts misexpressing WT Trbl or 141Q and identify methylated Arg141 and phosphorylated Thr147. Starvation may induce methylation at R141 (to prevent Akt activation more strongly), so fat body collected from larvae misexpressing Trbl under starvation condition would probably be more suitable for the detection of methylation at R141 site.

Trbl inhibits the TORC2 complex activity

TORC2 is a multi-protein complex consisting of TOR (target of rapamycin), RICTOR (rapamycin-insensitive companion of mTOR), GβL, SIN1 (stress-activated protein kinase interacting protein 1), Protor 1/2, DEPTOR, TTI1 and TEL2 (Frias et al., 2006; Sarbassov et al., 2004; Sarbassov et al., 2005). TORC2 phosphorylates Akt at Ser473 (Sarbassov et al., 2005) (equivalent to Ser505 of dAkt). Both TORC1 and TORC2 are evolutionarily conserved protein complexes with a multitude of

functions in cell division and nutritional homeostasis [reviewed in (Loewith and Hall 2011)]. One observation I made while testing the ability of Trbl to inhibit insulin signaling in various *Drosophila* tissues is the following - misexpression of Trbl alone in larval body wall muscle by *Mef2Gal4* driver does not change muscle size, however, co-misexpression of Trbl with Akt can prevent muscle hypertrophy caused by Akt misexpression alone (see Figure 3.4). If Trbl inhibits insulin signaling only by inhibiting Akt, Trbl misexpression alone by *Mef2Gal4* should have resulted in muscle hypotrophy, as seen with classical inhibitors of insulin signaling pathway, such as PTEN (Demontis and Perrimon 2009). The absence of such muscle phenotypes upon Trbl misexpression indicates a more complex regulation of nutrient homeostasis by Trbl. It has been shown in the mouse model system that skeletal muscle-specific inhibition of mTORC2 (mammalian TORC2) by deleting the *raptor* gene has no physiological effect (Bentzinger et al., 2008). Another genetic evidence of the regulation of TORC2 complex by Trbl comes from my observation of *trbl* null mitotic clones in the follicle cells. I observed that if the edge of the mitotic clone reaches nurse cell-oocyte boundary, it disrupts supracellular organization of the actin networks present at that boundary. mTORC2 has been reported to control actin polymerization and organization (Huang et al., 2013). Therefore, it is possible that absence of Trbl in the clone cells alters TORC2 activity, resulting in the disruption of the actin network organization. Based on these observations, I propose the following model of the inhibition of the insulin signaling by Trbl: in addition to binding to Akt, Trbl's inhibitory action on insulin signaling also comes from binding and inhibiting dTORC2 (*Drosophila* TORC2) complex. A very strong support for this hypothesis

comes from cited but unpublished data suggesting that Trib3 may bind to Rictor (Cunard 2013).

Inhibition of TORC2 by Trbl can be directly tested by misexpressing Trbl in TORC2 sensitive tissues such as fat body (Cybulski et al., 2009) and looking for association between Trbl and components of the TORC2 complex (such as Rictor) in the eluate from co-immunoprecipitated Trbl by western blot. In addition to Akt, mTORC2 is also known to phosphorylates PKC- α (protein kinase C- α) (Guertin et al., 2006). So, another way of testing Trbl's action specifically on TORC2 would be to test the adipose tissue extract for the change in the levels of phosphorylated PKC- α upon Trbl misexpression (by western blot using commercially available total PKC- α and phospho- PKC α antibody).

REFERENCES

- Abdelilah-Seyfried S, Chan YM, Zeng C, Justice NJ, Younger-Shepherd S, Sharp LE, Barbel S, Meadows SA, Jan LY, Jan YN. 2000. A gain-of-function screen for genes that affect the development of the *Drosophila* adult external sensory organ. *Genetics* 155(2):733-752.
- Ables ET, Drummond-Barbosa D. 2010. The steroid hormone ecdysone functions with intrinsic chromatin remodeling factors to control female germline stem cells in *Drosophila*. *Cell Stem Cell* 7(5):581-92.
- Andreozzi F, Formoso G, Prudente S, Hribal ML, Pandolfi A, Bellacchio E, Di Silvestre S, Trischitta V, Consoli A, Sesti G. 2008. TRIB3 R84 variant is associated with impaired insulin-mediated nitric oxide production in human endothelial cells. *Arterioscler Thromb Vasc Biol* 28(7):1355-60.
- Angyal A, Kiss-Toth E. 2012. The tribbles gene family and lipoprotein metabolism. *Curr Opin Lipidol* 23(2):122-6.
- Ashton-Chess J, Giral M, Mengel M, Renaudin K, Foucher Y, Gwinner W, Braud C, Dugast E, Quillard T, Thebault P et al. . 2008. Tribbles-1 as a novel biomarker of chronic antibody-mediated rejection. *J Am Soc Nephrol* 19(6):1116-27.
- Auger KR, Serunian LA, Soltoff SP, Libby P, Cantley LC. 1989. PDGF-dependent tyrosine phosphorylation stimulates production of novel polyphosphoinositides in intact cells. *Cell* 57(1):167-75.
- Bailey FP, Byrne DP, Oruganty K, Evers CE, Novotny C, Shokat KM, Kannan N, Evers PA. 2015. The Tribbles 2 (TRB2) pseudokinase binds to ATP and autophosphorylates in a metal-independent manner. *Biochem J*.
- Barcelo H, Stewart MJ. 2002. Altering *Drosophila* S6 kinase activity is consistent with a role for S6 kinase in growth. *Genesis* 34(1-2):83-5.

- Battle E, Sancho E, Franci C, Dominguez D, Monfar M, Baulida J, Garcia De Herreros A. 2000. The transcription factor snail is a repressor of E-cadherin gene expression in epithelial tumour cells. *Nat Cell Biol* 2(2):84-89.
- Bentzinger CF, Romanino K, Cloetta D, Lin S, Mascarenhas JB, Oliveri F, Xia J, Casanova E, Costa CF, Brink M et al. . 2008. Skeletal muscle-specific ablation of raptor, but not of rictor, causes metabolic changes and results in muscle dystrophy. *Cell Metab* 8(5):411-24.
- Bezy O, Vernochet C, Gesta S, Farmer SR, Kahn CR. 2007. TRB3 blocks adipocyte differentiation through the inhibition of C/EBPbeta transcriptional activity. *Mol Cell Biol* 27(19):6818-31.
- Bi XP, Tan HW, Xing SS, Wang ZH, Tang MX, Zhang Y, Zhang W. 2008. Overexpression of TRB3 gene in adipose tissue of rats with high fructose-induced metabolic syndrome. *Endocr J* 55(4):747-52.
- Bischof J, Basler K. 2008. Recombinases and their use in gene activation, gene inactivation, and transgenesis. *Methods Mol Biol* 420:175-95.
- Bramble DM, Lieberman DE. 2004. Endurance running and the evolution of Homo. *Nature* 432(7015):345-52.
- Britton JS, Lockwood WK, Li L, Cohen SM, Edgar BA. 2002. Drosophila's Insulin/PI3-Kinase Pathway Coordinates Cellular Metabolism with Nutritional Conditions. *Developmental Cell* 2(2):239-249.
- Broggiolo W, Stocker H, Ikeya T, Rintelen F, Fernandez R, Hafen E. 2001. An evolutionarily conserved function of the Drosophila insulin receptor and insulin-like peptides in growth control. *Curr Biol* 11(4):213-21.
- Burkhardt R, Toh S-A, Lagor WR, Birkeland A, Levin M, Li X, Robblee M, Fedorov VD, Yamamoto M, Satoh T et al. . 2010. Trib1 is a lipid- and myocardial infarction-associated gene that regulates hepatic lipogenesis and VLDL production in mice. *J Clin Invest* 120(12):4410-4414.
- Butterworth FM BD, King RC. 1965 Adipose tissue of drosophila melanogaster. I. An experimental study of larval fat body. *J Exp Zool Mar* 158: 141-53.

- Calera MR, Martinez C, Liu H, Jack AK, Birnbaum MJ, Pilch PF. 1998. Insulin increases the association of Akt-2 with Glut4-containing vesicles. *J Biol Chem* 273(13):7201-4.
- Canavoso LE, Jouni ZE, Karnas KJ, Pennington JE, Wells MA. 2001. Fat metabolism in insects. *Annu Rev Nutr* 21:23-46.
- Cano A, Perez-Moreno MA, Rodrigo I, Locascio A, Blanco MJ, del Barrio MG, Portillo F, Nieto MA. 2000. The transcription factor snail controls epithelial-mesenchymal transitions by repressing E-cadherin expression. *Nat Cell Biol* 2(2):76-83.
- Carpenter CL, Duckworth BC, Auger KR, Cohen B, Schaffhausen BS, Cantley LC. 1990. Purification and characterization of phosphoinositide 3-kinase from rat liver. *J Biol Chem* 265(32):19704-11.
- Chambers JC, Zhang W, Sehmi J, Li X, Wass MN, Van der Harst P, Holm H, Sanna S, Kavousi M, Baumeister SE et al. . 2011. Genome-wide association study identifies loci influencing concentrations of liver enzymes in plasma. *Nat Genet* 43(11):1131-1138.
- Chan MC, Nguyen PH, Davis BN, Ohoka N, Hayashi H, Du K, Lagna G, Hata A. 2007. A novel regulatory mechanism of the bone morphogenetic protein (BMP) signaling pathway involving the carboxyl-terminal tail domain of BMP type II receptor. *Mol Cell Biol* 27(16):5776-89.
- Chen C, Jack J, Garofalo RS. 1996. The *Drosophila* insulin receptor is required for normal growth. *Endocrinology* 137(3):846-56.
- Choksi SP, Southall TD, Bossing T, Edoff K, de Wit E, Fischer BE, van Steensel B, Micklem G, Brand AH. 2006. Prospero acts as a binary switch between self-renewal and differentiation in *Drosophila* neural stem cells. *Dev Cell* 11(6):775-89.
- Ciruna B, Rossant J. 2001. FGF signaling regulates mesoderm cell fate specification and morphogenetic movement at the primitive streak. *Dev Cell* 1(1):37-49.
- Coffer PJ, Jin J, Woodgett JR. 1998. Protein kinase B (c-Akt): a multifunctional mediator of phosphatidylinositol 3-kinase activation. *Biochem J* 335 (Pt 1):1-13.

- Colombani J, Bianchini L, Layalle S, Pondeville E, Dauphin-Villemant C, Antoniewski C, Carre C, Noselli S, Leopold P. 2005. Antagonistic actions of ecdysone and insulins determine final size in *Drosophila*. *Science* 310(5748):667-70.
- Cunard R. 2013. Mammalian tribbles homologs at the crossroads of endoplasmic reticulum stress and Mammalian target of rapamycin pathways. *Scientifica (Cairo)* 2013:750871.
- Cybulski N, Polak P, Auwerx J, Ruegg MA, Hall MN. 2009. mTOR complex 2 in adipose tissue negatively controls whole-body growth. *Proc Natl Acad Sci U S A* 106(24):9902-7.
- Das R, Sebo Z, Pence L, Dobens LL. 2014. *Drosophila* tribbles antagonizes insulin signaling-mediated growth and metabolism via interactions with Akt kinase. *PLoS One* 9(10):e109530.
- Datta SR, Dudek H, Tao X, Masters S, Fu H, Gotoh Y, Greenberg ME. 1997. Akt phosphorylation of BAD couples survival signals to the cell-intrinsic death machinery. *Cell* 91(2):231-41.
- Dedhia PH, Keeshan K, Uljon S, Xu L, Vega ME, Shestova O, Zaks-Zilberman M, Romany C, Blacklow SC, Pear WS. 2010. Differential ability of Tribbles family members to promote degradation of C/EBPalpha and induce acute myelogenous leukemia. *Blood* 116(8):1321-8.
- Demontis F, Perrimon N. 2009. Integration of Insulin receptor/Foxo signaling and dMyc activity during muscle growth regulates body size in *Drosophila*. *Development* 136(6):983-93.
- DiAngelo JR, Birnbaum MJ. 2009. Regulation of fat cell mass by insulin in *Drosophila melanogaster*. *Mol Cell Biol* 29(24):6341-52.
- Ding J, Kato S, Du K. 2008. PI3K activates negative and positive signals to regulate TRB3 expression in hepatic cells. *Exp Cell Res* 314(7):1566-74.
- Dobens AC, Dobens LL. 2013. FijiWings: an open source toolkit for semiautomated morphometric analysis of insect wings. *G3 (Bethesda)* 3(8):1443-1449.

- Dobens LL, Jr., Bouyain S. 2012. Developmental roles of tribbles protein family members. *Dev Dyn* 241(8):1239-48.
- Downward J. 1998. Mechanisms and consequences of activation of protein kinase B/Akt. *Curr Opin Cell Biol* 10(2):262-7.
- Du K, Ding J. 2009. Insulin regulates TRB3 and other stress-responsive gene expression through induction of C/EBPbeta. *Mol Endocrinol* 23(4):475-85.
- Du K, Herzig S, Kulkarni RN, Montminy M. 2003. TRB3: a tribbles homolog that inhibits Akt/PKB activation by insulin in liver. *Science* 300(5625):1574-7.
- Duggan SP, Behan FM, Kirca M, Smith S, Reynolds JV, Long A, Kelleher D. 2010. An integrative genomic approach in oesophageal cells identifies TRB3 as a bile acid responsive gene, downregulated in Barrett's oesophagus, which regulates NF-kappaB activation and cytokine levels. *Carcinogenesis* 31(5):936-45.
- Eder K, Guan H, Sung HY, Francis SE, Crossman DC, Kiss-Toth E. 2008a. LDL uptake by monocytes in response to inflammation is MAPK dependent but independent of tribbles protein expression. *Immunol Lett* 116(2):178-83.
- Eder K, Guan H, Sung HY, Ward J, Angyal A, Janas M, Sarmay G, Duda E, Turner M, Dower SK et al. . 2008b. Tribbles-2 is a novel regulator of inflammatory activation of monocytes. *Int Immunol* 20(12):1543-50.
- Edgar BA. 2006. How flies get their size: genetics meets physiology. *Nat Rev Genet* 7(12):907-16.
- Farrell JA, O'Farrell PH. 2013. Mechanism and regulation of Cdc25/Twine protein destruction in embryonic cell-cycle remodeling. *Curr Biol* 23(2):118-26.
- Fichelson P, Gho M. 2004. Mother-daughter precursor cell fate transformation after Cdc2 down-regulation in the Drosophila bristle lineage. *Dev Biol* 276(2):367-77.
- Franke TF, Hornik CP, Segev L, Shostak GA, Sugimoto C. 2003. PI3K/Akt and apoptosis: size matters. *Oncogene* 22(56):8983-98.

- Frias MA, Thoreen CC, Jaffe JD, Schroder W, Sculley T, Carr SA, Sabatini DM. 2006. mSin1 is necessary for Akt/PKB phosphorylation, and its isoforms define three distinct mTORC2s. *Curr Biol* 16(18):1865-70.
- Gao X, Neufeld TP, Pan D. 2000. *Drosophila* PTEN regulates cell growth and proliferation through PI3K-dependent and -independent pathways. *Dev Biol* 221(2):404-418.
- Garami A, Zwartkuis FJ, Nobukuni T, Joaquin M, Rocco M, Stocker H, Kozma SC, Hafen E, Bos JL, Thomas G. 2003a. Insulin activation of Rheb, a mediator of mTOR/S6K/4E-BP signaling, is inhibited by TSC1 and 2. *Mol Cell* 11(6):1457-66.
- Garami A, Zwartkuis FJT, Nobukuni T, Joaquin M, Rocco M, Stocker H, Kozma SC, Hafen E, Bos JL, Thomas G. 2003b. Insulin activation of Rheb, a mediator of mTOR/S6K/4E-BP signaling, is inhibited by TSC1 and 2. *Mol Cell* 11(6):1457-1466.
- Gilby DC, Sung HY, Winship PR, Goodeve AC, Reilly JT, Kiss-Toth E. 2010. Tribbles-1 and -2 are tumour suppressors, down-regulated in human acute myeloid leukaemia. *Immunol Lett* 130(1-2):115-24.
- Gong H-p, Wang Z-h, Jiang H, Fang N-n, Li J-s, Shang Y-y, Zhang Y, Zhong M, Zhang W. 2009. TRIB3 functional Q84R polymorphism is a risk factor for metabolic syndrome and carotid atherosclerosis. *Diabetes Care* 32(7):1311-1313.
- Grosshans J, Wieschaus E. 2000. A genetic link between morphogenesis and cell division during formation of the ventral furrow in *Drosophila*. *Cell* 101(5):523-31.
- Guertin DA, Stevens DM, Thoreen CC, Burds AA, Kalaany NY, Moffat J, Brown M, Fitzgerald KJ, Sabatini DM. 2006. Ablation in mice of the mTORC components raptor, rictor, or mLST8 reveals that mTORC2 is required for signaling to Akt-FOXO and PKCalpha, but not S6K1. *Dev Cell* 11(6):859-71.
- He L, Simmen FA, Mehendale HM, Ronis MJ, Badger TM. 2006. Chronic ethanol intake impairs insulin signaling in rats by disrupting Akt association with the cell membrane. Role of TRB3 in inhibition of Akt/protein kinase B activation. *J Biol Chem* 281(16):11126-34.

- Hegedus Z, Czibula A, Kiss-Toth E. 2006. Tribbles: novel regulators of cell function; evolutionary aspects. *Cell Mol Life Sci* 63(14):1632-41.
- Hegedus Z, Czibula A, Kiss-Toth E. 2007. Tribbles: a family of kinase-like proteins with potent signalling regulatory function. *Cell Signal* 19(2):238-250.
- Herranz N, Pasini D, Diaz VM, Franci C, Gutierrez A, Dave N, Escrivà M, Hernandez-Munoz I, Di Croce L, Helin K et al. . 2008. Polycomb complex 2 is required for E-cadherin repression by the Snail1 transcription factor. *Mol Cell Biol* 28(15):4772-4781.
- Hua F, Mu R, Liu J, Xue J, Wang Z, Lin H, Yang H, Chen X, Hu Z. 2011. TRB3 interacts with SMAD3 promoting tumor cell migration and invasion. *J Cell Sci* 124(Pt 19):3235-46.
- Huang W, Zhu PJ, Zhang S, Zhou H, Stoica L, Galiano M, Krnjevic K, Roman G, Costa-Mattioli M. 2013. mTORC2 controls actin polymerization required for consolidation of long-term memory. *Nat Neurosci* 16(4):441-8.
- Huynh JR, St Johnston D. 2004. The origin of asymmetry: early polarisation of the *Drosophila* germline cyst and oocyte. *Curr Biol* 14(11):R438-49.
- Ikeya T, Galic M, Belawat P, Nairz K, Hafen E. 2002. Nutrient-dependent expression of insulin-like peptides from neuroendocrine cells in the CNS contributes to growth regulation in *Drosophila*. *Curr Biol* 12(15):1293-300.
- Ip YT, Gridley T. 2002. Cell movements during gastrulation: snail dependent and independent pathways. *Curr Opin Genet Dev* 12(4):423-9.
- Ishizuka Y, Nakayama K, Ogawa A, Makishima S, Boonvisut S, Hirao A, Iwasaki Y, Yada T, Yanagisawa Y, Miyashita H et al. . 2014. TRIB1 downregulates hepatic lipogenesis and glycogenesis via multiple molecular interactions. *J Mol Endocrinol* 52(2):145-58.
- Ilyedjian PB. 2005. Lack of evidence for a role of TRB3/NIPK as an inhibitor of PKB-mediated insulin signalling in primary hepatocytes. *Biochem J* 386(Pt 1):113-118.

- Johansson P, Eisele L, Klein-Hitpass L, Sellmann L, Duhrsen U, Durig J, Nuckel H. 2010. Percentage of smudge cells determined on routine blood smears is a novel prognostic factor in chronic lymphocytic leukemia. *Leuk Res* 34(7):892-8.
- Junger M, Rintelen F, Stocker H, Wasserman J, Vegh M, Radimerski T, Greenberg M, Hafen E. 2003. The Drosophila Forkhead transcription factor FOXO mediates the reduction in cell number associated with reduced insulin signaling. *Journal of Biology* 2(3):20.
- Kathiresan S, Melander O, Anevski D, Guiducci C, Burt NP, Roos C, Hirschhorn JN, Berglund G, Hedblad B, Groop L et al. . 2008. Polymorphisms associated with cholesterol and risk of cardiovascular events. *N Engl J Med* 358(12):1240-1249.
- Kato S, Du K. 2007. TRB3 modulates C2C12 differentiation by interfering with Akt activation. *Biochem Biophys Res Commun* 353(4):933-8.
- Keeshan K, Bailis W, Dedhia PH, Vega ME, Shestova O, Xu L, Toscano K, Uljon SN, Blacklow SC, Pear WS. 2010. Transformation by Tribbles homolog 2 (Trib2) requires both the Trib2 kinase domain and COP1 binding. *Blood* 116(23):4948-57.
- Keeshan K, He Y, Wouters BJ, Shestova O, Xu L, Sai H, Rodriguez CG, Maillard I, Tobias JW, Valk P et al. . 2006. Tribbles homolog 2 inactivates C/EBPalpha and causes acute myelogenous leukemia. *Cancer Cell* 10(5):401-11.
- Keeshan K, Shestova O, Ussin L, Pear WS. 2008. Tribbles homolog 2 (Trib2) and HoxA9 cooperate to accelerate acute myelogenous leukemia. *Blood Cells Mol Dis* 40(1):119-21.
- Kiss-Toth E. 2011. Tribbles: 'puzzling' regulators of cell signalling. *Biochem Soc Trans* 39(2):684-7.
- Koh HJ, Arnolds DE, Fujii N, Tran TT, Rogers MJ, Jessen N, Li Y, Liew CW, Ho RC, Hirshman MF et al. . 2006. Skeletal muscle-selective knockout of LKB1 increases insulin sensitivity, improves glucose homeostasis, and decreases TRB3. *Mol Cell Biol* 26(22):8217-27.

- Kohn AD, Summers SA, Birnbaum MJ, Roth RA. 1996. Expression of a constitutively active Akt Ser/Thr kinase in 3T3-L1 adipocytes stimulates glucose uptake and glucose transporter 4 translocation. *J Biol Chem* 271(49):31372-8.
- Koo SH, Satoh H, Herzig S, Lee CH, Hedrick S, Kulkarni R, Evans RM, Olefsky J, Montminy M. 2004. PGC-1 promotes insulin resistance in liver through PPAR-alpha-dependent induction of TRB-3. *Nat Med* 10(5):530-4.
- Koyama T, Mendes CC, Mirth CK. 2013. Mechanisms regulating nutrition-dependent developmental plasticity through organ-specific effects in insects. *Front Physiol* 4:263-263.
- Lee G, Park JH. 2004a. Hemolymph sugar homeostasis and starvation-induced hyperactivity affected by genetic manipulations of the adipokinetic hormone-encoding gene in *Drosophila melanogaster*. *Genetics* 167(1):311-23.
- Lee G, Park JH. 2004b. Hemolymph sugar homeostasis and starvation-induced hyperactivity affected by genetic manipulations of the adipokinetic hormone-encoding gene in *Drosophila melanogaster*. *Genetics* 167(1):311-323.
- Levine B, Hackney JF, Bergen A, Dobens L, 3rd, Truesdale A, Dobens L. 2010. Opposing interactions between *Drosophila cut* and the C/EBP encoded by slow border cells direct apical constriction and epithelial invagination. *Dev Biol* 344(1):196-209.
- Liew CW, Bochenski J, Kawamori D, Hu J, Leech CA, Wanic K, Malecki M, Warram JH, Qi L, Krolewski AS et al. . 2010. The pseudokinase tribbles homolog 3 interacts with ATF4 to negatively regulate insulin exocytosis in human and mouse beta cells. *J Clin Invest* 120(8):2876-88.
- Lin K-R, Lee S-F, Hung C-M, Li C-L, Yang-Yen H-F, Yen JJY. 2007. Survival factor withdrawal-induced apoptosis of TF-1 cells involves a TRB2-Mcl-1 axis-dependent pathway. *J Biol Chem* 282(30):21962-21972.
- Liu J, Wu X, Franklin JL, Messina JL, Hill HS, Moellering DR, Walton RG, Martin M, Garvey WT. 2010. Mammalian Tribbles homolog 3 impairs insulin action in skeletal muscle: role in glucose-induced insulin resistance. *Am J Physiol Endocrinol Metab* 298(3):E565-76.

- Liu J, Zhang W, Chuang GC, Hill HS, Tian L, Fu Y, Moellering DR, Garvey WT. 2012. Role of TRIB3 in regulation of insulin sensitivity and nutrient metabolism during short-term fasting and nutrient excess. *Am J Physiol Endocrinol Metab* 303(7):E908-16.
- Loewith R, Hall MN. 2011. Target of rapamycin (TOR) in nutrient signaling and growth control. *Genetics* 189(4):1177-201.
- Manning BD, Cantley LC. 2007. AKT/PKB signaling: navigating downstream. *Cell* 129(7):1261-74.
- Masoner V, Das R, Pence L, Anand G, LaFerriere H, Zars T, Bouyain S, Dobens LL. 2013. The kinase domain of *Drosophila* Tribbles is required for turnover of fly C/EBP during cell migration. *Dev Biol* 375(1):33-44.
- Mata J, Curado S, Ephrussi A, Rorth P. 2000. Tribbles coordinates mitosis and morphogenesis in *Drosophila* by regulating string/CDC25 proteolysis. *Cell* 101(5):511-22.
- Mathieu J, Sung H-H, Pugieux C, Soetaert J, Rorth P. 2007. A sensitized PiggyBac-based screen for regulators of border cell migration in *Drosophila*. *Genetics* 176(3):1579-1590.
- Matsumoto M, Han S, Kitamura T, Accili D. 2006. Dual role of transcription factor FoxO1 in controlling hepatic insulin sensitivity and lipid metabolism. *J Clin Invest* 116(9):2464-72.
- Matsushima R, Harada N, Webster NJ, Tsutsumi YM, Nakaya Y. 2006. Effect of TRIB3 on insulin and nutrient-stimulated hepatic p70 S6 kinase activity. *J Biol Chem* 281(40):29719-29.
- Mayumi-Matsuda K, Kojima S, Suzuki H, Sakata T. 1999. Identification of a novel kinase-like gene induced during neuronal cell death. *Biochem Biophys Res Commun* 258(2):260-4.
- Miron M, Lasko P, Sonenberg N. 2003. Signaling from Akt to FRAP/TOR Targets both 4E-BP and S6K in *Drosophila melanogaster*. *Molecular and Cellular Biology* 23(24):9117-9126.

- Miyoshi N, Ishii H, Mimori K, Takatsuno Y, Kim H, Hirose H, Sekimoto M, Doki Y, Mori M. 2009. Abnormal expression of TRIB3 in colorectal cancer: a novel marker for prognosis. *Br J Cancer* 101(10):1664-70.
- Montagne J, Stewart MJ, Stocker H, Hafen E, Kozma SC, Thomas G. 1999. *Drosophila* S6 kinase: a regulator of cell size. *Science* 285(5436):2126-9.
- Montell DJ, Rorth P, Spradling AC. 1992. slow border cells, a locus required for a developmentally regulated cell migration during oogenesis, encodes *Drosophila* C/EBP. *Cell* 71(1):51-62.
- Mora A, Komander D, van Aalten DM, Alessi DR. 2004. PDK1, the master regulator of AGC kinase signal transduction. *Semin Cell Dev Biol* 15(2):161-70.
- Mukherjee T, Schafer U, Zeidler MP. 2006. Identification of *Drosophila* genes modulating Janus kinase/signal transducer and activator of transcription signal transduction. *Genetics* 172(3):1683-97.
- Musselman LP, Fink JL, Narzinski K, Ramachandran PV, Hathiramani SS, Cagan RL, Baranski TJ. 2011. A high-sugar diet produces obesity and insulin resistance in wild-type *Drosophila*. *Dis Model Mech* 4(6):842-9.
- Na J, Musselman LP, Pendse J, Baranski TJ, Bodmer R, Ocorr K, Cagan R. 2013. A *Drosophila* model of high sugar diet-induced cardiomyopathy. *PLoS Genet* 9(1):e1003175.
- Naiki T, Saijou E, Miyaoka Y, Sekine K, Miyajima A. 2007. TRB2, a mouse Tribbles ortholog, suppresses adipocyte differentiation by inhibiting AKT and C/EBPbeta. *J Biol Chem* 282(33):24075-82.
- Norga KK, Gurganus MC, Dilda CL, Yamamoto A, Lyman RF, Patel PH, Rubin GM, Hoskins RA, Mackay TF, Bellen HJ. 2003. Quantitative Analysis of Bristle Number in *Drosophila* Mutants Identifies Genes Involved in Neural Development. *Current Biology* 13(16):1388-1396.
- Oberkofler H, Pfeifenberger A, Soyal S, Felder T, Hahne P, Miller K, Krempler F, Patsch W. 2010. Aberrant hepatic TRIB3 gene expression in insulin-resistant obese humans. *Diabetologia* 53(9):1971-5.

- Ohoka N, Yoshii S, Hattori T, Onozaki K, Hayashi H. 2005. TRB3, a novel ER stress-inducible gene, is induced via ATF4-CHOP pathway and is involved in cell death. *EMBO J* 24(6):1243-1255.
- Okamoto H, Latres E, Liu R, Thabet K, Murphy A, Valenzeula D, Yancopoulos GD, Stitt TN, Glass DJ, Sleeman MW. 2007. Genetic deletion of Trb3, the mammalian *Drosophila* tribbles homolog, displays normal hepatic insulin signaling and glucose homeostasis. *Diabetes* 56(5):1350-6.
- Parisi F, Riccardo S, Daniel M, Saqcena M, Kundu N, Pession A, Grifoni D, Stocker H, Tabak E, Bellosta P. 2011. *Drosophila* insulin and target of rapamycin (TOR) pathways regulate GSK3 beta activity to control Myc stability and determine Myc expression in vivo. *BMC Biol* 9:65.
- Parrini MC, Lei M, Harrison SC, Mayer BJ. 2002. Pak1 kinase homodimers are autoinhibited in trans and dissociated upon activation by Cdc42 and Rac1. *Mol Cell* 9(1):73-83.
- Pasco MY, Leopold P. 2012. High sugar-induced insulin resistance in *Drosophila* relies on the lipocalin Neural Lazarillo. *PLoS One* 7(5):e36583.
- Porstmann T, Griffiths B, Chung Y-L, Delpuech O, Griffiths JR, Downward J, Schulze A. 2005. PKB//Akt induces transcription of enzymes involved in cholesterol and fatty acid biosynthesis via activation of SREBP. *Oncogene* 24(43):6465-6481.
- Porstmann T, Santos CR, Griffiths B, Cully M, Wu M, Leever S, Griffiths JR, Chung YL, Schulze A. 2008. SREBP activity is regulated by mTORC1 and contributes to Akt-dependent cell growth. *Cell Metab* 8(3):224-36.
- Price DM, Jin Z, Rabinovitch S, Campbell SD. 2002. Ectopic expression of the *Drosophila* Cdk1 inhibitory kinases, Wee1 and Myt1, interferes with the second mitotic wave and disrupts pattern formation during eye development. *Genetics* 161(2):721-31.
- Prudente S, Baratta R, Andreozzi F, Morini E, Farina MG, Nigro A, Copetti M, Pellegrini F, Succurro E, Di Pietrantonio L et al. . 2010. TRIB3 R84 variant affects glucose homeostasis by altering the interplay between insulin sensitivity and secretion. *Diabetologia* 53(7):1354-61.

- Prudente S, Hribal ML, Flex E, Turchi F, Morini E, De Cosmo S, Bacci S, Tassi V, Cardellini M, Lauro R et al. . 2005. The functional Q84R polymorphism of mammalian Tribbles homolog TRB3 is associated with insulin resistance and related cardiovascular risk in Caucasians from Italy. *Diabetes* 54(9):2807-11.
- Prudente S, Morini E, Marselli L, Baratta R, Copetti M, Mendonca C, Andreozzi F, Chandalia M, Pellegrini F, Bailetti D et al. . 2013. Joint effect of insulin signaling genes on insulin secretion and glucose homeostasis. *J Clin Endocrinol Metab* 98(6):1143-1147.
- Prudente S, Scarpelli D, Chandalia M, Zhang Y-Y, Morini E, Del Guerra S, Perticone F, Li R, Powers C, Andreozzi F et al. . 2009. The TRIB3 Q84R polymorphism and risk of early-onset type 2 diabetes. *J Clin Endocrinol Metab* 94(1):190-196.
- Prudente S, Sesti G, Pandolfi A, Andreozzi F, Consoli A, Trischitta V. 2012. The mammalian tribbles homolog TRIB3, glucose homeostasis, and cardiovascular diseases. *Endocr Rev* 33(4):526-46.
- Puig O, Marr MT, Ruhf ML, Tjian R. 2003. Control of cell number by *Drosophila* FOXO: downstream and feedback regulation of the insulin receptor pathway. *Genes Dev* 17(16):2006-20.
- Puig O, Tjian R. 2005. Transcriptional feedback control of insulin receptor by dFOXO/FOXO1. *Genes Dev* 19(20):2435-46.
- Qi L, Heredia JE, Altarejos JY, Screatton R, Goebel N, Niessen S, Macleod IX, Liew CW, Kulkarni RN, Bain J et al. . 2006. TRB3 links the E3 ubiquitin ligase COP1 to lipid metabolism. *Science* 312(5781):1763-6.
- Rorth P, Szabo K, Texido G. 2000. The level of C/EBP protein is critical for cell migration during *Drosophila* oogenesis and is tightly controlled by regulated degradation. *Mol Cell* 6(1):23-30.
- Ruud AF, Lam G, Thummel CS. 2011. The *Drosophila* NR4A nuclear receptor DHR38 regulates carbohydrate metabolism and glycogen storage. *Mol Endocrinol* 25(1):83-91.
- Rulifson EJ, Kim SK, Nusse R. 2002. Ablation of insulin-producing neurons in flies: growth and diabetic phenotypes. *Science* 296(5570):1118-20.

- Saltiel AR, Pessin JE. 2002. Insulin signaling pathways in time and space. *Trends Cell Biol* 12(2):65-71.
- Sarbassov DD, Ali SM, Kim DH, Guertin DA, Latek RR, Erdjument-Bromage H, Tempst P, Sabatini DM. 2004. Rictor, a novel binding partner of mTOR, defines a rapamycin-insensitive and raptor-independent pathway that regulates the cytoskeleton. *Curr Biol* 14(14):1296-302.
- Sarbassov DD, Ali SM, Sengupta S, Sheen JH, Hsu PP, Bagley AF, Markhard AL, Sabatini DM. 2006. Prolonged rapamycin treatment inhibits mTORC2 assembly and Akt/PKB. *Mol Cell* 22(2):159-68.
- Sarbassov DD, Guertin DA, Ali SM, Sabatini DM. 2005. Phosphorylation and regulation of Akt/PKB by the rictor-mTOR complex. *Science* 307(5712):1098-101.
- Sathyanarayana P, Dev A, Fang J, Houde E, Bogacheva O, Bogachev O, Menon M, Browne S, Pradeep A, Emerson C et al. . 2008. EPO receptor circuits for primary erythroblast survival. *Blood* 111(11):5390-5399.
- Schulz C, Kiger AA, Tazuke SI, Yamashita YM, Pantalena-Filho LC, Jones DL, Wood CG, Fuller MT. 2004. A misexpression screen reveals effects of bag-of-marbles and TGF beta class signaling on the Drosophila male germ-line stem cell lineage. *Genetics* 167(2):707-23.
- Schwarzer R, Dames S, Tondera D, Klippel A, Kaufmann J. 2006. TRB3 is a PI 3-kinase dependent indicator for nutrient starvation. *Cell Signal* 18(6):899-909.
- Seher TC, Leptin M. 2000. Tribbles, a cell-cycle brake that coordinates proliferation and morphogenesis during Drosophila gastrulation. *Curr Biol* 10(11):623-9.
- Selim E, Frkanec JT, Cunard R. 2007. Fibrates upregulate TRB3 in lymphocytes independent of PPAR alpha by augmenting CCAAT/enhancer-binding protein beta (C/EBP beta) expression. *Mol Immunol* 44(6):1218-29.
- Shang YY, Wang ZH, Zhang LP, Zhong M, Zhang Y, Deng JT, Zhang W. 2009. TRB3, upregulated by ox-LDL, mediates human monocyte-derived macrophage apoptosis. *FEBS J* 276(10):2752-61.

- Shingleton AW, Das J, Vinicius L, Stern DL. 2005. The temporal requirements for insulin signaling during development in *Drosophila*. *PLoS Biol* 3(9):e289.
- Sievers F, Wilm A, Dineen D, Gibson TJ, Karplus K, Li W, Lopez R, McWilliam H, Remmert M, Soding J et al. . 2011. Fast, scalable generation of high-quality protein multiple sequence alignments using Clustal Omega. *Mol Syst Biol* 7:539.
- Sung HY, Guan H, Czibula A, King AR, Eder K, Heath E, Suvarna SK, Dower SK, Wilson AG, Francis SE et al. . 2007. Human tribbles-1 controls proliferation and chemotaxis of smooth muscle cells via MAPK signaling pathways. *J Biol Chem* 282(25):18379-87.
- Szafranski P, Goode S. 2004. A Fasciclin 2 morphogenetic switch organizes epithelial cell cluster polarity and motility. *Development* 131(9):2023-2036.
- Taguchi A, White MF. 2008. Insulin-like signaling, nutrient homeostasis, and life span. *Annu Rev Physiol* 70:191-212.
- Takahashi Y, Ohoka N, Hayashi H, Sato R. 2008. TRB3 suppresses adipocyte differentiation by negatively regulating PPARgamma transcriptional activity. *J Lipid Res* 49(4):880-92.
- Takasato M, Kobayashi C, Okabayashi K, Kiyonari H, Oshima N, Asashima M, Nishinakamura R. 2008. *Trb2*, a mouse homolog of tribbles, is dispensable for kidney and mouse development. *Biochem Biophys Res Commun* 373(4):648-52.
- Taylor CR, Heglund NC. 1982. Energetics and Mechanics of Terrestrial Locomotion. *Annual Review of Physiology* 44(1):97-107.
- Teleman AA. 2010. Molecular mechanisms of metabolic regulation by insulin in *Drosophila*. *Biochem J* 425(1):13-26.
- Teleman AA, Hietakangas V, Sayadian AC, Cohen SM. 2008. Nutritional control of protein biosynthetic capacity by insulin via Myc in *Drosophila*. *Cell Metab* 7(1):21-32.

- Thibault ST, Singer MA, Miyazaki WY, Milash B, Dompe NA, Singh CM, Buchholz R, Demsky M, Fawcett R, Francis-Lang HL et al. . 2004. A complementary transposon tool kit for *Drosophila melanogaster* using P and piggyBac. *Nat Genet* 36(3):283-7.
- Thompson SN. 2003. Trehalose – The Insect ‘Blood’ Sugar. *Advances in Insect Physiology* 31:205-285.
- Tzivion G, Dobson M, Ramakrishnan G. 2011. FoxO transcription factors; Regulation by AKT and 14-3-3 proteins. *Biochim Biophys Acta* 1813(11):1938-45.
- Varbo A, Nordestgaard BG, Tybjaerg-Hansen A, Schnohr P, Jensen GB, Benn M. 2011. Nonfasting triglycerides, cholesterol, and ischemic stroke in the general population. *Ann Neurol* 69(4):628-634.
- Wang S-P, Wang W-L, Chang Y-L, Wu C-T, Chao Y-C, Kao S-H, Yuan A, Lin C-W, Yang S-C, Chan W-K et al. . 2009. p53 controls cancer cell invasion by inducing the MDM2-mediated degradation of Slug. *Nat Cell Biol* 11(6):694-704.
- Weismann D, Erion DM, Ignatova-Todorava I, Nagai Y, Stark R, Hsiao JJ, Flannery C, Birkenfeld AL, May T, Kahn M et al. . 2011. Knockdown of the gene encoding *Drosophila* tribbles homologue 3 (Trib3) improves insulin sensitivity through peroxisome proliferator-activated receptor-gamma (PPAR-gamma) activation in a rat model of insulin resistance. *Diabetologia* 54(4):935-44.
- Wennemers M, Bussink J, Scheijen B, Nagtegaal ID, van Laarhoven HW, Raleigh JA, Varia MA, Heuvel JJ, Rouschop KM, Sweep FC et al. . 2011. Tribbles homolog 3 denotes a poor prognosis in breast cancer and is involved in hypoxia response. *Breast Cancer Res* 13(4):R82.
- Wilkin F, Savonet V, Radulescu A, Petermans J, Dumont JE, Maenhaut C. 1996. Identification and characterization of novel genes modulated in the thyroid of dogs treated with methimazole and propylthiouracil. *J Biol Chem* 271(45):28451-7.
- Wilkin F, Suarez-Huerta N, Robaye B, Peetermans J, Libert F, Dumont JE, Maenhaut C. 1997. Characterization of a phosphoprotein whose mRNA is regulated by the mitogenic pathways in dog thyroid cells. *Eur J Biochem* 248(3):660-8.

- Xu T, Rubin GM. 1993. Analysis of genetic mosaics in developing and adult *Drosophila* tissues. *Development* 117(4):1223-37.
- Yacoub Wasef SZ, Robinson KA, Berkaw MN, Buse MG. 2006. Glucose, dexamethasone, and the unfolded protein response regulate TRB3 mRNA expression in 3T3-L1 adipocytes and L6 myotubes. *Am J Physiol Endocrinol Metab* 291(6):E1274-80.
- Yamagata K, Daitoku H, Takahashi Y, Namiki K, Hisatake K, Kako K, Mukai H, Kasuya Y, Fukamizu A. 2008. Arginine methylation of FOXO transcription factors inhibits their phosphorylation by Akt. *Mol Cell* 32(2):221-31.
- Yamamoto M, Uematsu S, Okamoto T, Matsuura Y, Sato S, Kumar H, Satoh T, Saitoh T, Takeda K, Ishii KJ et al. . 2007. Enhanced TLR-mediated NF-IL6 dependent gene expression by Trib1 deficiency. *J Exp Med* 204(9):2233-9.
- Yokoyama T, Nakamura T. 2011. Tribbles in disease: Signaling pathways important for cellular function and neoplastic transformation. *Cancer Sci* 102(6):1115-22.
- Zanella F, Renner O, Garcia B, Callejas S, Dopazo A, Peregrina S, Carnero A, Link W. 2010. Human TRIB2 is a repressor of FOXO that contributes to the malignant phenotype of melanoma cells. *Oncogene* 29(20):2973-82.
- Zdychova J, Komers R. 2005. Emerging role of Akt kinase/protein kinase B signaling in pathophysiology of diabetes and its complications. *Physiol Res* 54(1):1-16.
- Zhang X, Tang N, Hadden TJ, Rishi AK. 2011. Akt, FoxO and regulation of apoptosis. *Biochim Biophys Acta* 1813(11):1978-86.
- Zinzalla V, Stracka D, Oppliger W, Hall MN. 2011. Activation of mTORC2 by association with the ribosome. *Cell* 144(5):757-68.

VITA

Rahul Das was born on June 13, 1986 in Kolkata, India. He graduated from Nabajiban Vidyamandir, Kolkata in 2001. In 2006, he obtained Bachelor of Science degree in Microbiology from University of Calcutta and graduated from University of Calcutta with a Master of Science in Biochemistry in 2008. He worked in Chembiotek International, a biotechnology company from 2008-2009.

He began graduate school in 2009 at the School of Biological Sciences of the University of Missouri-Kansas City and joined the laboratory of Dr. Leonard Dobens in 2010. During the course of his PhD, he studied the evolutionarily conserved roles of the *Drosophila* protein Tribbles in development and Insulin signaling pathway.